The Role of TET Proteins in the Epigenetic Regulation of Neural Gene Expression and

Behavior

by

Aaron Joseph Towers

University Program in Genetics and Genomics
Duke University

Date:_____
Approved:

_____
Yong-hui Jiang, Advisor

_____
Beth Sullivan, Chair

_____
Anne West

_____
Simon Gregory

Dissertation submitted in partial fulfillment of
the requirements for the degree of Doctor of Philosophy,
in the University Program in Genetics and Genomics
in the Graduate School
of Duke University

2016

ABSTRACT

The Role of TET Proteins in the Epigenetic Regulation of Neural Gene Expression and

Behavior

by

Aaron Joseph Towers

University Program in Genetics and Genomics
Duke University

Date:_____
Approved:

_____
Yong-hui Jiang, Advisor

_____
Beth Sullivan, Chair

_____
Anne West

_____
Simon Gregory

An abstract of a dissertation submitted in partial
fulfillment of the requirements for the degree
of Doctor of Philosophy, in the University Program in
Genetics and Genomics in the Graduate School of
Duke University

2016

Abstract

Understanding how genes affect behavior is critical to develop precise therapies for human behavioral disorders. The ability to investigate the relationship between genes and behavior has been greatly advanced over the last few decades due to progress in gene-targeting technology. Recently, the *Tet* gene family was discovered and implicated in epigenetic modification of DNA methylation by converting 5-methylcytosine to 5-hydroxymethylcytosine (5hmC). 5hmC and its catalysts, the TET proteins, are highly abundant in the postnatal brain but with unclear functions. To investigate their neural functions, we generated new lines of *Tet1* and *Tet3* mutant mice using a gene targeting approach. We designed both mutations to cause a frameshift by deleting the largest coding exon of *Tet1* (*Tet1*$^{\Delta e4}$) and the catalytic domain of *Tet3* (*Tet3*$^{\Delta e7\text{-}9}$). As *Tet1* is also highly expressed in embryonic stem cells (ESCs), we generated *Tet1* homozygous deleted ESCs through sequential targeting to compare the function of *Tet1* in the brain to its role in ESCs. To test our hypothesis that TET proteins epigenetically regulate transcription of key neural genes important for normal brain function, we examined transcriptional and epigenetic differences in the *Tet1*$^{\Delta e4}$ mouse brain. The oxytocin receptor (*OXTR*), a neural gene implicated in social behaviors, is suggested to be epigenetically regulated by an unknown mechanism. Interestingly, several human studies have found associations between *OXTR* DNA hypermethylation and a wide

iv

spectrum of behavioral traits and neuropsychiatric disorders including autism spectrum

disorders. Here we report the first evidence for an epigenetic mechanism of *Oxtr*

transcription as expression of *Oxtr* is reduced in the brains of *Tet1*$^{\Delta e4-/-}$ mice. Likewise,

the CpG island overlapping the promoter of *Oxtr* is hypermethylated during early

embryonic development and persists into adulthood. We also discovered altered histone

modifications at the hypermethylated regions, indicating the loss of TET1 has broad

effects on the chromatin structure at *Oxtr*. Unexpectedly, we discovered an array of

novel mRNA isoforms of *Oxtr* that are selectively reduced in *Tet1*$^{\Delta e4-/-}$ mice. Additionally,

Tet1$^{\Delta e4-/-}$ mice display increased agonistic behaviors and impaired maternal care and

short-term memory. Our findings support a novel role for TET1 in regulating *Oxtr*

expression by preventing DNA hypermethylation and implicate TET1 in social

behaviors, offering novel insight into *Oxtr* epigenetic regulation and its role in

neuropsychiatric disorders.

Dedication

To my wife Angela and two boys, Kai and Asher, who endured too many nights and weekends away from their husband and daddy in pursuit of this degree.

Contents

List of Tables

List of Figures

Acknowledgements

I would like to thank Dr. Jiang for his mentoring, especially the confidence he showed in me. I would like to thank UPGG and Peds admin for their support and my committee for advice and stimulating questions. I would like to thank all the folks over at CAPS: Ayesha Chaudhary for her wisdom; Kelly Crace for exposing my perfectionist tendencies; Yan Li, Holly Rogers, Margaret Maytan, Libby Webb, and Kate Davies-Adams for introducing me to mindfulness; and Gary Glass for meaningful conversations and encouragement in expanding GradConvos. I would like to thank the Graduate Student Affairs staff including Dean Looney, Melissa Bostrom, Alan Kendrick, and Sondra Ponzi for always showing genuine interest in graduate student well-being and making sure there was great programing. I would also like to thank GPSC for electing me as Director of Advocacy and giving me a chance to advocate for graduate students in D.C. Duke has been a wonderful place to complete my graduate work and I fully took advantage of many performances, athletic events, and intramural sports. My lab mates and UPGG classmates were critical for their intellectual engagement and peer support as friends who "got it", especially Lomax Boyd for capturing my story as a graduate student on film. I would like to thank my friends and family, especially my parents, for always believing I could finish this degree. Finally, I would like to thank Angela for carrying the family load through this long and arduous process. I owe her big time.

1. Epigenetics, Gene Regulation, and Disease

Epigenetic modifications can affect gene expression through their effect on chromatin structure, whether it be promoting open or condensed chromatin, or by affecting access to specific DNA regulatory elements (Cedar and Bergman, 2009; Jones, 2012; Lam et al., 2005). DNA methylation is one form of epigenetic modification which serves in a regulatory role during mammalian development (Smith and Meissner, 2013) but is also important for neuronal gene expression in the adult (Wu et al., 2010).

DNA methyltransferases (DNMTs) methylate DNA by catalyzing the reaction of the base cytosine to the "fifth base" 5-methylcytosine (5mC). The DNMTs accomplish this by transferring a methyl group from S-adenosyl methionine to a cytosine, usually adjacent to a guanine in DNA sequence (Jabbari and Bernardi, 2004). 5mC is a significant epigenetic mark, as it is enriched in heterochromatin (Ficz et al., 2011) and silenced gene promoters (Brenet et al., 2011). On the contrary, enzymes responsible for DNA demethylation have remained elusive.

Abnormal DNA methylation has been implicated in many human diseases (Bergman and Cedar, 2013). Over the last decade, data have been accumulating that suggest the epigenome is sensitive to environmental influences (Brummelte et al., 2016; Waterland and Jirtle, 2004). The environment could potentially affect the epigenome by over or under supplying of methyl groups, such as methionine, or by influencing the expression of epigenetically modifying genes (Waterland, 2006). A more complete

understanding of the complex interplay between genes, epigenetics, and the environment would contribute to our ability to treat human conditions that are influenced by environmental modulation of the epigenome.

1.1 Intersection of epigenetics and disease

The discovery of epigenetic marks and the ability to routinely profile them, has opened up a whole new field of study into the mechanisms of human disease. Due to the relative stability of epigenetic modifications, there has been a growing interest in using them as biomarkers for disease diagnosis and prognosis. Some of the greatest demonstrations in feasibility have come from profiling DNA methylation in cancer (Zhu and Yao, 2009). Hypermethylation at the glutathione S-transferase pi 1 (GSTP1) gene is effective at diagnosing prostate cancer while hypermethylation at the O6-methylguanine-DNA methyltransferase (MGMT) gene is effective at predicting drug response in gliomas (Esteller et al., 2000; Lee et al., 1994). Several studies have also found associations between epigenetic marks and neurodevelopmental disorders but epigenetic therapies for these disorders are lacking (Millan, 2013). A better understanding of the factors that influence epigenetics is needed to develop new and improved therapies. Potential therapies could target epigenetic marks themselves or the factors that produce or remove them. Currently, pharmaceuticals that inhibit histone deacetylases and DNA methyltransferases are being used to treat a variety of cancers

but the treatments are not locus-specific and can trigger epigenome-wide changes with unintended consequences (Piekarz and Bates, 2009).

1.2 DNA methylation and neurodevelopmental disorders

Among the several hundred genes implicated in intellectual disabilities and related cognitive disorders are genes encoding epigenetic modifiers (van Bokhoven, 2011). Among them are gene mutations in DNA methyltransferase *DNMT3b* which causes Immunodeficiency, Centromere instability and Facial anomalies syndrome (ICF) and *MECP2* which causes Rett syndrome (Amir et al., 1999; Hansen et al., 1999). In addition to the genes themselves, abnormal epigenetic marks such as DNA hyper- or hypomethylation have been implicated in autism spectrum disorders (ASD), fragile X, Angelman syndromes and other genomic imprinting disorders (Colak et al., 2014; Jiang et al., 2004; Nardone et al., 2014). Of particular note, hypermethylation at specific gene loci, including *OXTR* and *SHANK3*, have been implicated in autism spectrum disorders (Gregory et al., 2009; Zhu et al., 2014). Understanding the regulation of DNA methylation in the brain might give insight into how these disorders progress.

1.3 Unknown mechanistic cause for abnormal DNA methylation of neural genes

While it was an important endeavor to document methylation changes and their associations for diseases, there was no mechanistic cause to explain the hypermethylation observed in both the *OXTR* and *SHANK3* studies. Was the

hypermethylation causal for autism phenotypes or an effect of the phenotypes? When

did the hypermethylation occur, during prenatal development or childhood? Was the

hypermethylation a genetic or environmental cause? Was the hypermethylation due to

increased activity of DNA methyltransferases or a lack of activity from putative DNA

demethylases? An active DNA demethylation pathway had been suggested most

strongly from the observance of rapid demethylation of the paternal genome after

fertilization but the mechanism remained unknown (Hajkova et al., 2008; Kafri et al.,

1992). While a few proteins including AID, TDG, and Gadd45b have been implicated in

the DNA demethylation process, a complete mechanism was still lacking (Ma et al.,

2009; Morgan et al., 2004; Zhu et al., 2001).

1.4 Discovery of the TET family of proteins and 5-hydroxymethylcytosine

A computational study aimed at identifying protein domains that could modify

5mC, was the first to suggest the involvement of the TET family in the oxidation of DNA

methylation (Iyer et al., 2009). Shortly thereafter, two studies discovered the novel base

5-hydroxymethylctysine (5hmC) and showed that overexpression of TET1 led to a

decrease in 5mC with 5hmC identified as the conversion product (Kriaucionis and

Heintz, 2009; Tahiliani et al., 2009). TET1, Ten Eleven Translocation, was first discovered

as a fusion partner with MLL histone methyltransferase in acute myeloid leukemia

(Lorsbach et al., 2003; Ono et al., 2002). Its name is derived from its location on

chromosome ten while MLL is located on chromosome 11.

The discovery of the TET family of methylcytosine dioxygenases has shed light on the regulation of DNA methylation during development and in post-mitotic cells (Kriaucionis and Heintz, 2009; Tahiliani et al., 2009). TET proteins can partner with other proteins to demethylate DNA in a stepwise process that begins with oxidation of 5-methylcytosine (5mC) to 5-hydroxymethylcytosine (5hmC), followed by further oxidation to 5-formylcytosine (5fC) and 5-carboxylcytosine (5caC). Finally, thymidine DNA glycosylase-mediated base excision repair replaces 5fC or 5caC with unmodified cytosine (He et al., 2011; Ito et al., 2011).

The mouse *Tet* gene family (*Tet1-3*) is differentially regulated during development and in adult brain tissues (Szwagierczak et al., 2010). *Tet1* expression is relatively enriched in embryonic stem cells (ESCs) (Szwagierczak et al., 2010; Wossidlo et al., 2011) and has been implicated in regulating genes important for cellular differentiation, pluripotency, and neurogenesis (Ito et al., 2010; Koh et al., 2011; Xu et al., 2011). *Tet1-3*, along with other putative DNA demethylation machinery *Gadd45*, *Tdg*, and *Mbd4*, are all expressed in the brain suggesting that DNA demethylation occurs in the brain (Guo et al., 2011a; Guo et al., 2011b; Ma et al., 2009). In addition to being a DNA demethylation intermediate, 5hmC is a stable DNA modification as opposed to 5fC and 5caC (Munzel et al., 2010). 5hmC is present at variable levels in ESCs and adult tissues but is specifically enriched in postnatal brains (Bachman et al., 2014; Globisch et al., 2010) where it accumulates with age (Song et al., 2011). 5hmC is enriched in active

genes (Song et al., 2011), absent in heterochromatin (Ficz et al., 2011), and is bound by the methyl binding protein, Mbd3 (Yildirim et al., 2011). Further demonstrating a relationship between 5hmC and expression, a study showed that differentiation-dependent transcriptional enhancers accumulate 5hmC along with active histone modifications upon differentiation (Serandour et al., 2012).

Similar to other epigenetic modifications, the primary role of 5hmC is believed to involve transcriptional regulation, but the exact function of 5hmC and TET proteins in the brain is largely unknown. One hypothesis for brain enrichment of 5hmC is that key neural genes important for brain function are regulated by TET-mediated hydroxymethylation. Identification of such genes would be the first critical step to investigate the function of TET proteins and 5hmC in the brain.

1.5 Using the mouse to study TET1 function

As DNA methylation is a dynamic process, being able to manipulate the process and measure the effects at different times in development and under different physiological conditions is necessary to more completely understand the process. The mouse presents attractive advantages for being able to manipulate the DNA methylation process by either targeting genes involved in DNA methylation or by manipulating the environment.

2. Generation and Molecular Characterization of Tet1 Mutant (Tet1Δe4) Embryonic Stem Cells and Mice[1]

2.1 Introduction

The important role of transcriptional regulation in synaptic plasticity and memory formation has been well documented (Agranoff et al., 1967; Guan et al., 2002; Ramamoorthi et al., 2011). But how exactly the act of learning can trigger long-lasting changes in gene expression remains poorly understood. The genes which are triggered after learning or neuronal stimulation are termed activity-dependent genes. The regulation of activity-dependent neuronal gene expression plays a role in modulating synaptic activity and plasticity (Lubin et al., 2008; West et al., 2001). Several knowledge gaps still remain, however, in the cellular mechanisms for how learning and experience trigger gene expression important for synaptic remodeling.

One possible way could be through chromatin remodeling. There is some evidence to suggest that neurons employ this method as recent research demonstrated a role for histone acetylation and methylation in regulating memory formation (Guan et al., 2009; Gupta et al., 2010). DNA methylation has also been shown to change at genes implicated in memory formation after learning or neuronal stimulation (Guo et al.,

---

[1] Chapter 2 onward contain modified parts of a manuscript under review in Cell Reports. The authors were Aaron J Towers (myself), Xin-lei Li, Alexandra L Bey, Martine W Tremblay, Wenhao Zhang, Xinyu Cao, Xiaoming Wang, Ping Wang, Leeyup Chung, Lara J Duffney, Stephen K Siecinski, Sonia Xu, Yuna Kim, Xiangyin Kong, Wei Xie, Yong-hui Jiang. I wrote and was involved, at minimum, in the design and analysis of every experiment in the manuscript.

2011a; Lubin et al., 2008; Ma et al., 2009). The recent discovery of the TET proteins

presented a new opportunity to explore the role of demethylation in the regulation of

neural genes important for cognitive function.

One of the classic reverse genetics approaches to understanding gene function is

through gene targeting by homologous recombination. We decided to use a mouse gene

knockout approach to study the function of TET1 (described in this chapter) and TET3

(described in Chapter 4) in the epigenetic regulation of neural gene expression.

2.2 Methods

2.2.1 Generation of *Tet1*$^{\Delta e4-/-}$ mice

We created a floxed construct of *Tet1* exon 4 using the recombineering

(recombination-mediated genetic engineering) method described by Liu and colleagues

(Liu et al., 2003). The 129SvEv BAC clone (bMQ-258L12) covering the *Tet1* gene was first

identified *in silico* using the Ensembl mouse genome browser (www.ensembl.org) and

obtained from Geneservice (www.geneservice.co.uk) (Adams et al., 2005). A 13.7 kb

genomic fragment containing exon 4 of the *Tet1* gene from the BAC clone was retrieved

into a plasmid by electroporation. A neomycin (neo) selectable marker flanked by FRT

sites was inserted into the plasmid. Two loxP sites were inserted into the plasmid

flanking exon 4. The 5′ loxP was introduced at the genomic site of 62,304,376bp and the

3′ loxP/neo cassette at 62,300,243bp (www.genome .ucsc.edu; mm9). The finalized

plasmid was linearized with NotI and electroporated into R1 129/Sv mouse embryonic

stem cells (ESCs) at the Duke Neurotransgenic Laboratory. Neo-resistant colonies were picked after 7-8 days of selection and correctly recombinant clones were identified by Southern blot analysis using both a 5′ and 3′ probe. $Tet1^{e4+/f}$ ESCs were injected into blastocysts resulting in 9 high percentage chimeric male mice. These were bred with CMV-Cre females (Jackson Labs, Stock No. 006054, Bar Harbor, ME) to obtain germline transmission of the $Tet1$ deleted allele. $Tet1^{\Delta e4+/-}$ mice were backcrossed to C57BL/6J mice (Jackson Labs, Stock No. 000664) for more than 6 generations (N6) before molecular experiments and behavioral analysis unless otherwise noted. We segregated out a naturally occurring mutation in the $Disc1$ gene in the 129R1 mouse strain from which ESCs were derived during the backcrossing. Multiple cohorts of $Tet1^{\Delta e4-/-}$ mice and wild-type control (WT/$Tet1^{+/+}$) littermates were obtained from heterozygous breeding. Mice used for behavior tests were between 2-6 months of age. The age of mice used for molecular experiments varied and are indicated in the text. Mice were sex-matched for all experiments. All experiments were conducted with protocols approved by the Institutional Animal Care and Use Committee at Duke University.

2.2.2 Generation of Tet1$^{\Delta e4-/-}$ ESCs

We generated homozygous $Tet1^{\Delta e4-/-}$ ESCs through sequential targeting with our $Tet1$ construct. Briefly, heterozygous $Tet1^{e4+/f}$ ESCs were electroporated with a Flp plasmid containing puromycin resistance. Colonies were picked, expanded, and split in order to perform selection with puromycin and neomycin in parallel. We confirmed

excision of the neo cassette by PCR in those clones that survived puromycin selection

but were susceptible to neomycin. Neo(-) cells were electroporated with the original

construct again to generate homozygous *Tet1*e4f/f ESCs. After selection with neomycin,

homozygous *Tet1*e4f/f ESCs were identified by Southern blot using both a 5′ and 3′ probe.

Homozygous *Tet1*e4f/f ESCs were then electroporated with a Cre plasmid containing

puromycin resistance. After selection with puromycin, we identified *Tet1*Δe4-/- ESCs by

PCR confirmation of deleted exon 4.

2.2.3 PCR genotyping

DNA and cDNA genotyping was routinely performed by PCR using the primers

listed in Appendix A. The DNA primers of GF1 and GR1 are for wild-type (217bp) and

floxed (304bp), and GF2 and GR1 are for exon4 deletion (151bp). The cDNA primers CF1

and CR1 are for wild-type (246 bp), and CF2 and CR1 are for exon4 deletion (182 bp).

2.2.4 Preparation of nuclear protein and immunoblot analysis

Hippocampal tissue was dissected from whole brains and homogenized in

HEPES-buffered sucrose (0.32 M sucrose, 4 mM HEPES, pH 7.4) and centrifuged at 800 ×

g for 10 min at 4°C. The pellet including nuclear proteins was washed one time with 1 ×

PBS and then centrifuged at 2000 × g for 10 min at 4°C. The washed pellet was dissolved

in RIPA buffer and protein concentration was measured by a BCA kit (ThermoFisher

Scientific, Grand Island, NY). Equal amount of protein was separated by SDS-PAGE

and then transferred to PVDF membranes (Bio-Rad, Hercules, CA). After blocking the

membrane at room temperature for 1 hr in TRIS-buffered saline (pH 7.4, TBS) with 5%
non-fat milk, the blots were incubated with an anti-Tet1 antibody (cat. no. GTX125888,
GeneTex, Irvine, CA), anti-β-tubulin III antibody (cat. no. ab18207, Abcam, Cambridge,
MA), or anti-actin antibody (cat. no. sc-1615, Santa Cruz Biotechnology, Santa Cruz, CA)
at 4°C overnight. The blots were washed in TBS containing 0.1% Tween-20 (TBST) and
incubated with HRP-conjugated secondary antibodies for 60 min at room temperature.
Following 3 washes in TBST, the blots were incubated with ECL reagent (GE Healthcare
Life Sciences, Piscataway, NJ) and exposed to Kodak X-ray film (Rochester, NY).

2.2.5 RNA isolation, qRT-PCR, & 5′ Rapid Amplification of cDNA Ends (RACE)

RNA from tissue or ESCs was isolated using SV Total RNA Isolation System
(Promega) with DNase treatment. cDNA was prepared from 2ug of total RNA using
Superscript III Reverse Transcriptase and oligo(dT) primer (ThermoFisher). cDNA was
quantified by using SsoAdvanced Universal SYBR Green (Bio-rad) on a LightCycler 480
II (Roche) with a 10s denaturing step at 95ºC and 20s annealing step at 59ºC for 40 cycles.
All qPCR results were normalized to *Gapdh*. *Oxtr* isoform qRT-PCR results were
confirmed by using random primers to generate cDNA in a second round of testing. 5′
RACE products were generated from RNA using the 5′/3′ RACE kit, 2nd generation
(Roche). 5′ RACE products were gel separated, excised, cloned, and sequenced. All
primers used are listed in Appendix A.

2.2.6 5hmC dot blot

Control DNA was prepared by PCR amplifying a 100bp template with dNTPs

containing either cytosine (C), 5mC, or 5hmC. Primers and template are listed in

Appendix A. Purified DNA was spotted on an Amersham Hybond-N+ nylon membrane

(GE Healthcare). Dried spots were then crosslinked using the CL-1000 Ultraviolet

Crosslinker (UVP). Crosslinked membranes were blocked with 5% milk in TBST for 2

hours at room temperature (RT). Membranes were incubated overnight with the 5hmC

antibody (1:10000, Active Motif). The next day, membranes were washed 3 times for 15

minutes each with TBST. Washed membranes were incubated with an HRP-conjugated

secondary antibody in 5% milk in TBST for 2 hours at RT. Membranes were washed

again 3 times for 15 minutes each with TBST and visualized by Amersham ECL Prime

(GE Healthcare). Images were processed in ImageJ by subtracting background noise and

measuring integrated intensity of each dot with respect to 5hmC control. Intensities

were then normalized to Tet+/+ controls. Data is presented as the mean ± SEM.

2.2.7 Electroconvulsive shock

Electroconvulsive shock (ECS) was administered via alligator clamps applied

bilaterally to the ears of the mouse using a stimulator (Digitimer) and waveform

generator (Agilent Trueform 33500 series). The following optimized parameters were

used to generate a tonic-clonic seizure: 100 Hz, 0.2-ms pulse width, 18 mA stimulation

for 1.15 seconds. Seizures typically lasted less than 1 min and mice typically recovered in

30-90 seconds by self-righting. We treated sham mice by applying the clamps without administering the shock. Hippocampi from *Tet1*$^{\Delta e4-/-}$ and *Tet1*$^{+/+}$ mice (ECS and sham) were harvested 1.5-2 hours after stimulation, a timeframe when activity-dependent genes are known to be upregulated (Brakeman et al., 1997; Nibuya et al., 1995).

2.2.8 Whole transcriptome sequencing (RNA-seq)

RNA was isolated using Trizol Reagent (ThermoFisher) from ECS-treated hippocampal tissue from 3 *Tet1*$^{\Delta e4-/-}$ and 3 *Tet1*$^{+/+}$ mice and sent to the Genomic Analysis Facility at the Duke Center for Human Genome Variation for sequencing. RNA libraries were prepared and sequenced using the Illumina HiSeq 2000 machine as per manufacturer's protocols (Illumina, San Diego, CA). We used TopHat (version 2.0.9) to align reads to mouse genome (mm10) and Cufflinks (version 2.1.1) to find differentially expressed genes with default parameters. Only genes that had a status of "OK" were used in subsequent analyses (14601 out of 23360 genes). The list of significantly differentially expressed genes was defined at false discovery rate (FDR)<0.05. Gene Ontology analysis was performed using DAVID to investigate whether dysregulated genes were enriched in any particular category of genes.

2.2.9 Generation of neuronal activity-dependent gene list and gene list comparisons

A list of neuronal activity-dependent genes was generated by searching the literature and including genes that have been implicated in at least two independent studies (Appendix B) (Crepaldi et al., 2013; French et al., 2001; Kim et al., 2010; Lin et al.,

2008; Malik et al., 2014; Park et al., 2006; Spiegel et al., 2014). $Tet1^{\Delta e4-/-}$ dysregulated genes

were not significantly overlapped with known activity-dependent genes (number of

overlap genes=11, Odds ratio=1.477801, p=0.1932, Fisher's exact test). Our set of

dysregulated genes was compared to dysregulated genes reported in $Tet1$ exon 5

deficient ($\Delta e5$) hippocampus (Rudenko et al., 2013) $Tet1$ exon 11-13 deletion ($\Delta e11-13$)

neural progenitor cells (Zhang et al., 2013), $Tet1$-knockdown ESCs (Wu et al., 2011), and

$Tet1$ gene-trap primordial germ cells (Yamaguchi et al., 2012). Significant overlap was

determined by Fisher's exact test in R (http://www.r-project.org/), 14,601 genes were

used as background.

2.2.10 Targeted bisulfite sequencing

2ug DNA from each sample was bisulfite-converted using the EpiTect bisulfite

kit (Qiagen, Valencia, CA, USA) according to the manufacturer's protocol. Bisulfite-

converted DNA was amplified in 40 cycles using EpiMark Hot Start Taq DNA

polymerase (NEB). Specific primers and annealing temperatures are listed in Appendix

A. PCR fragments were recovered by gel excision and cloned into the pGEM-T easy

vector (Promega, Madison, WI, USA). Typically, 16 clones from each PCR product were

sequenced with M13R primers at Beckman Coulter Genomics (Danvers, MA, USA) or

EtonBio (Research Triangle Park, NC, USA). A minimum of 10 clones with a lower

threshold conversion rate of 90% of cytosines and lower threshold sequence identity of

14

90% were obtained for each sample. Sequencing reads were analyzed using the online platform BISMA (Rohde et al., 2010).

2.2.11 Chromatin immunoprecipitation assay

Histone methylation at the *Oxtr* locus in *Tet1*$^{\Delta e4-/-}$ and *Tet1*$^{+/+}$ mice were analyzed by chromatin immunoprecipitation (ChIP) PCR. The ChIP assay was performed using ChIP-IT Express magnetic kit (Active Motif) according to the manufacturer's instructions. Briefly, cerebrum (hippocampus, olfactory bulb and cerebral cortex) samples were collected from two *Tet1*$^{\Delta e4-/-}$ and *Tet1*$^{+/+}$ mice. Chromatin was prepared from isolated nuclei of the cerebrum after cross-linking by 1% formaldehyde for 10 min, followed by enzymatic digestions to 150-500bp sized fragments. For each immunoprecipitation reaction, 7 ug of chromatin was used for each specific antibody (1 ∘g) or species IgG isotype control. Antibodies were anti-rabbit Histone H3 trimethyl K4 (Abcam, ab8580) and anti-mouse monoclonal Histone H3 dimethyl K27 (Abcam, ab6002). Protein G magnetic beads were used for recovering chromatin immunoprecipitates consisting of the antibody-chromatin complexes. RNase- and proteinase K-treated DNA was purified using PCR purification columns (Promega). Recovered DNA was quantified by real-time PCR performed on the LightCycler480 instrument (Roche) using SsoAdvanced Universal SYBR green Supermix (Biorad). qPCR reactions were performed with the following cycling parameters: at 95ºC/5min followed by 40 cycles of 95ºC/30sec, 60ºC/60sec. ChIP-qPCR data was analyzed by the percent

15

input method. The ChIP signals were normalized by both background levels of GAPDH and total input chromatin, and were shown as percent input ± SEM. Statistical significance was determined by two-tailed t-test. All samples were measured in triplicate. All primers are listed in Appendix A.

2.2.12 Methylome generation & analysis

Whole genome bisulfite sequencing – 6ug DNA was mixed with 25ng lambda DNA and sonicated to 200-500bp. DNA was end-repaired, adenylated, and ligated to TrueSeq sequencing adaptors. DNA was purified by AMPure beads or DNA purification kit according to the DNA amount after each step. Library DNA was amplified by PfuTurbo Cx Hotstart DNA polymerase (Agilent, for bisulfite treated DNA libraries). 2% agarose gel was used to select 200-500bp DNA fragments after PCR amplification. Bisulfite treatment was performed using commercial kit (Zymo research, Cat. D5005). DNA was amplified and 200-500bp fragments were gel selected.

Reads were mapped to mm9 reference using BSMAP (Xi and Li, 2009) with parameters -r 0 -w 100 -v 0.1, adaptor sequence was removed with parameter -A. PCR duplicates were removed. Only samples with CT conversion rate greater than 99% was accepted. Then, 200bp bin was chosen as basic unit for analysis. Bins with CG coverage less than 5 times were removed leaving a total of 32,424 bins. Methylation ratio was calculated using methylated CG verses total CG for each bin.

Fisher's exact test was used to discover altered mCG in each 200bp bins with a threshold of *p*-value <0.05. Random regions were chosen from regions also covered by our methylome data. The *p*-value for the enrichment of *Tet1*-DMRs in genome was also calculated using fisher's exact test.

2.3 Results

2.3.1 Generation of a Novel Line of *Tet1* Mice and Embryonic Stem Cells

We decided to target exon 4 as it is the largest coding exon and deletion of exon 4 causes a frameshift leading to a premature stop codon and disruption of the catalytic domain[2] (Figure 1A & 1B). Design of the mouse occurred prior to the publication of the frameshift-inducing *Tet1* exon 5 deletion (Δe5) mice (Rudenko et al., 2013) and the enzymatically-targeted *Tet1* exon 11-13 deletion (Δe11-13) mice (Zhang et al., 2013).

We first identified recombination of the *Tet1* exon 4-floxed allele (*Tet1*[e4f]) in 129R1 ESCs (Figure 1C & 1D) and then obtained germline transmission of the *Tet1*[e4f] allele in a mixed 129R1 and C57BL/6J background (Figure 1E). *Tet1*[e4+/f] mice were bred to CMV-Cre mice to obtain germline transmission of the deleted exon 4 (*Tet1*[Δe4+/-]) (Figure 1E). RT-PCR confirmed exon 4 deletion from mRNA and western blot analysis showed deficiency of TET1 protein from *Tet1*[Δe4-/-] mouse hippocampus (Figure 1F & 2A). The hippocampus was initially studied as 5hmc is enriched in the hippocampus (Bachman et

---

[2] Visiting student Xin-lei Li designed and created the *Tet1* targeting construct.

al., 2014; Globisch et al., 2010). In addition, human clinical cases have suggested an

important role for the hippocampus in memory formation (Scoville and Milner, 1957).
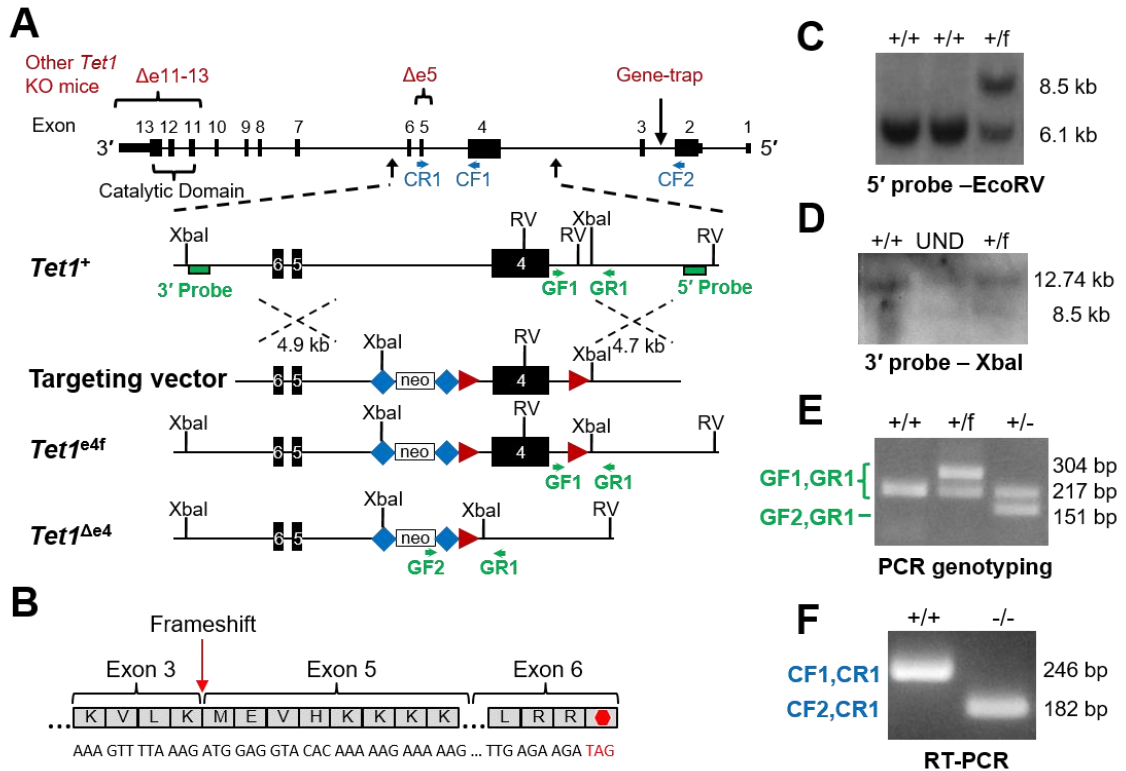
Figure 1: Generation of *Tet1* Mutant (*Tet1*^{Δe4}) Mice

(A) Gene targeting strategy for generating *Tet1*^{e4f} and *Tet1*^{Δe4} mice. *LoxP* sites (red arrowheads), *FRT* sites (blue diamonds), and primers for RT-PCR (blue arrows) and genotyping (green arrows) are indicated. Mutations of other published *Tet1* mutant mice are diagramed [Δe11-13, (Zhang et al., 2013); Δe5, (Dawlaty et al., 2011); Gene-trap, (Yamaguchi et al., 2012)]. (B) Diagram showing deletion of exon 4 leads to a frameshift causing a premature stop codon (stop sign) to appear in exon 6. Amino acid abbreviations with DNA sequence are indicated. (C) DNA Southern blot confirmation of *Tet1*^{e4f} (+/f) embryonic stem cells (ESCs) after EcoRV digestion using the 5' probe. +=wild-type allelle, f=floxed allele (D) DNA Southern blot confirmation of targeted ESCs after XbaI digestion using the 3' probe. UND=undetermined. (E) PCR genotyping with the indicated primers (green) to confirm germline transmission of the Tet1^{e4f} allele (+/f) and deletion of exon4 (+/-) after breeding with a CMV-Cre

mouse. (F) RT-PCR with the indicated primers (blue) to confirm absence of exon4 in Tet1$^{\Delta e4-/-}$ mice.

We did not, however, detect a significant difference in levels of 5hmC in the

hippocampus of *Tet1*$^{\Delta e4-/-}$ adult mice by DNA dot blot analysis (Figure 2B). We

hypothesized that upregulation of *Tet2* and/or *Tet3* might compensate for the lack of

Tet1 in *Tet1*$^{\Delta e4-/-}$ adult mouse brains, but found no difference in their expression (Figure

2C).
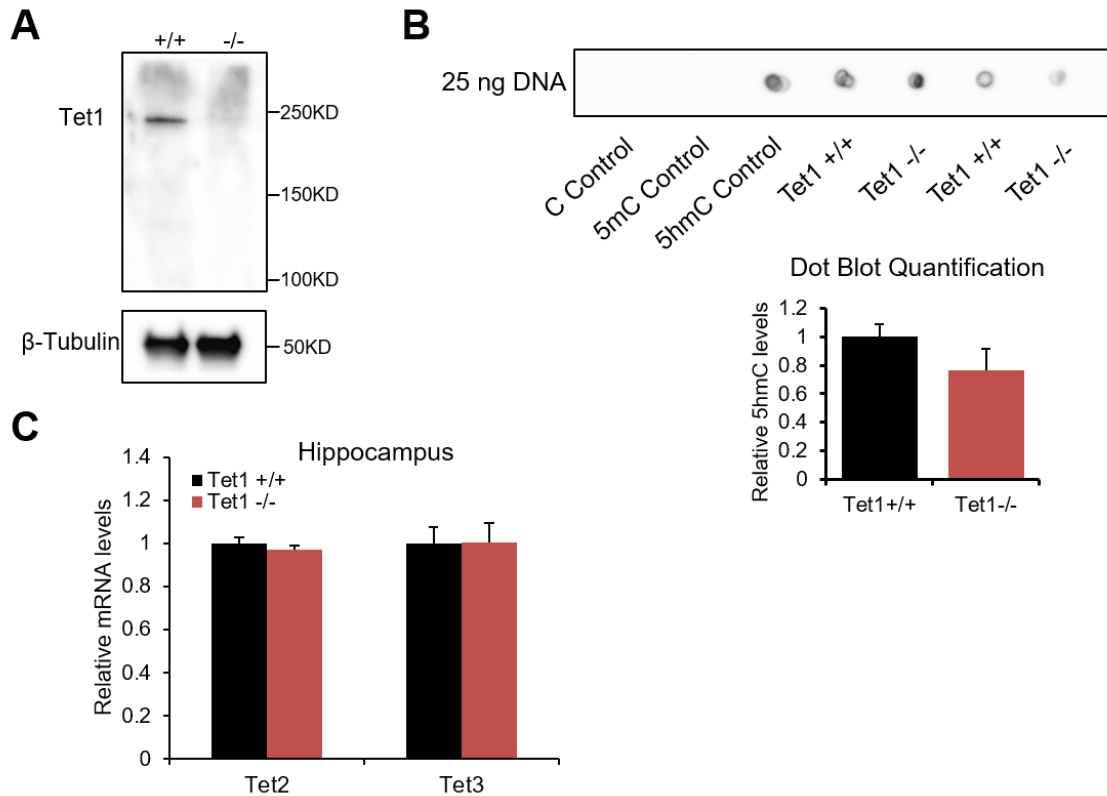
Figure 2: Molecular Characterization of *Tet1* Mutant (*Tet1*$^{\Delta e4}$) hippocampus

(A) Western blot analysis with a TET1 antibody confirmed deficiency of TET1 protein from *Tet1*$^{\Delta e4-/-}$ (-/-) hippocampus. β-tubulin used as loading control. (B) No significant difference detected in hippocampal 5hmC levels between *Tet1*$^{\Delta e4-/-}$ and *Tet1*$^{+/+}$ mice as measured by DNA dot blot using an anti-5hmC antibody. Representative dot blot

shown. Control DNA was prepared by PCR amplifying a 100bp template with dNTPs containing either cytosine (C), 5mC, or 5hmC. n=5/group (*p*=0.21, two-tailed t-test). Data are presented as mean ± SEM. **(C)** *Tet2* and *Tet3* were not differentially expressed in *Tet1*$^{\Delta e4-/-}$ hippocampus.

We also generated homozygous *Tet1*$^{\Delta e4-/-}$ ESCs by sequentially targeting the second allele of *Tet1*$^{e4+/f}$ ESCs (Figure 3A). Correct recombination at the second allele was confirmed by Southern blot using a 5' and 3' probe (Figure 3B & 3C). Finally, *Tet1*$^{e4f/f}$ ESCs were electroporated with a Cre plasmid to generate *Tet1*$^{\Delta e4-/-}$ ESCs (Figure 3D).
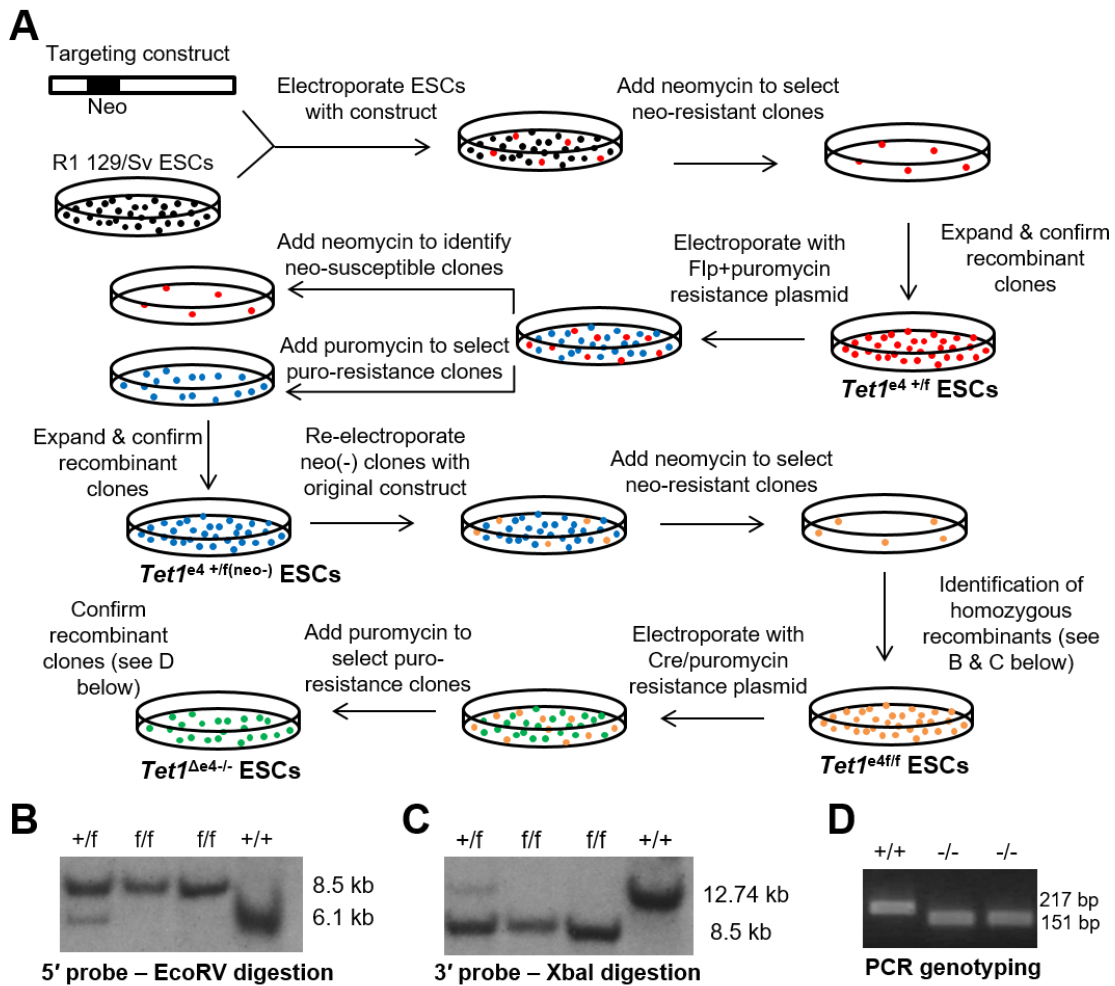
Figure 3: Generation of *Tet1*$^{\Delta e4-/-}$ embryonic stem cells (ESCs)

(A) Workflow for generating homozygous *Tet1*$^{\Delta e4-/-}$ ESCs through sequential targeting. (B) DNA Southern blot confirmation of *Tet1*$^{e4f/f}$ (f/f) ESCs after EcoRV digestion using the 5' probe. +=wild-type allelle, f=floxed allele (C) DNA Southern blot confirmation of targeted ESCs after XbaI digestion using the 3' probe. (D) PCR genotyping confirmation of exon4 deletion (-/-) after electroporation with Cre plasmid.

We first confirmed that *Tet1*$^{\Delta e4-/-}$ ESCs were depleted of TET1 protein by western blot

(Figure 4A). *Tet1*$^{\Delta e4-/-}$ ESCs were viable with no apparent abnormality in cellular

morphology but displayed a global reduction of 5hmC, in contrast to hippocampal

5hmC levels (Figure 4B). While *Tet1* and *Tet2* are highly expressed in ESCs, *Tet3* is not

(Szwagierczak et al., 2010; Wossidlo et al., 2011). Accordingly, we found *Tet2* but not

Tet3 upregulated in *Tet1*$^{\Delta e4-/-}$ ESCs (Figure 4C), suggesting a compensatory mechanism of

Tet2 in response to deficiency of *Tet1* in ESCs.
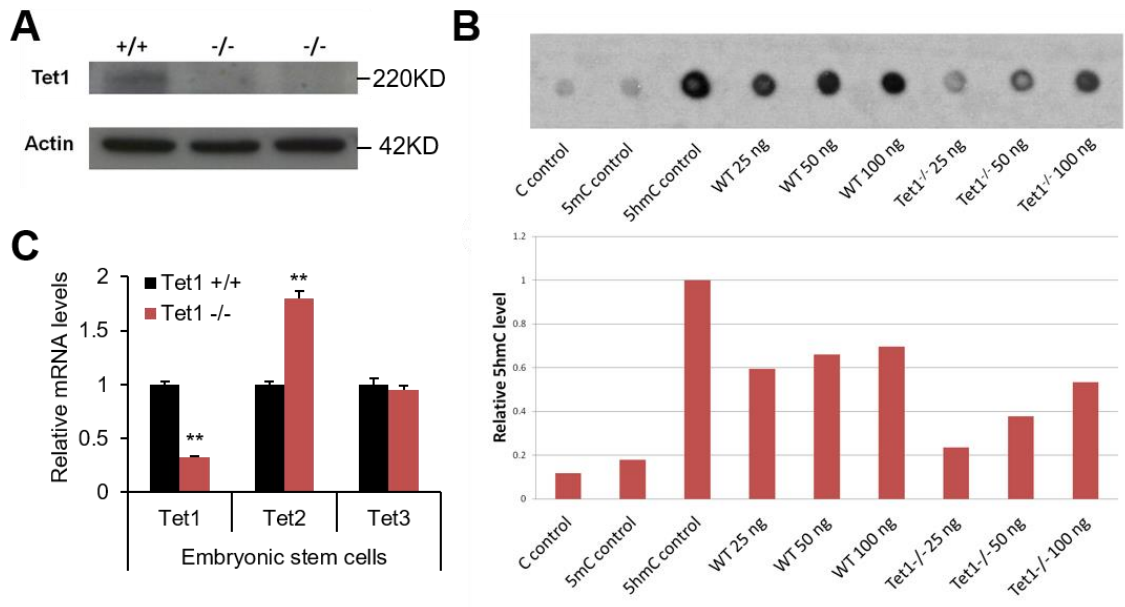
Figure 4: Molecular confirmation of *Tet1* depletion in *Tet1*$^{\Delta e4-/-}$ ESCs

(A) Western blot analysis with a TET1 antibody confirmed deficiency of TET1 protein from *Tet1*$^{\Delta e4-/-}$ (-/-) ESCs. β-actin used as loading control. (B) Visual difference observed

in 5hmC levels between *Tet1*^{Δe4-/-} and wild-type ESCs as measured by DNA dot blot using an anti-5hmC antibody. Representative dot blot shown (upper panel) and quantified (lower panel). Control DNA was prepared by PCR amplifying a 100bp template with dNTPs containing either cytosine (C), 5mC, or 5hmC. (C) *Tet1* and *Tet2* but not *Tet3* were differentially expressed in *Tet1*^{Δe4-/-} ESCs. **, *p*<0.005, two-tailed t-test. Data are presented as mean ± SEM.

Tet1^{Δe4-/-} mice displayed partial perinatal lethality and a deviation from expected Mendelian ratio of genotypes at weaning age, indicating a role for TET1 in early development (Figure 5A). The surviving *Tet1*^{Δe4-/-} mice showed a mild degree of growth retardation, as *Tet1*^{Δe4-/-} mice weighed significantly less than *Tet1*^{+/+} littermates at weaning which persisted into adulthood (Figure 5B). We also occasionally observed a variety of craniofacial abnormalities in *Tet1*^{Δe4-/-} mice (~10-15%), including midface hypoplasia mostly observed in mice on a mixed background and hydrocephalus mostly observed in the C57BL/6J backcrossed mice (Figure 5C). Overall cerebral morphology appeared normal by Nissl staining of 5 week-old *Tet1*^{Δe4-/-} and *Tet1*^{+/+} littermates (Figure 5D). *Tet1*^{Δe4-/-} mice did not have any apparent abnormal behavior in their home cage.
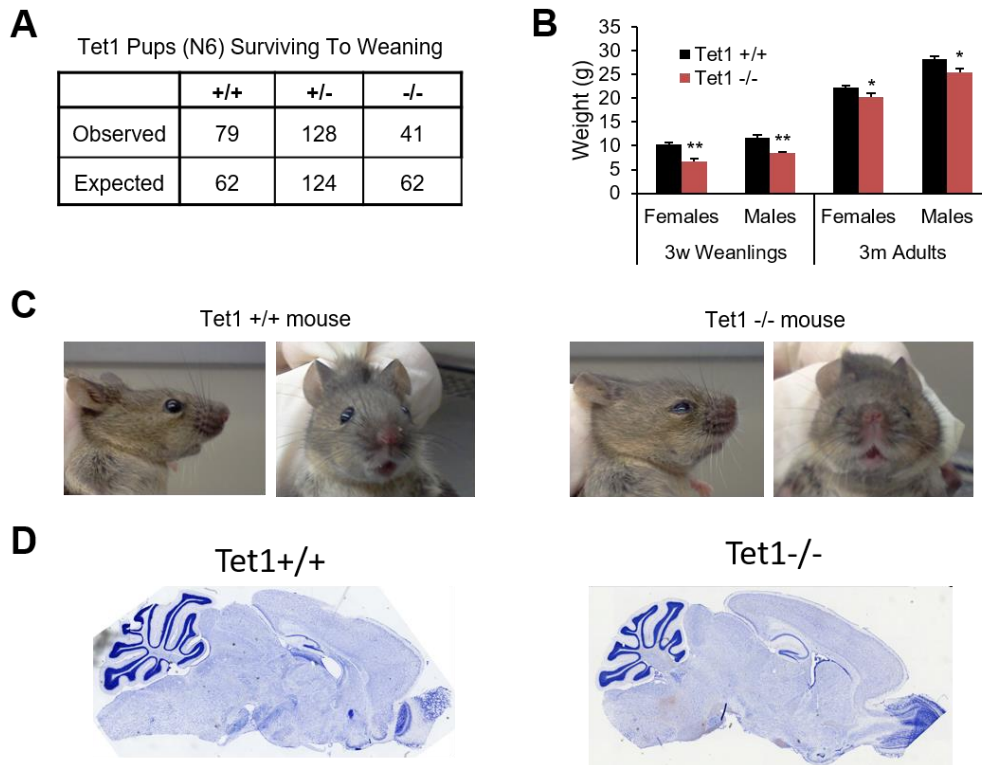
A

Tet1 Pups (N6) Surviving To Weaning

	+/+	+/-	-/-
Observed	79	128	41
Expected	62	124	62

B

C

Tet1 +/+ mouse   Tet1 -/- mouse

D

Tet1+/+   Tet1-/-

Figure 5: *Tet1*$^{\Delta e4-/-}$ **mice displayed partial perinatal lethality and mild growth retardation**

(A) Genotype ratio at weaning: Fewer *Tet1*$^{\Delta e4-/-}$ mice survived to weaning [x^2 (2, N=248)=11.903, *p*<0.001]. (B) *Tet1*$^{\Delta e4-/-}$ mice have reduced weight at weaning (3w) and adulthood (n=4-12/group at weaning and n=8-19/group at adult age). ∗, *p*<0.05; ∗∗, *p*<0.005, two-tailed t-test. Data are presented as mean ± SEM. (C) Facial profiles showing the midface hypoplasia in a *Tet1*$^{\Delta e4-/-}$ mouse compared to *Tet1*$^{+/+}$ littermate. (D) Nissl staining revealed normal cerebral morphology of 5 week-old *Tet1*$^{\Delta e4-/-}$ and *Tet1*$^{+/+}$ mice.

2.3.2 Transcriptional Dysregulation of Neural Genes in *Tet1*$^{\Delta e4}$ Mutant Mice

In order to test the role of TET proteins in activity-induced gene expression, we first optimized the electroconvulsive shock (ECS) paradigm to consistently produce a tonic-clonic seizure. ECS has been demonstrated as a valid paradigm to induce neural

activity (Cole et al., 1990). As both *de novo* methylation and demethylation has been to

occur after brain stimulation, including ECS, we hypothesized that TET1 was

responsible for the demethylation (Guo et al., 2011a). We then validated that activity-

dependent expression was stimulated by confirming upregulation of *Bdnf* and *Homer1a*

in the hippocampus 2 hours after ECS (Figure 6A) as previously reported (Brakeman et

al., 1997; Nibuya et al., 1995).
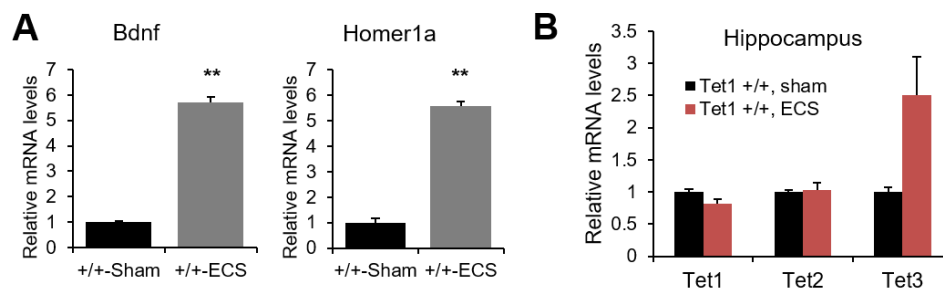
Figure 6: Validation of electroconvulsive shock paradigm

(A) Confirmation of upregulation of activity-dependent genes (*Bdnf* & *Homer1a*) in hippocampus after electroconvulsive stimulation. n=4/group, **, $p<0.005$, two-tailed t-test. (B) *Tet1* showed a trend for downregulation ($p=0.09$) and *Tet3* showed a trend for upregulation ($p=0.06$) 2 hours after ECS. n=3/group, two-tailed t-test. All data are presented as mean ± SEM.

Next we tested whether hippocampal expression of *Tet* genes was activity-dependent

and found *Tet1* downregulated but *Tet3* upregulated in *Tet1*^{+/+} mice after ECS, although

neither reached significance (Figure 6B). To examine the effect of TET1 deletion on

activity-dependent gene regulation, we isolated hippocampal RNA from 3 pairs of

Tet1[Δe4-/-] and their *Tet1*^{+/+} littermates two hours after ECS. RNA libraries were prepared

and sequenced, resulting in reads of high sequence alignment and depth (Figure 7A).

A

Genotype	Read pairs	Percentage aligned	Percentage exonic sequence	Depth
Tet1-/-	58,671,498	85.14%	78.05%	166.5
Tet1-/-	41,595,514	84.30%	78.45%	116.9
Tet1-/-	78,639,428	84.13%	78.29%	220.5
Tet1+/+	58,033,659	86.12%	79.82%	166.6
Tet1+/+	48,063,891	85.25%	79.40%	136.6
Tet1+/+	63,478,549	85.87%	79.16%	181.7

B
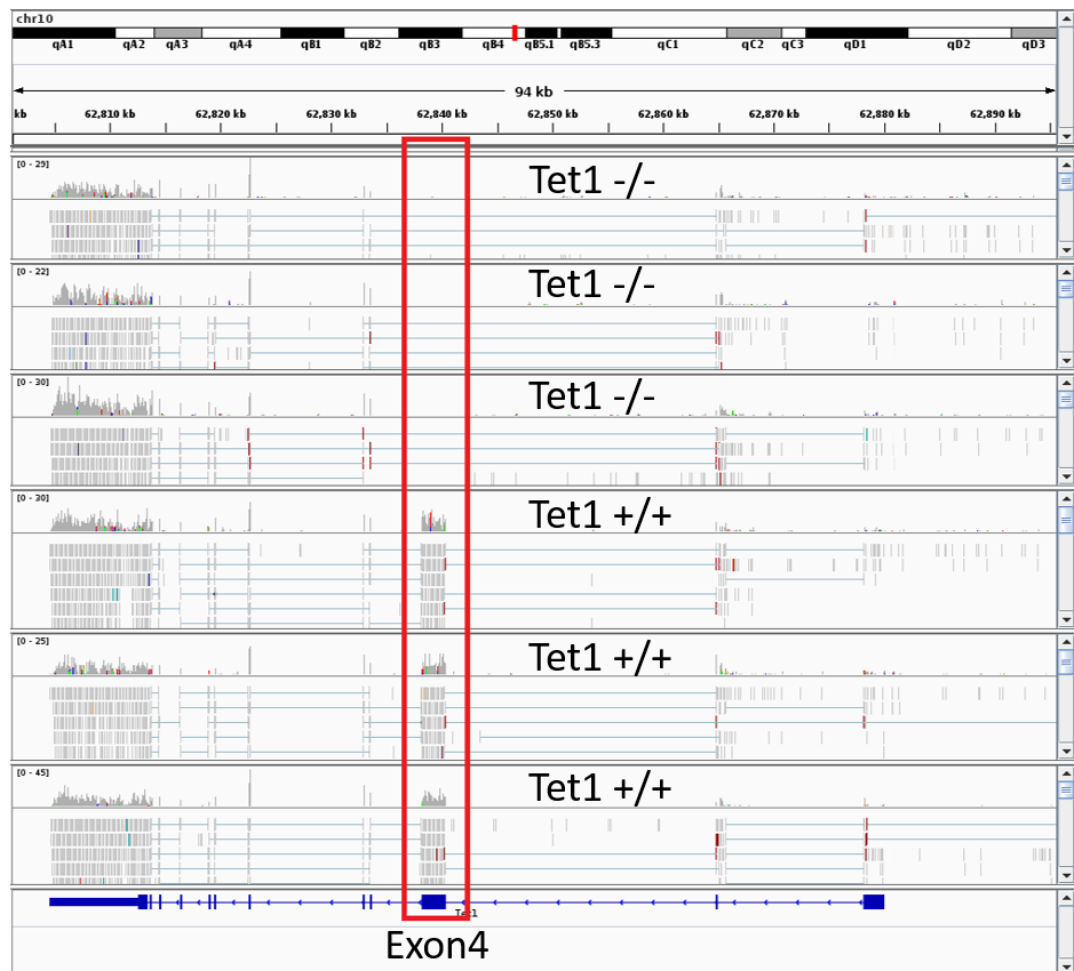
Figure 7: RNA-seq quality control

(A) Table showing high alignment and read depth obtained from RNA-seq experiment. (B) RNA-seq data mapped to *Tet1* showed absence of exon 4 reads (red rectangle) but no overall reduction of *Tet1* expression.

We first confirmed that Tet1 exon 4 reads were absent from the data but found other

exons of *Tet1* were not reduced (Figure 7B). Overall *Tet1* expression was also not

reduced in sham-treated hippocampus measured by qPCR, indicating that Tet1 RNA

lacking exon 4 is stable in the hippocampus (Figure 8B). By comparing RNA-seq

expression profiles from the *Tet1^{Δe4-/-}* and *Tet1^{+/+}* mice, we discovered that 34 genes were

significantly upregulated and 184 genes were downregulated in *Tet1^{Δe4-/-}* mice (Figure 8A

& Appendix B), suggesting a primary role for TET1 in activating gene expression. In

order to test the hypothesis that TET1 is responsible for regulating activity-dependent

genes, we cataloged a dataset of activity-dependent genes based on a literature review

(Appendix B). While there was not significant enrichment for activity-dependent genes

disrupted in *Tet1*-deficient mice, dysregulation of several activity-dependent genes were

identified including the master memory gene regulator, *Npas4* (Figure 8A)

(Ramamoorthi et al., 2011). *Npas4* downregulation was observed by qRT-PCR in the

hippocampus of sham-treated *Tet1^{Δe4-/-}* mice as well (Figure 8B). Gene Ontology analyses

of the dysregulated genes detected a significant enrichment for genes involved in the

extracellular region/matrix/space (Figure 8C). Interestingly, RNA-seq revealed

downregulation of *Oxtr*, the receptor which binds oxytocin. *Oxtr* downregulation was

also observed in untreated *Tet1^{Δe4-/-}* mice but not in *Tet1^{Δe4-/-}* ESCs (Figure 8D).
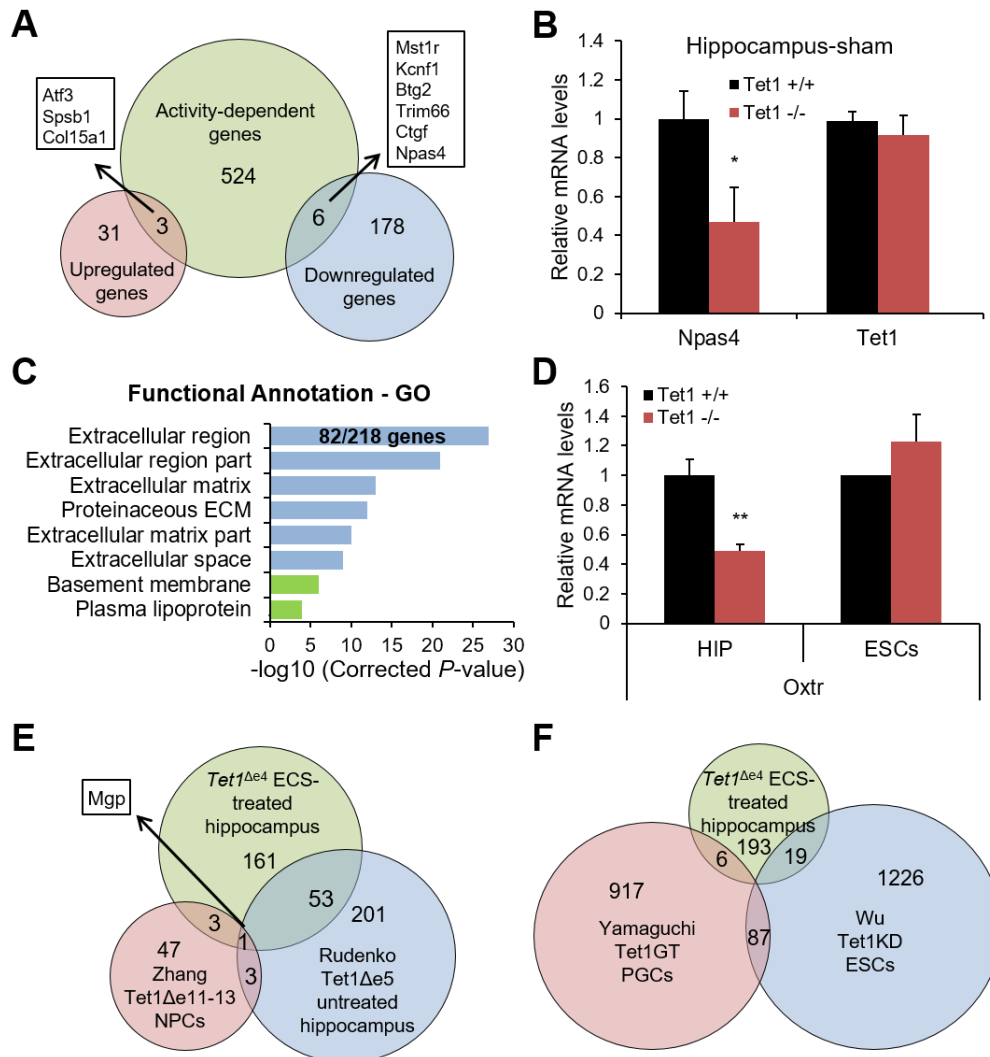
Figure 8: *Tet1* deficiency resulted in altered hippocampal expression of key neural genes, including *Npas4* and *Oxtr*

(A) RNA-seq transcriptional profiling of hippocampus 2 hours after ECS, revealed 184 downregulated genes and 34 upregulated genes (false discovery rate < 0.05) in *Tet1*^Δe4-/- mice (n=3/group). Dysregulated activity-dependent genes are indicated (boxes). (B) *Npas4* but not Tet1 was downregulated in hippocampus from *Tet1*^Δe4-/- mice (n=6/group) *p*=0.017, two-tailed t-test. (C) Gene ontology (cellular component classification) analysis revealed an enrichment of extracellular dysregulated genes (Benjamini corrected *p*-values indicated). (D) *Oxtr* was downregulated in hippocampus from *Tet1*^Δe4-/- mice but not in *Tet1*^Δe4-/- ESCs. Oxtr_ABEFG primers used. **, *p*<0.005, two-tailed t-test. (E) Significant overlap of ECS-treated *Tet1*^Δe4-/- hippocampal dysregulated genes with dysregulated genes from neural progenitor

cells (NPCs) of $Tet1^{\Delta e11\text{-}13}$ (OR=7.66, p=0.003) and untreated hippocampus of $Tet1^{\Delta e5}$ mice (OR=39.07, p=2.3E-57). (F) No significant overlap of ECS-treated $Tet1^{\Delta e4\text{-}/\text{-}}$ hippocampal dysregulated genes with dysregulated genes from $Tet1^{GeneTrap}$ primordial germ cells (PGCs) or Tet1-knockdown ESCs. *, p<0.05; **, p<0.005. All data are presented as mean ± SEM.

We compared our list of $Tet1^{\Delta e4\text{-}/\text{-}}$ dysregulated genes from ECS-treated hippocampus to the dysregulated genes reported in *Tet1* exon 5 deficient (Δe5) hippocampus (Rudenko et al., 2013) and *Tet1* exon 11-13 deletion (Δe11-13) neural progenitor cells (Zhang et al., 2013) and found significant overlap (Figure 8E). When we compared dysregulated genes from *Tet1*-knockdown ESCs (Wu et al., 2011) or *Tet1* gene-trap (Gt) primordial germ cells (Yamaguchi et al., 2012) however, we did not observe a significant overlap (Figure 8F). These comparisons indicate TET1 differentially regulates sets of genes in a tissue and development dependent manner.

2.3.3 DNA Hypermethylation of Neural Genes in $Tet1^{\Delta e4\text{-}/\text{-}}$ Mice

Based on the role of TET1 in DNA demethylation, we wanted to examine if the downregulation of *Npas4* and *Oxtr* were associated with increased CpG island DNA methylation. One of the traditional methods for measuring site-specific DNA methylation is bisulfite sequencing. It involves treating DNA with sodium bisulfite to convert unmodified cytosines to uracils, which are read as thymines in the sequencing reaction (Frommer et al., 1992). It was recently discovered that bisulfite sequencing cannot distinguish 5mC from 5hmC, and unmodified cytosine, 5fC and 5caC are all read as thymines (Booth et al., 2012; Huang et al., 2010). As TET1 converts 5mC to 5hmC, we

28

predicted that any hypermethylation detected by bisulfite sequencing would be an accumulation of 5mC and not 5hmC.

We bisulfite sequenced the CpG island associated with the *Npas4* promoter and found it hypermethylated in *Tet1^{Δe4-/-}* hippocampus (27.2±3.1%) compared to *Tet1^{+/+}* (8.1±0.6%) (Figure 9A). This is in line with previous data supporting a role for TET1 in
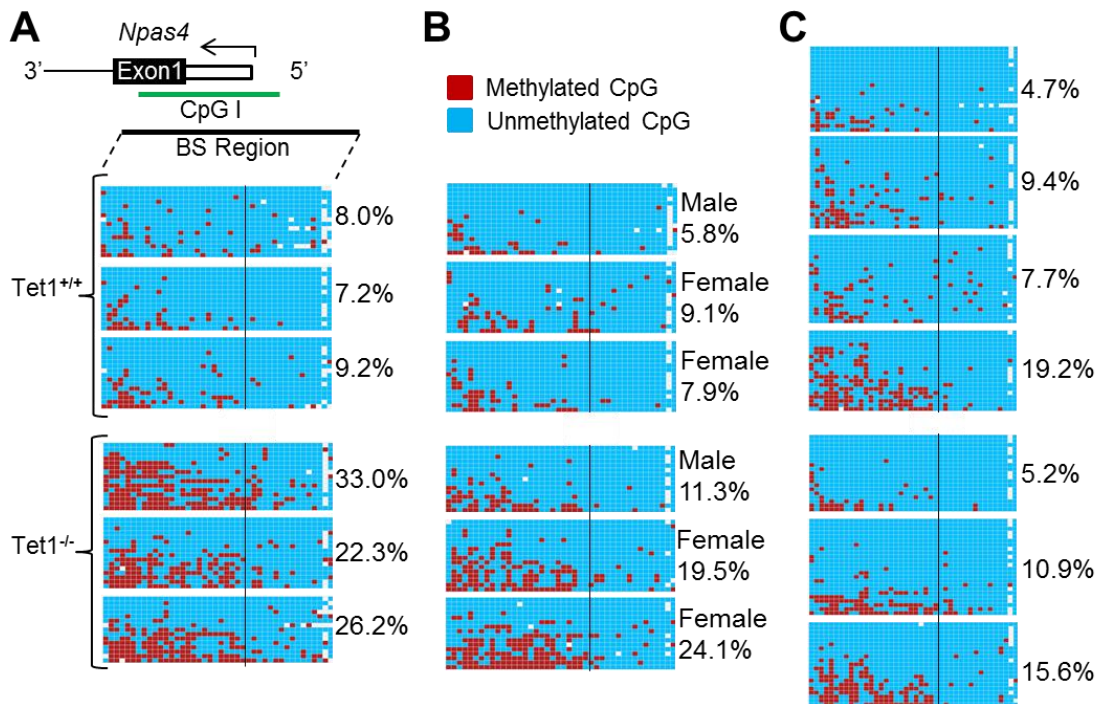
Figure 9: *Tet1^{Δe4-/-}* Mice Show Hypermethylation of the *Npas4* CpG Island

(A) Diagram of *Npas4* promoter (coding regions are shaded), associated CpG island (CpG I, green bar), and bisulfite-sequencing (BS) region (black bar). *Npas4* was hypermethylated in hippocampus of female 5-9 week old *Tet1^{Δe4-/-}* mice (n=3/group; *p*=0.004, two-tailed t-test). Black line indicates divide between the 5' upstream region and the beginning of the 5' UTR. Blue squares represent unmethylated CpG dinucleotides, red squares represent methylated CpGs, and white squares were undetermined. Percent methylation indicated. (B) *Npas4* was hypermethylated in hippocampus of 17-35 week old *Tet1^{Δe4-/-}* mice on a mixed C57Bl/6J & 129/Sv background (n=3/group; *p*=0.05, two-tailed t-test). (C) *Npas4* methylation not different in 1-year old mice from behavior cohort.

29

regulating the methylation state of *Npas4* (Rudenko et al., 2013). As the methylation

difference was more striking in knockout mice from a mixed background in the

Rudenko study, we also analyzed the same region in 17-35 week old F1 mice on a

C57Bl/6J & 129/Sv mixed background and found it hypermethylated but to a lesser

extent in *Tet1*$^{\Delta e4-/-}$ hippocampus (18.3±3.7%) compared to (7.6±1.0%) (Figure 9B). While

we did not have enough samples to perform a statistical analysis, the pair of male mice

from the mixed background appeared to have lower overall methylation compared to

females (Figure 9B). In order to see if age or experience had any effect on *Npas4*

methylation, we analyzed 1-year old mice that had been through a battery of behavioral

tests and surprisingly did not observe a difference in genotype (Figure 9C). In every case

when we examined *Npas4* methylation, the majority of the methylated CpGs were found

in the exonic sequence including the 5′ UTR and the first coding exon compared to the 5′

upstream sequence (Figure 9A-C).

The mouse *Oxtr* gene contains 4 exons (Kubota et al., 1996) including a 5′ UTR

which encompasses exons 1, 2, and part of exon 3 and overlaps with an 859bp CpG

island (Figure 10A). Interestingly, the human CpG island spans 2319bp extending to the

more 5′ region of *OXTR* (Figure 10A). The mouse also has high GC content in the

homologous region indicating the difference for CpG island length is likely due to

different computational programs used. We analyzed 3 potential regulatory elements

(BS1-3) of *Oxtr* to identify if the reduced hippocampal expression of *Oxtr* was associated

with DNA hypermethylation (Figure 10A). We first performed bisulfite sequencing on BS1, a region mostly upstream of the 5′ *Oxtr* transcription start site (TSS). Consistent with the association of low methylation in active promoter regions, BS1 was mostly unmethylated and comparable between *Tet1*$^{+/+}$ (8.1±0.5%) and *Tet1*$^{\Delta e4-/-}$ (9.9±0.7%) mice (Figure 10A).

We next examined BS2, a region just downstream of the most 5′ TSS. A portion of this region has been shown in humans to have activity for an alternative promoter that is suppressed by DNA methylation (region MT2 in Figure 10A)(Kusui et al., 2001). *Tet1*$^{\Delta e4-/-}$ mice had mild but significantly increased DNA methylation (10.7±1.7%) in BS2 compared to their *Tet1*$^{+/+}$ littermates (3.3±0.9%) (Figure 10A). The differential methylation in the BS2 region appears to be driven by only a few CpGs, including the CpG (BS2-CpG12) that aligns to the human CpG -924 which was hypermethylated in a small sample of autistic individuals (Gregory et al., 2009). BS2-CpG12 was methylated (16.4±5.7%) in *Tet1*$^{\Delta e4-/-}$ mice but always completely unmethylated in *Tet1*$^{+/+}$ littermates (Figure 10A).

Chromatin immunoprecipitation (ChIP) data from the Encode project (Consortium, 2012) indicated that the CpG island spanning *Oxtr* exon 3 includes a potential regulatory element. Strikingly, nearly every CpG assessed in this region (BS3) was hypermethylated in *Tet1*$^{\Delta e4-/-}$ mice (64.3±4.1%) compared to their *Tet1*$^{+/+}$ littermates (17.6±1.2%) (Figure 10A). To test for a gene dosage effect of TET1 on *Oxtr* DNA
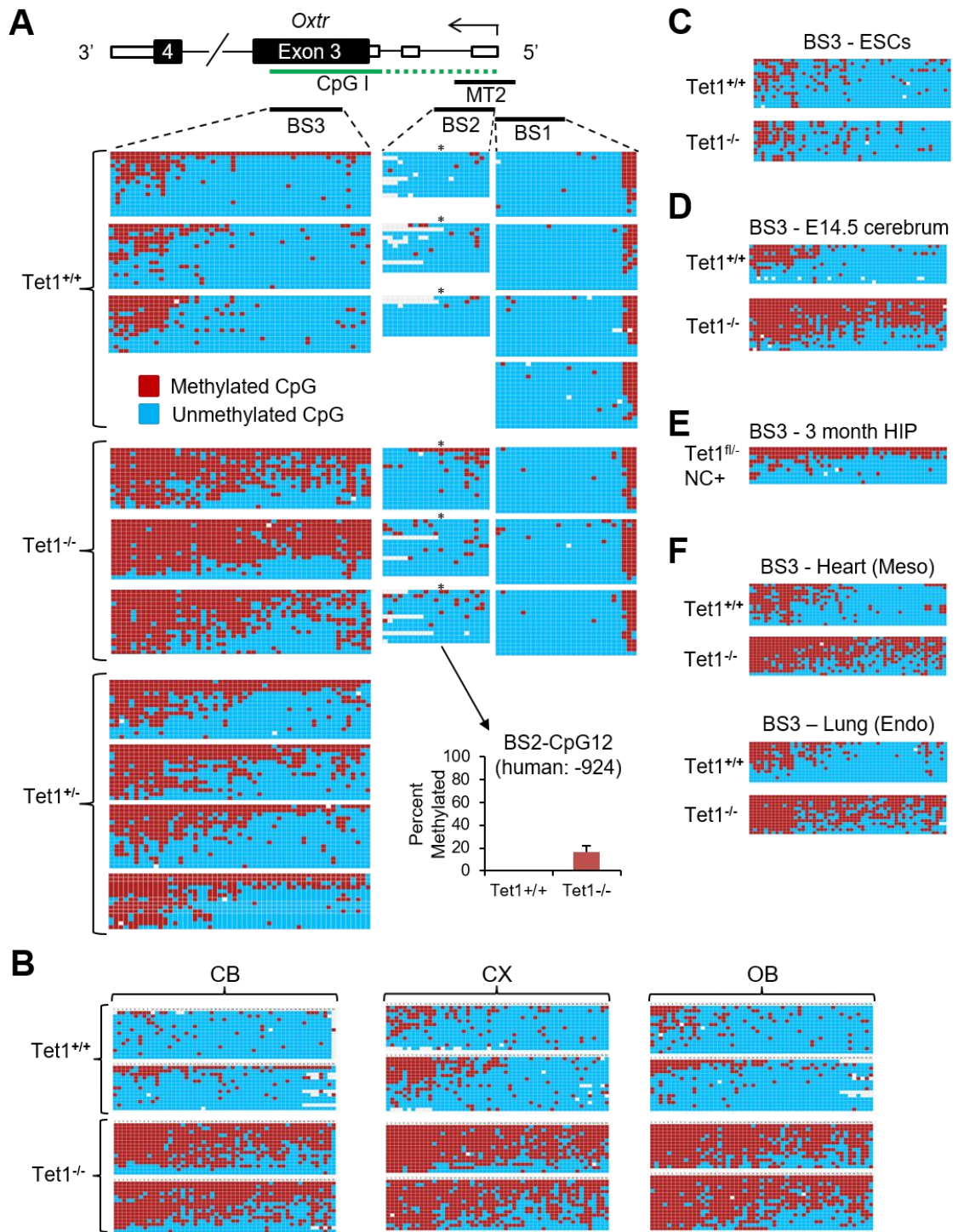
Figure 10: *Tet1*[Δe4-/-] **Mice Show Hypermethylation of the** *Oxtr* **CpG Island in early development which persists into adulthood**

(A) Diagram of *Oxtr* gene structure (coding regions are shaded), CpG island (green bar), and bisulfite-sequencing regions (BS, black bars). The human CpG island spans 2319bp extending to the more 5′ region of *OXTR* as indicated by a dotted green line. Human promoter MT2 region (Kusui et al., 2001) is indicated (black bar). BS2 & BS3 were hypermethylated but not BS1 in hippocampus of adult *Tet1*$^{\Delta e4-/-}$ mice (n=3/group; BS2, *p*=0.02; BS3, *p*=0.0004; two-tailed t-test). BS3 showed intermediate levels of hypermethylation in *Tet1*$^{\Delta e4+/-}$ mice (n=3-4/group; *p*=0.0019, two-tailed t-test). The mouse CpG aligning to the human *OXTR* CpG -924 is indicated by asterisks and methylation levels are plotted in the bar graph. Data are presented as mean ± SEM. (B) *Oxtr* BS3 is hypermethylated in cerebellum (CB), cortex (CX), olfactory bulb (OB) of adult *Tet1*$^{\Delta e4-/-}$ mice. (C) *Oxtr* BS3 was not hypermethylated in *Tet1*$^{\Delta e4-/-}$ ESCs. (D) *Oxtr* BS3 was hypermethylated in E14.5 neocortex of *Tet1*$^{\Delta e4-/-}$ mice. (E) *Oxtr* BS3 was 33.5% methylated in the hippocampus (HIP) of a *Tet1*$^{e4\ fl/-}$ mouse with Nestin-cre (NC) (F) *Oxtr* BS3 was hypermethylated in tissues from the other two germ layers (Meso=mesoderm, Endo=endoderm).

methylation, we examined the BS3 region in *Tet1*$^{\Delta e4+/-}$ mice and found an intermediate

level of methylation (42±3.3%) (Figure 10A). To examine tissue specificity of *Oxtr* CpG

island hypermethylation, we examined multiple brain regions and found similar levels

of hypermethylation in each *Tet1*$^{\Delta e4-/-}$ adult mouse brain region investigated (Figure 10B).

To test if the correlation between *Oxtr* gene expression and DNA methylation extended

to ESCs, we examined the level of BS3 methylation in ESCs. Consistent with our findings

that *Oxtr* was not differentially expressed in ESCs, BS3 methylation in *Tet1*$^{\Delta e4-/-}$ ESCs was

not different from *Tet1*$^{+/+}$ ESCs (Figure 10C). These data suggest that DNA methylation

of BS2 and BS3 regions is associated with altered *Oxtr* expression. To understand at

which time during development the *Oxtr* CpG island becomes hypermethylated, we

examined BS3 in embryonic brains and found a similar level of hypermethylation in

cerebrum as early as embryonic day 14.5 (E14.5) (Figure 10D). We next examined BS3 in

the hippocampus of a 3-month old $Tet1^{e4\,fl/-}$ mouse expressing Cre recombinase driven by

a Nestin promoter. This Cre is expressed in the central and peripheral nervous system

by embryonic day 11 (E11) (Tronche et al., 1999). Interestingly, this mouse which had

one $Tet1$ deleted allele and one floxed allele had a similar methylation pattern and level

to $Tet1$ heterozygote mice (33.5%), indicating that deleting $Tet1$ in the brain after E11 had

no effect on $Oxtr$ methylation at BS3 (Figure 10E). We speculated that if the

hypermethylation occurred prior to gastrulation, we would also find adult tissues from

the other two primary germ layers to be hypermethylated. Indeed, we observed BS3

hypermethylation in tissue from mesoderm (heart) and endoderm (lung) in adult $Tet1^{\Delta e4-/-}$

mice (Figure 10F). As BS3 methylation is similar between WT ESCs and E14.5 cerebrum

in $Tet1^{+/+}$ mice, these data suggest a critical window in early development for a dose

dependent TET1-mediated maintenance of $Oxtr$ methylation.

The TET1 protein contains a CXXC domain which preferentially binds to

unmethylated CpG rich sequences (Zhang et al., 2010). To investigate the genome-wide

effect of TET1-defiency on DNA methylation in the brain, we performed whole-genome

bisulfite sequencing in adult cortex tissue[3]. We identified 666 differentially methylated

regions ($Tet1$-DMRs) between $Tet1^{\Delta e4-/-}$ and $Tet1^{+/+}$, with an enrichment for

hypermethylated $Tet1$-DMRs (522 hypermethylated vs 144 hypomethylated). We next

wanted to understand whether these hypermethylated $Tet1$-DMRs were distributed

---

[3] Methylome data were generated and analyzed in the laboratory of Wei Xie at Tsinghua University.

randomly or enriched in specific genomic regions. We discovered an enrichment of

hypermethylated *Tet1*-DMRs in CpG islands (380 CpG islands ΔmCG ≥20%), including

the *Oxtr* CpG island (Figure 11, 1.2 fold observed/random, *p*=1.25e-07). Stratifying CpG

islands by location (promoter vs intragenic), revealed *Tet1*-DMRs preferentially enriched

in intragenic CpG islands (Figure 11 and Appendix D, 4.5 fold observed/random,

p=2.65e-38), indicating a more prominent role for TET1 in regulating intragenic CpG

island methylation.
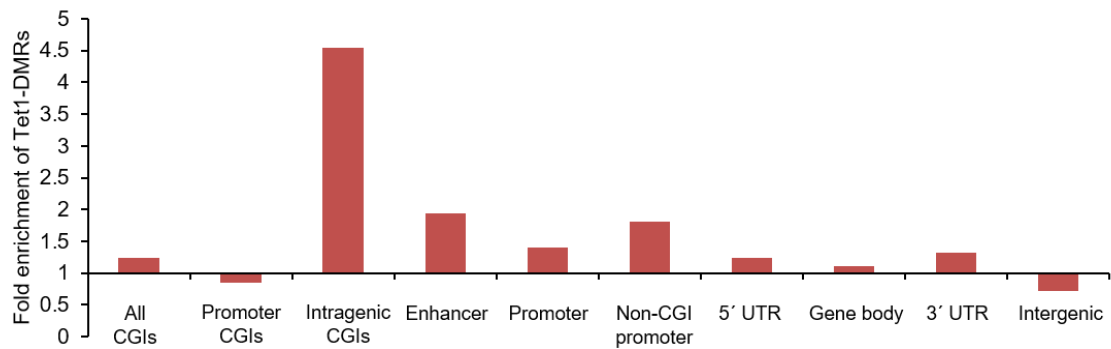
Figure 11: Stratification of *Tet1*-DMRs in genomic regions

Whole-genome bisulfite sequencing revealed *Tet1*-DMRs are enriched in intragenic CpG islands (CGI) (*p*=2.65e-38, fisher's exact test).

2.3.4 Identification of Novel *Oxtr* Gene mRNA Isoforms and Altered Histone Modifications

The specific pattern of *Oxtr* hypermethylation indicated that *Oxtr* may have a

more complex transcript structure than that described in literature. A single *Oxtr*

transcript has been previously characterized with an open reading frame (ORF)

spanning exons 3 & 4 and encodes a 388 amino acid protein (*Oxtr-A*) (Kubota et al.,

1996). Examining the *Oxtr* gene structure in the UCSC genome browser (mm9,

http://genome.ucsc.edu/), revealed a predicted mRNA isoform lacking exons 1 & 2

(*Oxtr-B*) as well as a previously deposited isoform originating from intron 3 (*Oxtr-C*).

We validated the presence of all three isoforms in the hippocampus by RT-PCR and

sequencing (Figure 12A). In addition, we identified a fourth isoform by RT-PCR and

sequencing in which exon 3 is skipped (*Oxtr-D*) (Figure 12A). Our RNA-seq read depth

data also suggested a potential novel TSS originating from the 3' end of exon 3 (data not

shown). To examine if there were additional TSSs not previously reported that could be

affected by the exonic hypermethylation of the BS3 region, we performed 5' RACE using

primers from exon 4 in a pair of *Tet1*$^{+/+}$ and *Tet1*$^{\Delta e4-/-}$ mice. Interestingly, the sequences of

5' RACE products revealed four novel transcription starting sites[4], including one

originating from intron 3 (Oxtr E-H) (Figure 12A).

We first made cDNA using random primers and then measured the relative

abundance of the various *Oxtr* transcripts by qRT-PCR with several primer sets

indicated in Figure 12A. Our results indicate that isoform B is the most dramatically

reduced (20% of WT), while full-length isoforms A and novel isoform H are not different

in *Tet1*$^{\Delta e4-/-}$ hippocampus (Figure 12B). We then confirmed these results with cDNA

made with oligo dT primers (Figure 12C). Transcript levels of isoforms C & D were

---

[4] *Oxtr* mRNA isoform sequencing data has been deposited in GenBank under accession
numbers KU686795- KU686801.

below our detection threshold, and unique primers for isoforms E, F, G could not be

designed because of transcript overlap.
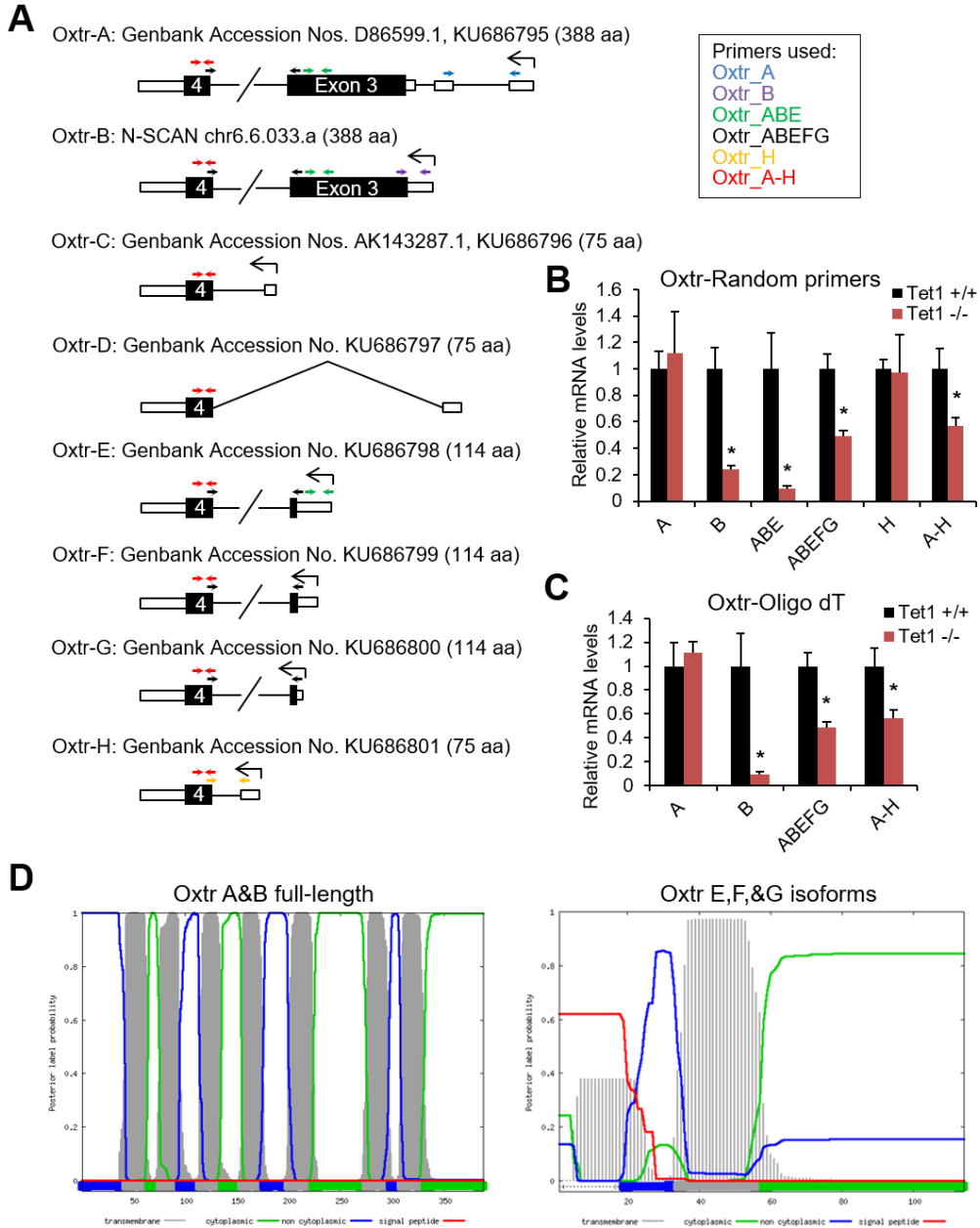
Figure 12: *Tet1*[Δe4-/-] **mice show complex transcriptional dysregulation of** *Oxtr*

(A) *Oxtr* isoforms A to C known or predicted *in silico* prior to this study. Novel *Oxtr* mRNA isoforms D to H identified by RT-PCR and 5' RACE (predicted coding regions are shaded). qRT-PCR primers indicated (multicolored arrows). Accession numbers are noted along with predicted amino acids (aa) in parentheses. **(B)** qRT-PCR data from cDNA made using random primers revealed downregulation of isoform B but not A or H (n=3-4/group, *$p<0.05$, two-tailed t-test). **(C)** qRT-PCR data from cDNA made using oligo dT primers confirmed downregulation of isoform B but not A (n=3-4/group, *$p<0.05$, two-tailed t-test). **(D)** Protein domain analysis using the online tool Phobius predicted the short *Oxtr* mRNA isoforms E,F&G to only have 1 ½ of the 7 *Oxtr* transmembrane domains (shaded gray). All data are presented as mean ± SEM.

Oxtr isoforms A and B have the same full length ORF while the other mRNA isoforms have shorter predicted ORFs ranging from 75 to 114 amino acids (Figure 12A). We used Phobius, an online protein domain predictor tool, to show the predicted short isoforms E, F, and G would only retain one and half of the seven transmembrane domains (http://phobius.sbc.su.se/) (Figure 12D). However, whether the shorter mRNA isoforms are translated endogenously and possess a function similar to *Oxtr* warrants further investigation. Our data together indicate a complex transcript structure of *Oxtr* with selectively reduced transcripts in *Tet1$^{\Delta e4-/-}$* mice.

Based on the DNA hypermethylation and reduced transcripts of *Oxtr*, we hypothesized that the chromatin structure in the promoter region was altered in *Tet1$^{\Delta e4-/-}$* mice. Encode ChIP data from E14.5 whole brain tissue indicate the *Oxtr* promoter has two active H3K4me3 peaks that overlap a repressive H3K27me3 peak (Figure 13A), typical of a bivalent domain (Bernstein et al., 2006). Interestingly, TET1 is known to preferentially bind to these transcriptionally poised bivalent domains which are generally hypomethylated in ESCs (Wu et al., 2011). We performed chromatin

immunoprecipitation of adult cerebrum followed by quantitative PCR and found both H3K4me3 and H3K27me3 histone marks reduced in exon 3, while H3K4me3 was increased in the 5'UTR of *Tet1*^{-/-} mice (Figure 13B). Although there was no difference in DNA methylation at the 5' UTR region in *Tet1*^{-/-} mice, the increase in H3K4me3 could be the result of a compensatory mechanism due to the reduced transcription at the downstream promoter. Consistent with the finding of dramatic hypermethylation of the *Oxtr* BS3 region in *Tet1*^{-/-} mice, we find more significant differences in histone modifications overlapping the same region suggesting an altered chromatin structure particularly in exon 3.
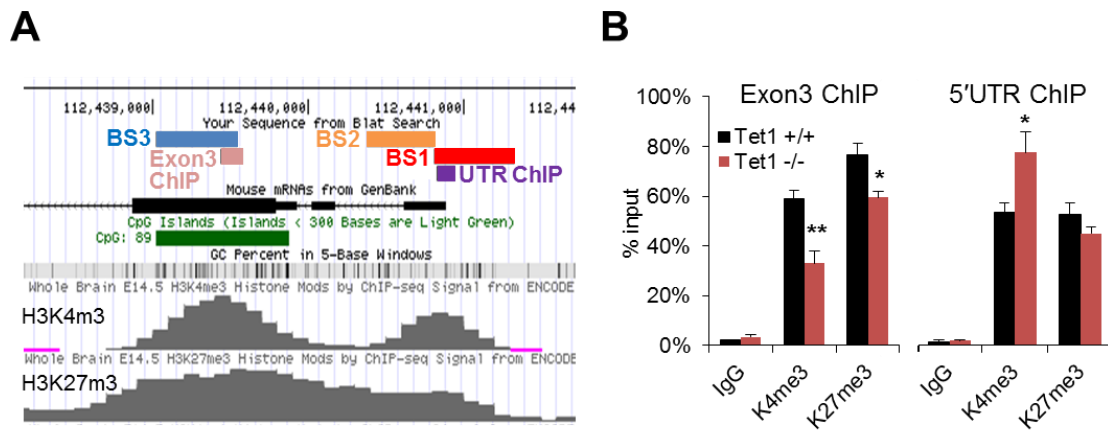
Figure 13: Altered histone modifications at *Oxtr* promoter regions

(A) A second putative regulatory was identified within exon 3 (large black bar) of *Oxtr* which overlaps a CpG island (green bar) (mm9, http://genome.ucsc.edu/). Selection of *Oxtr* regions for bisulfite sequencing (BS1-3) and ChIP-PCR are indicated. Encode ChIP data shown is from E14.5 whole brain produced in the laboratory of Bing Ren (H3K4me3, GEO:GSM1000095; H3K27me3, GEO:GSM1000143). (B) ChIP-qPCR revealed altered histone modifications at the bivalent promoter region of *Oxtr* in the cerebrum of *Tet1*[Δe4-/-] mice. H3K4me3 (K4me3, active mark), H3K27me3 (K27me3, repressive mark), and IgG (isotype negative

control) were assessed in two regions overlapping coding exon 3 and exon 1 in the 5′ UTR. (n=2/group, each sample ran in triplicate; *$p < 0.05$; **$p < 0.005$; two-tailed t-test). All data are presented as mean ± SEM.

2.4 Conclusions

We generated a novel *Tet1* knockout mouse and null ESCs by deleting the largest coding exon, exon 4. To date, 3 lines of *Tet1* mutant mice have been generated by deleting different coding exons of *Tet1* (Dawlaty et al., 2011; Zhang et al., 2013) or by inserting a gene-trap in intron 2 (Yamaguchi et al., 2012)(Figure1A). Although these deletions result in frameshift or truncated TET1 protein that are predicted to be loss of function mutations, further study of these mutant mice in parallel is warranted to determine whether there is any difference at the molecular level among different lines. For example, a mutation may result in a truncated but stable protein that retains some residual TET1 function or gains a new function.

Consistent with previous reports in other lines, *Tet1*$^{\Delta e4-/-}$ mice are viable but have partial perinatal lethality and mild growth retardation (Dawlaty et al., 2011; Yamaguchi et al., 2012). While 5hmC is abundant in the postnatal brain, its exact function remains poorly understood (Globisch et al., 2010; Munzel et al., 2010). We found a similar reduction in 5hmC in *Tet1*$^{\Delta e4-/-}$ ESCs as previously reported (Dawlaty et al., 2011) but not in the adult brain suggesting a more prominent role for TET1 in generating 5hmC in ESCs. It is possible that global levels of 5hmC remain unchanged in adult brain due to a compensatory role of TET2 and TET3. Our data and others support that *Tet1* expression

is significantly higher than *Tet2* and *Tet3* in embryonic stem cells but drops dramatically upon differentiation, while in the adult brain *Tet2* and *Tet3* expression are significantly higher than *Tet1* (Szwagierczak et al., 2010). It may also be the case that a slight difference in 5hmC levels was not observed due to the insensitive nature of DNA dot blot analysis. Indeed, 5hmC brains levels were reported to be decreased in *Tet1* knockout studies using more quantitative mass spectrometry methods (Kumar et al., 2015; Rudenko et al., 2013).

Contrary to early studies which showed striking morphological changes and loss or skew of pluripotency in ESCs targeted by *Tet1* small hairpin RNAs (shRNAs) (Ito et al., 2010; Koh et al., 2011), we did not observe any noticeable change in cell morphology in our *Tet1*$^{\Delta e4-/-}$ ESCs. While fewer *Tet1*$^{\Delta e4-/-}$ mice survive to weaning and the majority of those that do are smaller in total body size, the observance of viable and fertile *Tet1*$^{\Delta e4-/-}$ mice suggests that the absence of TET1 is not sufficient to disrupt the pluripotency potential of *Tet1*$^{\Delta e4-/-}$ ESCs. The first *in vivo* study of *Tet1*$^{\Delta e5-/-}$ ESCs and mice corroborates our results although partial perinatal lethality was not previously reported (Dawlaty et al., 2011). The difference in partial lethality observed in our mice could be due to a difference in background as we backcrossed six generations to C57BL/6J mice while Dawlaty et al. used a mixed background. The observed results of the *Tet1* knockdown studies could be restricted to an *in vitro* context or be due to undetected off-target effects

or difference in ESC background. Whichever the reason, our results suggest caution in interpreting results from RNA interference studies.

While the *Tet1* downregulation 2-hours after ECS did not reach significance in our study, another study found downregulation of *Tet1* 3-hours after inducing seizure (Kaas et al., 2013). Consistent with previous reports, we found the total number of *Tet1*-dysregulated genes was skewed towards downregulated genes suggesting a primary role for TET1 in activating gene expression in the hippocampus (Rudenko et al., 2013; Zhang et al., 2013). Although we found TET1 important for regulating several activity-dependent genes including *Npas4*, we did not observe significant overlap between the dysregulated genes from ECS-treated *Tet1*$^{\Delta e4-/-}$ brain and known activity dependent genes. Interestingly, we found that genes involved in the extracellular region/matrix/space were preferentially dysregulated in *Tet1*$^{\Delta e4-/-}$ mice. Genes involved in the extracellular matrix have been strongly implicated in synaptic plasticity and homeostasis (Dityatev et al., 2010). Further investigation is clearly warranted to elucidate how TET1 regulates this set of genes and whether specific aspects of synaptic function may be affected.

Our dysregulated genes had a 25% overlap with untreated *Tet1*$^{\Delta e5}$ mice indicating many commonalities but also highlighting many differences. Future studies may investigate if differences are due to ECS treatment, mouse background, or the nature of the mutation. Only a single gene, *Mgp*, was found to be downregulated in

Tet1$^{\Delta e5}$ hippocampus, *Tet1*$^{\Delta e11-13}$ neural progenitor cells, and our ECS-treated *Tet1*$^{\Delta e4-/-}$ hippocampus (Figure 7F). *Mgp* is implicated in Keutel syndrome (OMIM 245150), a rare autosomal disorder characterized by abnormal skeletal developments and other features including mild intellectual disability (Munroe et al., 1999). Further investigation is warranted to investigate if *Mgp* dysregulation is related to the partial perinatal lethality, midface hypoplasia, and growth retardation observed in our TET1-deficient mice.

A previous study of *Tet1*$^{\Delta e5}$ mice also found downregulation and hypermethylation of *Npas4* (Rudenko et al., 2013). While we observed downregulation of *Npas4*, the amount of hypermethylation was less in *Tet1*$^{\Delta e4-/-}$ versus *Tet1*$^{\Delta e5}$ mouse hippocampus (~27% vs ~45%). We did not detect hypermethylation of *Npas4* in the cortex in our genome-wide analysis although Rudenko et al. found hypermethylation of *Npas4* more striking in the hippocampus (~45%) than in cortex (~20%) in *Tet1*$^{\Delta e5}$ mice, suggesting a tissue-dependent effect of TET1 depletion.

Of particular interest is our discovery of the complex transcriptional regulation, altered histone modifications, and hypermethylation of *Oxtr* in *Tet1*$^{\Delta e4-/-}$ mice. The association between DNA methylation and suppression of the oxytocin receptor has been documented in several different tissues and cell lines from different species *in vitro* (Kusui et al., 2001; Mamrut et al., 2013). 5-azacytidine (Aza-C) treatment of low *Oxtr*-expressing mouse cell line (4T1) resulted in a dose-dependent increase in Oxtr mRNA and accompanying decrease in DNA methylation (Mamrut et al., 2013). Human *OXTR*

gene expression was significantly increased in HepG2 liver carcinoma cells after a 2-day treatment with the demethylating agent, 5-azacytidine (Aza-C) (Kusui et al., 2001). Kusui et al also used luciferase assays to show that promoter activity is higher in clones containing the CpG island of *OXTR* (MT2 region which overlaps our BS2 region) than clones containing fragments primarily upstream of the TSS. In addition, *in vitro* methylation of the MT2 region dramatically suppressed luciferase activity.

Our study provides the first direct *in vivo* evidence to support that *Oxtr* is epigenetically regulated during early development. We found hypermethylation in two select regions (BS2 and BS3) downstream of the most 5′ TSS, but not upstream (BS1). Accordingly, the full-length isoform A was unaltered in *Tet1*$^{\Delta e4-/-}$ mice. Isoform B, however, appeared most affected by the hypermethylation. The discovery of several novel mRNA isoforms presents many questions about their function. Although it remains to be determined whether each mRNA isoform has brain-region or cell-type specific expression or if each isoform is translated into protein, our finding does raise interesting questions about whether each isoform may possess a specific function in the developing mouse or adult brain.

3. Behavior and Physiological Analysis of Tet1 Mutant (Tet1Δe4) Mice

One of the primary goals of medicine is to identify treatments for symptoms of disease. In order for a treatment to have the highest likelihood of success, the underlying cause needs to be clearly identified. Human heritability studies can give good clues to whether the symptoms have a genetic basis. Around the turn of the century, genetic linkage studies were widely used to study human diseases but were mostly only successful in identifying mutations in single-gene Mendelian disorders. While the advent of genome-wide association studies and next generation sequencing has made identifying disease variants more feasible for complex disease, it still remains difficult to pinpoint a single gene mutation to a disease when multiple mutations are identified. In addition, even when a gene mutation is identified, the genetic heterogeneity in humans makes it difficult to clearly identify the phenotype. Therefore reverse genetics serves as a power tool to assess behavioral changes caused by mutations to a single gene on a uniform genetic background. By generating and studying gene knockout mice, we can get a better understanding of the influence of genes on the brain and behavior.

3.1 Introduction

3.1.1 Evidence for a role of DNA methylation in cognitive function

Among the several hundred genes implicated in intellectual disabilities and related cognitive disorders are genes encoding epigenetic modifiers (van Bokhoven,

2011). Learning and memory processes have been shown to involve epigenetic

modifications, such as DNA methylation, to maintain long-lasting changes in gene

expression (Lubin et al., 2008). In addition, *Dnmt1/Dmnt3a* brain-conditional double-

knockout mice show learning and memory deficits, impaired synaptic plasticity, and

dysregulated genes that have been implicated in memory (Feng et al., 2010). Based on

the observed downregulation and hypermethylation of the memory-related gene *Npas4*

and dysregulation of extracellular matrix genes in *Tet1*$^{\Delta e4-/-}$ mice, we hypothesized that

learning and memory would be impaired in these mice.

3.1.2 Behavioral summary of *Oxt* and *Oxtr* knockout mice

The discovery of the hypermethylation and downregulation of *Oxtr* transcripts

led us to consider what behavioral effect that might have on the *Tet1*$^{\Delta e4-/-}$ mice. Oxytocin

is synthesized in the paraventricular and supraoptic nuclei of the hypothalamus and

secreted by the posterior pituitary gland where it diffuses throughout the limbic system

and prefrontal cortex where it acts as a neuromodulator by activating neurons

expressing the oxytocin receptor (Russell et al., 2003). In addition, *Oxtr* knockout mice

show decreased sociability, increased aggression, and reduced maternal care

(Takayanagi et al., 2005). We hypothesized that we would see similar deficits if the

dysregulation of *Oxtr* in *Tet1*$^{\Delta e4-/-}$ mice was having a physiological effect.

46

3.2 Methods

We employed a battery of behavioral tests on multiple cohorts of mice at the Duke Mouse Behavior and Neuroendocrine Core Facility according to protocols described below. All experimenters handling animals or scoring behavioral data were blinded to genotype throughout the studies. We did not control for the estrus cycle in any of the tests. Mice in all cohorts were housed on a 14-hr light/ 10-hr dark cycle with most testing occurring during the light cycle, 4-5 mice per cage, and *ad libitum* access to food and water, unless otherwise specified.

3.2.1 Neurophysiological Screen

Mice were examined for general appearance, orientation to a moving object, reflexes, posture, and grip strength using methods previously described (Ribar et al., 2000; Taylor et al., 2008).

3.2.2 Open field

Spontaneous activity in the open field was conducted over 1 hr in an automated Omnitech Digiscan apparatus (AccuScan Instruments, Columbus, OH). Accuscan software scored the total distance traveled, vertical activity (beam-breaks), and time spent in the center zone.

3.2.3 Rotarod

Balance and coordination were examined using a rotarod (Med-Associates) as described (Ribar et al., 2000). On day 1 the rod accelerated from 4 to 40 rpm over 5 min,

47

and mice were given 4 successive 5-min trials with an inter-trial interval of 30 min. Trials

were terminated when the mouse fell from the rod or at 300 s. On day 2 the rod was

maintained at a steady speed of 24 rpm, and 4 trials were conducted in the same manner

as on day 1.

3.2.4 Light-dark emergence

Mice were placed into the darkened side (~2 lux) of a 2-chambered apparatus

(Med-Associates, St. Albans, VT) and given 5 min to freely explore the darkened and

lighted (~750 lux) chambers. Infrared diodes within the test chamber tracked the location

and activity of the animal throughout testing. The scored behaviors comprised the

latency to enter into the lighted chamber, activity (beam breaks) within each chamber,

and the numbers of crossings between the lighted and darkened chambers.

3.2.5 Resident-Intruder

Mice were individually housed for 3 weeks in order to increase propensity for

aggressive behaviors in both male and female mice (Goldsmith et al., 1978; More, 2008).

Sex-matched, non-familiar C3H mice (Jackson Labs, Stock No. 000659) of the same age

and approximate weight were used as intruders. The test was performed in the dark, 2-6

hr after onset of the dark cycle in the resident's home cage. The home cage with the test

mice was placed in the test arena and allowed to acclimatize for 5 minutes before an

intruder mouse was added to the cage. The mice were allowed to freely interact for 5

minutes before the intruder was removed. All tests were filmed and interactions were

later scored by an observer blinded to the genotype of the mice. The behavioral

ethogram was established at the Duke Mouse Behavioral and Neuroendocrine Core

Facility (Rodriguiz et al., 2011); individual behaviors were collapsed into six categories:

mild social investigation, non-social behaviors, withdrawal/disengagement, stationary

reactivity, threatening postures, and attacks. Only one animal engaged in fighting

necessitating early termination of the experiment and another animal left the testing

arena during the last minute of the test. For these two animals we adjusted the final

interactions proportionally based on levels of interactions up until the moment the test

was ended.

3.2.6 3-chamber sociability and social preference test

Mice were examined for sociability as described with a few modifications (Moy

et al., 2004). Testing was conducted in a white acrylic three-chambered apparatus with

small openings between chambers. Two small mesh cages (10 cm diameter x 11 cm high;

silver mesh pencil cups with weights on top of the cup, OfficeMax) were placed in the

outer two chambers and a clear plexiglass sheet was placed over the chamber to prevent

escape. Three days prior to testing, one Tet1$^{+/+}$ cagemate from each test cage were trained

to sit inside the wire-mesh cages in the test arena for 20 min a day for 3 consecutive

days. These animals were used subsequently as the social stimuli during testing. Testing

was divided into three phases. During each test phase, the mesh cages were placed in

the center of the two outer chambers. Test phase 1 began when a mouse was placed into

the center chamber and given free exploration of the apparatus. Identical objects (non-social stimuli) were placed in the mesh cages for phase 1. At the end of 10 min, the test mouse was removed and one of the objects was replaced with a Tet1$^{+/+}$ cagemate. Test phase 2 (sociability) began with reintroduction of the test mouse into the center chamber. At the end of 10 min, the test mouse was removed and the remaining object was replaced with a novel Tet1$^{+/+}$ mouse from a different cage. Test phase 3 (social preference) began as test phase 2 and was terminated after 10 min. All tests were filmed and the digital videos were analyzed subsequently using EthoVision software (Noldus) that included the frequency and duration of contacts with each cage. Preference scores were calculated, where time spent with one stimulus (non-social stimulus 1, social stimulus 1, or novel social stimulus 2) was subtracted from the time spent with the other stimulus (non-social stimulus 2, non-social stimulus, and familiar social stimulus 1, respectively) and divided by the total time spent exploring both stimuli. Positive scores indicated a preference for the novel social stimulus relative to the non-social or familiar social stimulus, whereas negative scores reflected preference for the non-social or familiar stimulus; and scores approximating "0" indicated no preference.

3.2.7 Virgin pup retrieval

Maternal behavior can be induced in virgin female mice by repeated exposure to pups (Alsina-Llanes et al., 2015; Brown et al., 1996; Noirot, 1969; Stolzenberg and Rissman, 2011). Maternal behaviors were tested in the home cage of each virgin female.

Cagemates were removed during testing. For three consecutive days, 3-5 day-old pups were gently placed in the corners of the cage. Pups were left with the test mice for 1 hour and the first and last 15 minutes were recorded. Only wild-type C57BL/6J pups were used in order to limit the effect of pups' behavior on the behavior of the test females. Retrieval times were calculated from the first 15 minutes of the test. Crouching time was calculated from the last 15minutes of the test. Aggressive behaviors scored included tail rattling and attacks on the pups during the first 15 minutes of Day 1.

3.2.8 Novel object recognition

Mice were examined for short- and long-term memory in this task as described (Porton et al., 2010; Roberts et al., 2009). Testing was conducted over 5 min in four phases; object training (train), short-term recall at 30 min (STM), and long-term recall at 24 hr (LTM). At training, mice were exposed to a pair of identical objects (2 x 2 x 3 cm in size) affixed with double-sided tape to the floor of a white Plexiglas arena (41 x 18 x 30 cm); these objects constituted the "familiar" objects for the tests. In the short- and long-term memory tests, one of the two familiar objects was replaced with a novel object with similar dimensions to the former but with different colors, patterns, and shapes. All tests were filmed with digital cameras and the videos were analyzed with Noldus Ethovision XT 7 software that automatically tracked the location of each animal as well as the location and movement of the animal's head and nose during testing. From these data, the total numbers of contacts and durations of object contacts were measured.

Orientation and time spent with objects was defined as the animal's head oriented towards the object with the nose positioned within 2 cm of the object. Recognition scores were calculated by subtracting the time spent with the familiar from the time spent with the novel object, and dividing this difference by the total time spent with both objects. Positive scores signified recognition of the novel object, negative scores indicated preferences for the familiar object, and scores approaching 'zero' denoted preference for neither object.

3.2.9 Morris water maze

Spatial learning and memory, and plasticity were examined in the Morris water maze as described (Wang et al., 2011). All training and testing were conducted under ~125 lux illumination in a 120 cm diameter stainless-steel pool filled with water, made opaque with white non-toxic poster paint (Crayola LLC, Easton, PA) and maintained at 24°C. The pool was divided into four quadrants; northeast (NE), northwest (NW), southeast (SE) and southwest (SW). Before testing, mice were handled for 10 min and then acclimated to standing in water for 1 min over 5 consecutive days. Mice were trained next to sit on the hidden platform (1 cm below the water's surface and 20 cm from the rim of the pool) in the NE quadrant for 20 s and then allowed to swim freely for 60 s before being returned to the platform for 15s. On the following day, water-maze testing began with testing divided into 2 phases: acquisition (days 1-6) with the hidden platform in the NE quadrant and reversal (days 7-12) with the platform in the SW

quadrant. Each day the mice received 4 trials in pairs that were separated by 60 min.

Release points were randomized across test-trials and test-days. On days 2, 4, 6, 8, 10,

and 12, a single probe trial was given 1 hr after the 4 test-trials. For probe trials, the

platform was removed from the water and the mice were released from the southern-

most point on days 2, 4, and 6, and from the northern-most point on days 8, 10, and 12.

Performance on all tests was scored by Ethovision XT 7 (Noldus) using a high-resolution

camera suspended 180 cm above the center of the pool. Tracking profiles were generated

by Ethovision software and were used to measure swim time. Except for probe trials (60

s in duration), all trials ended when the animal reached the platform or after 60 s of

swimming.

3.2.10 Social transmission of food preference

Mice were examined for their abilities to select a familiar over a non-familiar

food source as described (Porton et al., 2010; Roberts et al., 2009). Test mice were housed

in groups of 3-4 animals with a WT littermate selected as the demonstrator. Three days

prior to testing, animals were placed on food restriction. On the first test day, two

flavored diets were prepared by mixing 50 g of ground mouse chow (Lab Diet Formula

5001; Purina Mills Inc., Richmond, VA) with 50 ml of water flavored with banana or

maple extract. The demonstrator mouse was introduced into the test arena (41 x 18 x 30

cm) with a single 4 cm bowl containing 10 g of one of the flavored diets. The choice of

the banana or maple diet was randomized among demonstrator mice such that genotype

and sex of the test mice would be equally represented for each diet. The demonstrator

was allowed to consume the flavored diet for 30 min and was returned to its home cage.

Interactions between the demonstrator and test mice were filmed for 20 min, at which

time the demonstrator was removed and housed separately for the duration of the

study. Test mice were first examined in a two-way choice test beginning 20 min (short-

term memory) after demonstrator removal. Individual test mice were placed into the

center of the arena and were given 15 min of free access to two 4 cm test-bowls placed at

opposite ends of the chamber. One bowl contained the familiar demonstrator diet and

the other contained the second or novel diet. Following testing, mice were returned to

the home cage without the demonstrator animal. Twenty-four hours later, tester mice

were re-examined in the same test arena with the familiar demonstrator diet and another

novel diet flavored butter extract. Behaviors were filmed and later analyzed with the

Noldus Observer XT 7 by trained observers blinded to the genotype and sex of the mice.

For the choice tests with the tester mice, the bowls were weighed before and after

testing; spillage was recovered and noted. Preference for a diet was determined by

calculating the amount of novel diet consumed minus the amount of demonstrator diet

consumed divided by the total amount eaten. Positive scores indicated preference for the

familiar demonstrator diet, whereas negative scores denoted preferences for the novel or

unfamiliar diet. Scores approaching zero indicated no preference for either diet.

3.2.11 Olfaction Test

The ability of the mice to discriminate urine from pooled adult females relative to almond extract and water was examined. Thirty µL of urine, almond extract (diluted 1:100 in water) or water (unscented) were applied to filter paper (Whatman 3MM; Sigma-Aldrich, St Louis, MO) and placed in the center of the empty cage. Mice were habituated to an empty cage for 1 min prior to introduction of the filter paper (cue). Each mouse was given 1 min with each cue which were presented in a randomized order. The total time spent sniffing each cue was recorded by a blind observer with a stopwatch.

3.2.12 Fear conditioning

Animals were tested for contextual and cued fear conditioning as described (Wetsel et al., 2013). Mice were conditioned and tested in Med-Associates fear conditioning chambers under ~100 lux illumination. On day 1, mice were placed in the chamber for 2 min, after which a 72-dB 12-kHz tone (conditioned stimulus, CS) was presented for 30 s, which terminated simultaneously with a 2 s 0.4-mA scrambled foot-shock (unconditioned stimulus, UCS), which was repeated two subsequent times with an inter-stimulus interval of 60 seconds. Mice were removed from the conditioning chamber to the home cage 30 s later. For context testing on day 2, animals were returned to the chamber in which they had been conditioned for 5 min in the absence of the CS and UCS. For cued testing on day 3, the dimensions, texture and shape of the conditioning chamber were modified. Mice were introduced into the chamber for 2 min,

after which the CS was presented for 3 min. For all tests, behavior was videotaped and scored in an automated fashion by FreezeScan (Cleversys, Reston VA) for freezing.

3.2.13 Shock-threshold test

The shock-threshold test has been described (Grove et al., 2004; Taylor et al., 2008). Briefly, mice were acclimated to a single test chamber (MedAssociates) for 2 min before being presented with seven different foot-shock intensities (0, 0.1, 0.2, 0.3, 0.4, 0.5 and 0.6 mA) for 2 s. Inter-shock intervals were 60 s. Behavioral responses were scored by automation on a scale of 0-2000 (0 being no response). Behavioral scores were analyzed as a function of genotype and shock intensity.

3.2.14 General Statistical Analyses

The data were analyzed with SPSS 21 (SPSS Inc., Chicago, IL) or Microsoft Excel and expressed as means ± SEM. Simple comparisons between $Tet1^{\Delta e4-/-}$ and $Tet1^{+/+}$ mice without regards to sex were conducted with independent t-tests. When comparisons between genotypes were made for within-subject measurements across different phases of the same test (e.g., test days, locations within a test arena, or different intensities of stimuli), the data were analyzed with repeated measures ANOVA (RMANOVA). For RMANOVAs, a Bonferroni-correction for multiple comparisons was applied to post-hoc t tests. Statistical significance was defined as $p<0.05$. Sample sizes were based on previous experience with similarly designed experiments.

3.2.15 Electrophysiology

Six to 8 week-old mice were used for the long-term potentiation (LTP) experiment. The hippocampus was cut in transverse sections at 400 μm in the slicing solution containing (in mM) 75 sucrose, 87 NaCl, 2.5 KCl, 1.25 NaH_2PO_4, 26 $NaHCO_3$, 10 glucose, 7 $MgCl_2$, 0.5 $CaCl_2$. Slices were recovered at least 2 hours at 30 °C in ACSF containing (mM) 124 NaCl, 3 KCl, 1.25 NaH_2PO_4, 26 $NaHCO_3$, 10 glucose, 1 $MgCl_2$ and 2 $CaCl_2$. In the submersion recording chamber (30°C) a glass recording electrode (1-3 MΩ) filled with ACSF was placed in CA1 radiatum. At baseline, stimulations (200 μsec, DS301 or Isoflex) were applied to the Schaffer collaterals every 30 sec with a concentric bipolar tungsten electrode. The input-output relationship was obtained from increasing stimulation intensities (5, 10, 15, 20, 25, 30, 40, 50, 60, 100 μA). Paired-pulse ratios were obtained from the fEPSP slope of the second to the first stimulus at a given inter-stimulus intervals (25-2000 ms). For LTP, the stimulus strength was adjusted to evoke a field excitatory postsynaptic potential (fEPSP) at half of the maximal response. After recording a stable baseline for 20 min (less than 5 % drift), high frequency stimulation (100 Hz, 1 sec) was applied. For the following 60 min, activity to a single pulse was recorded. The slope at 55 to 60 min were compared to the pre-conditioning baseline response (last 5 min of baseline). Values are expressed as means ± SEM.

3.3 Results

3.3.1 *Tet1*$^{\Delta e4-/-}$ Mice Display Abnormal Social Behaviors and Impaired Episodic Memory

Due to the observed dysregulation of *Npas4* and *Oxtr*, we wanted to test whether there would be cognitive and social deficits in *Tet1*$^{\Delta e4-/-}$ mice. We performed a battery of behavioral tests using multiple cohorts of backcrossed (N6) C57BL/6J mice (Table 1).

Table 1: Behavioral cohorts and tests listed in the order performed

Behavioral Test	Cohort 1	Cohort 2	Cohort 3	Cohort 4	Conclusion
Light-Dark Emergence		14(+/+) 10(-/-)			Tet1+/+ females had increased activity in 1st minute, otherwise normal
Open Field	17(+/+) 11(-/-)	13(+/+) 10(-/-)			Tet1-/- mice are hypoactive (reduced distance traveled & rearing) and spend less time in the center
Accelerating Rotarod	17(+/+) 12(-/-)	14(+/+) 10(-/-)			Tet1-/- mice show enhanced performance
Steady-Speed Rotarod	17(+/+) 12(-/-)	14(+/+) 10(-/-)			No difference in performance between genotypes
Neurophysiological Screen	17(+/+) 12(-/-)				Tet1-/- mice have slightly reduced grip strength, otherwise normal
Novel Object Recognition	16(+/+) 11(-/-)	13(+/+) 10(-/-)			Tet1-/- mice display impaired short-term episodic memory
Morris Water Maze	16(+/+) 11(-/-)				No difference between genotypes in spatial memory and reversal
Social Transmission of Food Preference	10(+/+) 11(-/-)	8(+/+) 10(-/-)			No difference in preference between genotypes

Olfaction Test	16(+/+) 11(-/-)				Tet1-/- mice show normal olfaction but spend less overall time with cues
3-chamber sociability and social preference	10(+/+) 11(-/-)	8(+/+) 10(-/-)			Test results were inconclusive
Fear Conditioning	16(+/+) 11(-/-)	14(+/+) 10(-/-)			No difference between genotypes in contextual & cued memory
Shock Threshold	16(+/+) 11(-/-)				No difference in nociception
Resident Intruder		14(+/+) 9(-/-)		13(+/+) 6(-/-)	Increased threatening and stationary reactive postures in Tet1-/- females
Virgin Pup Retrieval			7(+/+) 3(-/-)	3(+/+) 4(-/-)	Delayed retrieval, decreased crouching, increased aggression in Tet1-/- females

We backcrossed the mice to reduce genetic heterogeneity, and chose the C57BL/6J strain as it is the most widely used strain and has moderate phenotypes compared to other strains in behavioral studies (1997; Voikar et al., 2001). For mice backcrossed six generations (N6), C57BL/6J would make up 98.375% of their genetic background, while 129/Sv would make up the remaining 1.625%. Any animal showing hydrocephalus was excluded from the behavioral analyses. In order to identify any other confounding factors that might influence behavioral testing we performed a neurophysiological screen in the first cohort of animals. Other than observing a slight reduction in grip strength in females, $Tet1^{\Delta e4-/-}$ mice appeared grossly normal (Table 2).

Table 2: Neurophysiological Screen

	Tet1+/+ Males	*Tet1*-/- Males	*Tet1*+/+ Females	*Tet1*-/- Females
General Evaluation				
Body Posture	Normal (11/11)	Normal (7/8)	Normal (6/6)	Normal (4/4)
Tail Elevation	Normal (10/11)	Normal (7/8)	Normal (6/6)	Normal (4/4)
Pelvic Elevation	Normal (11/11)	Normal (7/8)	Normal (6/6)	Normal (4/4)
Hair Loss/Barbering	None (11/11)	None (8/8)	None (6/6)	None (4/4)
Skin Color	Normal (11/11)	Normal (8/8)	Normal (6/6)	Normal (4/4)
Body Tone	Normal (11/11)	Normal (7/8)	Normal (6/6)	Normal (4/4)
Tremor/Convulsions	Absent (11/11)	Absent (8/8)	Absent (6/6)	Absent (4/4)
Piloerection	Absent (11/11)	Absent (8/8)	Absent (6/6)	Absent (4/4)
Whiskers appearance	Normal (11/11)	Normal (8/8)	Normal (6/6)	Normal (4/4)
Ear appearance	Normal (11/11)	Normal (8/8)	Normal (6/6)	Normal (4/4)
Lacrimation	Normal (11/11)	Normal (8/8)	Normal (6/6)	Normal (3/4)
Eye appearance	Normal (11/11)	Normal (7/8)	Normal (6/6)	Normal (3/4)
No. of urination during test	0.0 ± 0.0	0.13 ± 0.13	0.17 ± 0.17	0.75 ± 0.25
No. of boli during test	0.18 ± 0.18	0.63 ± 0.26	1.5 ± 0.76	2.0 ± 0.71
Orientation/Reflexes				
Ear Reflex	Normal (11/11)	Normal (8/8)	Normal (6/6)	Normal (4/4)
Eye Reflex	Normal (9/11)	Normal (7/8)	Normal (6/6)	Normal (4/4)
Whisker Reflex	Normal (11/11)	Normal (8/8)	Normal (6/6)	Normal (4/4)
Visual Placement (cm)	2.5 ± 0.07	2.31 ± 0.09	2.42 ± 0.15	2.0 ± 0.2
Orients to moving object (%)	100 ± 0.0	100 ± 0.0	100 ± 0.0	100 ± 0.0
Hindpaw Grasp	Normal (11/11)	Normal (8/8)	Normal (6/6)	Normal (4/4)
Grip Strength				
Front Paws (g-force)	98.5 ± 4.6	98.4 ± 4.1	91.8 ± 2.2	71.9 ± 9.0*
Whole Body (g-force)	178.8 ± 5.7	179.7 ± 12.6	189.6 ± 7.0	142.3 ± 6.7**

In addition to the neurophysiological screen, we tested olfaction through a preference test and nociception through the shock threshold test. *Tet1*$^{\Delta e4-/-}$ mice showed the expected preference for scented tissue paper over unscented although they spent less total time

investigating the scented cues (Figure 14A). In the shock threshold test, $Tet1^{\Delta e4-/-}$ mice

showed similar reactivity to increasing shock magnitude as their $Tet1^{+/+}$ littermates

(Figure 14B). Both genotypes showed increasing response to shock intensity until

receiving a shock of 0.3mA when they reached the maximum threshold for detection.
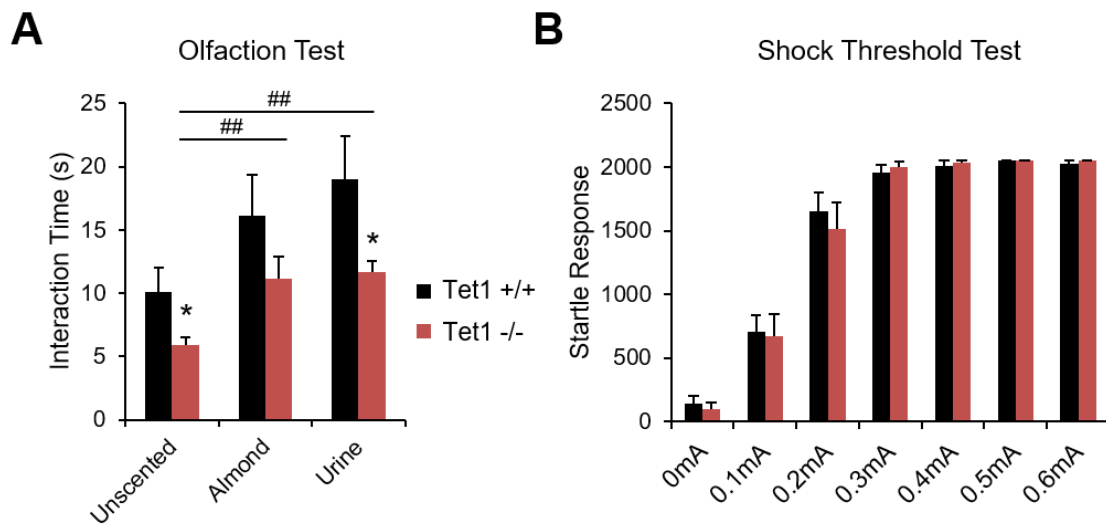
Figure 14: $Tet1^{\Delta e4-/-}$ mice have normal olfaction and nociception

(A) $Tet1^{\Delta e4-/-}$ mice show preference for almond and urine but interact less with the scented paper in the olfaction test. n= 11 (-/-) & 16 (+/+) (B) $Tet1^{\Delta e4-/-}$ mice react similarly to $Tet1^{+/+}$ littermates in the shock threshold test. n= 11 (-/-) & 16 (+/+). *p<0.05, +/+ vs -/- ; ##p<0.005, within genotype comparisons. All data are presented as mean ± SEM.

The open field test, one of the oldest rodent tests, is used to measure locomoter

activity and anxiety-like behaviors (Hall and Ballachey, 1932). $Tet1^{\Delta e4-/-}$ mice traveled less

distance, reared less, and spent less time in the center of the open-field (Figure 15A). In

order to test motor learning, muscle coordination and endurance, we performed the

rotarod test (Jones and Roberts, 1968). We hypothesized that the reduced grip strength
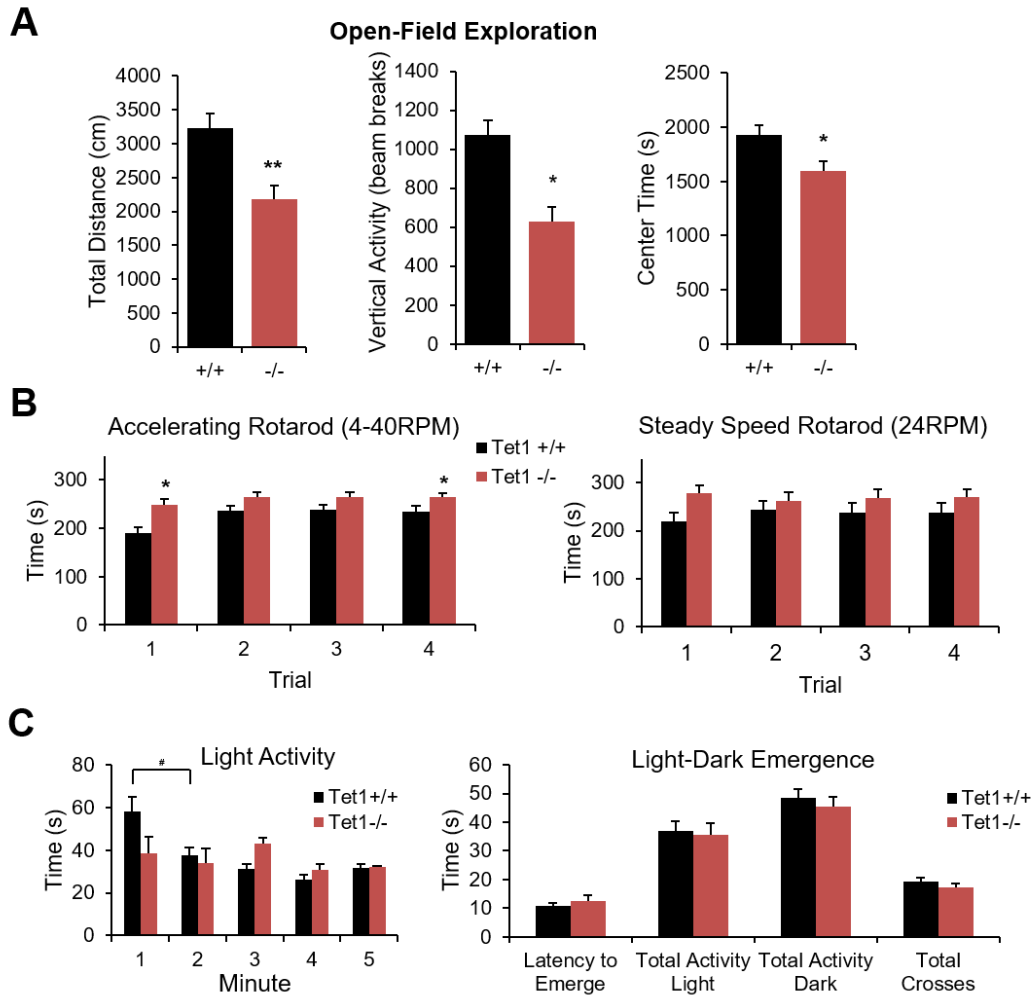
Figure 15: *Tet1*^Δe4-/- mice were hypoactive but showed enhanced coordination

(A) *Tet1*^Δe4-/- mice were hypoactive as measured by distance traveled and vertical activity (rearing) as measured by beam breaks in the open-field test. *Tet1*^Δe4-/- mice also spent less time in the center of the field (distance traveled p=0.0005, vertical activity p=9.7E-05, center time, p=0.04; two-tailed t-test). n= 21 (-/-) & 30(+/+). (B) *Tet1*^Δe4-/- mice display enhanced coordination on the accelerating Rotarod (4-40 RPM) and perform normally in steady speed Rotarod (24RPM). n= 22 (-/-) & 31(+/+). (C) *Tet1*^+/+ mice had increased activity in the lighted chamber during the first minute while *Tet1*^Δe4-/- mice had similar levels of activity throughout the 5 minute test [minute x genotype: F(4,88)=3.338, p=0.014]. Otherwise *Tet1*^Δe4-/- mice performed normally in the light-dark emergence test. n= 10 (-/-) & 14 (+/+). *p<0.05, **, p<0.005 +/+ vs -/-; #p<0.05, within genotype for post-hoc comparisons. All data are presented as mean ± SEM.

observed in female $Tet1^{\Delta e4-/-}$ mice might have a negative effect on their ability to stay on the rotarod. However, $Tet1^{\Delta e4-/-}$ mice showed an enhanced ability to stay on the accelerating rotarod (Figure 15B), suggesting the hypoactivity in the open-field was more likely anxiety-related than a motor-impairment. As locomoter activity and rearing have been associated with reduced emergence latencies, we performed the light-dark emergence test (Lalonde and Strazielle, 2008). An anxiety phenotype would be suggested by a reduced latency to emerge from the dark chamber and decreased time spent in the light chamber (Crawley and Goodwin, 1980). However, $Tet1^{\Delta e4-/-}$ mice did not have a strong anxiety phenotype in the light-dark emergence test (Figure 15C).

The role of OXTR has been well studied in the context of social and maternal care behaviors. We performed the three-chamber sociability and preference for social novelty, resident intruder, and virgin pup retrieval tests due to the observed decreased sociability, increased aggression, and reduced maternal care observed in $Oxtr-/-$ mice (Takayanagi et al., 2005). The three-chamber test not only measures sociability but also hippocampal-dependent social memory in the social preference part of the test (Hitti and Siegelbaum, 2014). Unfortunately, the results of the three chamber test were inconclusive as $Tet1^{\Delta e4-/-}$ mice showed an errant preference in phase one while their $Tet1^{+/+}$ littermates failed to show the typical sociability observed in wild-type C57BL/6 mice (Figure 16). In support of the hypoactivity observed in the open-field test, $Tet1^{\Delta e4-/-}$

mice also traveled less distance and interacted with the targets less in the three-chamber

test (Figure 16).

Three-chamber sociability and preference for social novelty
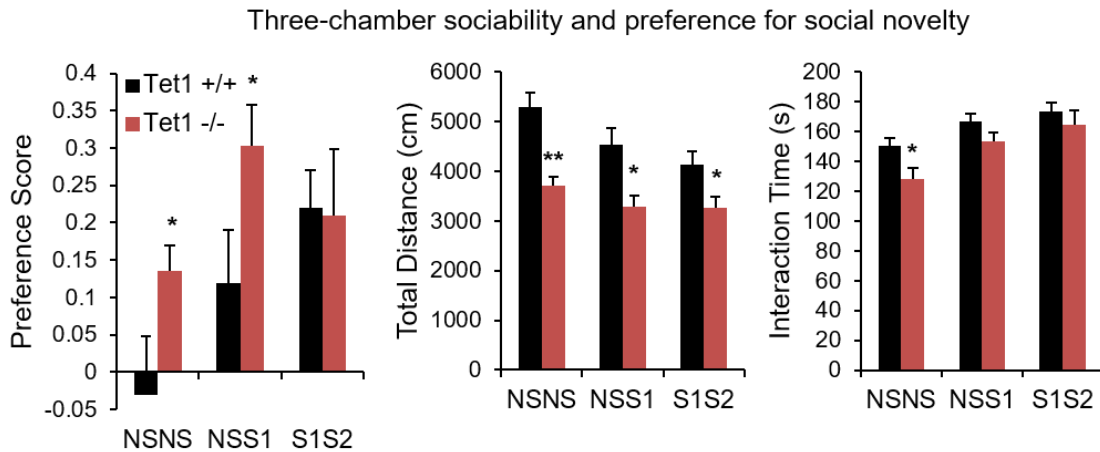
Figure 16: Three-chamber sociability test was inconclusive

(Left panel) *Tet1$^{\Delta e4-/-}$* **mice show an errant preference in the nonsocial-nonsocial (NSNS) phase and differ from** *Tet1$^{+/+}$* **in the NSNS phase and NS-familiar social (NSS1) test of sociability phase but not in the S1-novel social (S1S2) test of social preference phase. (Center panel)** *Tet1$^{\Delta e4-/-}$* **mice travel less distance in all three phases of the test. (Right panel)** *Tet1$^{\Delta e4-/-}$* **mice interact less with the objects in the NSNS phase and show a trend for reduced interactivity in the NSS1 and S1S2 phases. *p<0.05, **, *p*<0.005. All data are presented as mean ± SEM.**

In the sex-matched resident intruder test, there was a significant increase in

stationary reactivity and threatening postures in female *Tet1$^{\Delta e4-/-}$* mice and a trend

towards an increase in threatening postures in male *Tet1$^{\Delta e4-/-}$* mice (Figure 17A). These

trends were largely driven by the test mouse holding the intruder in the case of

stationary reactivity and climb-grooming in the case of threatening postures (Figure

17A). Other behavioral categories that did not differ between genotypes include mild-

social investigation, non-social behaviors, withdrawal/disengagement, and attacks

(Figure 17B).
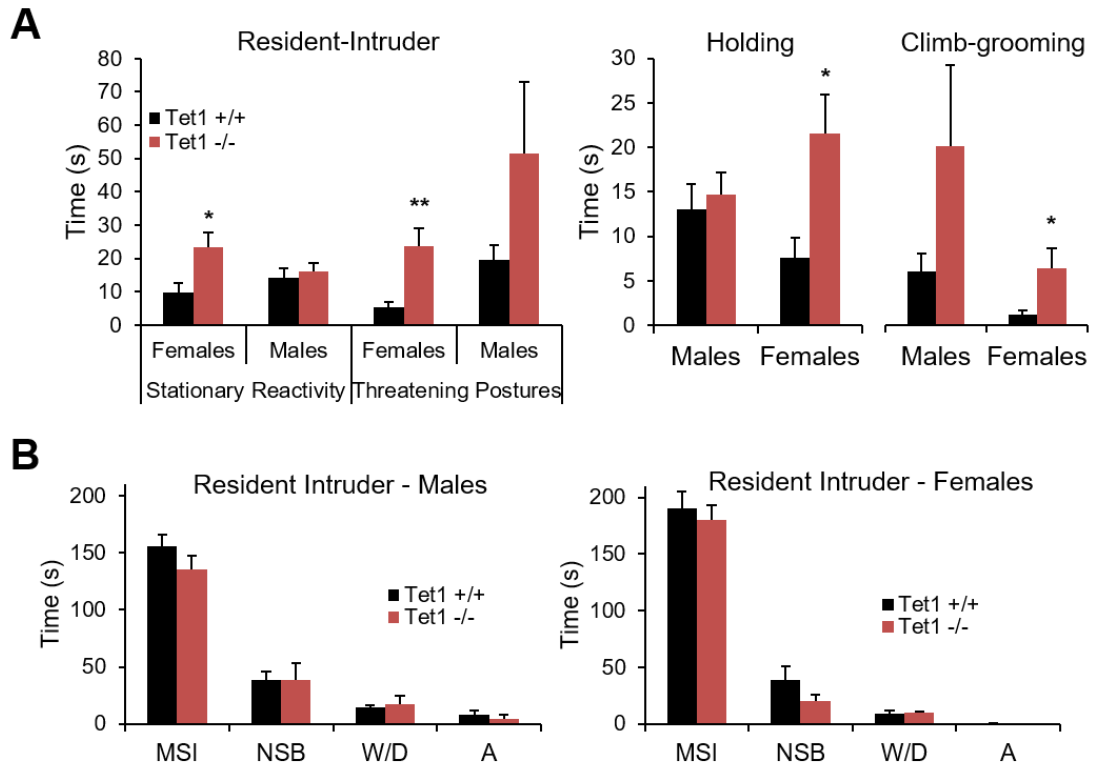
Figure 17: *Tet1^{Δe4-/-}* **female mice showed an increase of agonistic behaviors**

(A) *Tet1^{Δe4-/-}* **female mice display significantly increased stationary reactivity (p=0.017, two-tailed t-test) and threatening postures in the resident intruder test (p=0.001, two-tailed t-test). Males show a trend toward increased threatening postures (p=0.062, two-tailed t-test). Two single behaviors of holding and climb-grooming are driving the significance in each respective catergory. n= 7M&8F(-/-) & 14M&13F(+/+). (B)** *Tet1^{Δe4-/-}* **mice display similar levels of mild social investigation (MSI), non-social behaviors (NSB), withdrawal/disengagement (W/D), and attacks (A) as WT in the resident intruder test. n= 7M&8F(-/-) & 14M&13F(+/+). *p<0.05, **, p<0.005. All data are presented as mean ± SEM.**

Maternal behavior was only tested in virgin females as $Tet1^{\Delta e4-/-}$ female mice had reduced fertility and could not produce enough pups for dam pup retrieval. Increased maternal responsiveness after repeated exposures to pups is associated with increase oxytocin expression in the brain of wild-type virgin female mice (Noirot, 1969; Stolzenberg et al., 2012). Interestingly, the virgin pup retrieval test revealed that $Tet1^{\Delta e4-/-}$ female mice showed no improvement in latency to retrieve pups, spent less time crouching over pups, and showed an increase in aggressive interactions on the first day of pup exposure (Figure 18). Male mice were not tested in virgin pup retrieval, as males are known to attack non-offspring (Lonstein and De Vries, 2000).
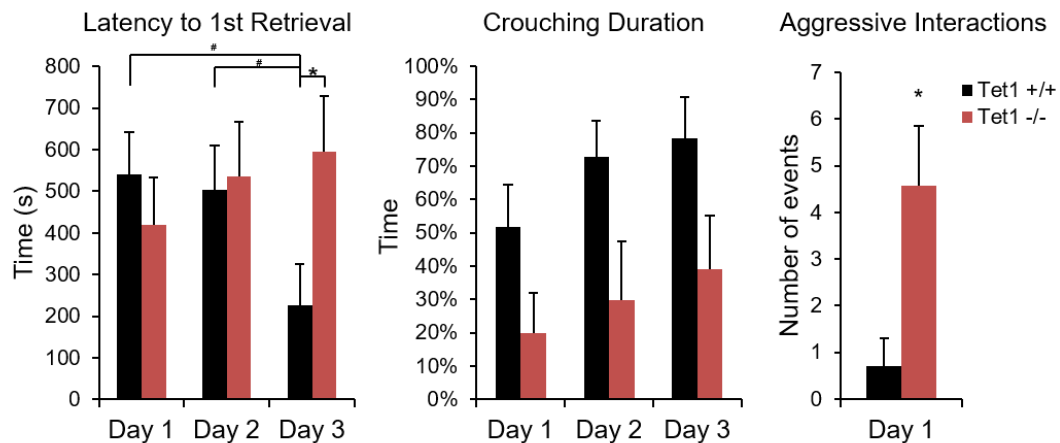
Figure 18: $Tet1^{\Delta e4-/-}$ mice display impaired maternal care in pup retrieval test

(Left panel) $Tet1^{\Delta e4-/-}$ mice showed no improvement in pup retrieval over time [genotype x day: F(2,30)=7.244, p=0.003]. (Center panel) $Tet1^{\Delta e4-/-}$ mice showed reduced overall crouching time [effect of genotype: F(1,15)=5.357, p=0.035]. Both genotypes show an increase in crouching over time [effect of day: F(2,30)=3.534, p=0.042]. (Right panel) $Tet1^{\Delta e4-/-}$ mice showed increased aggressive interactions in the first 15 minutes of the first day of virgin pup retrieval (p=0.008, two-tailed t-test). n= 7 (-/-) & 10 (+/+). All data are presented as mean ± SEM.

As *Npas4* has been implicated in memory formation, we performed several tests of cognition (Ramamoorthi et al., 2011). In the novel object recognition test, *Tet1^Δe4-/-* mice showed short-term (1 hr) memory deficits, indicating impairment in episodic memory (Figure 19). Long-term (24 hr) memory was not significantly different between
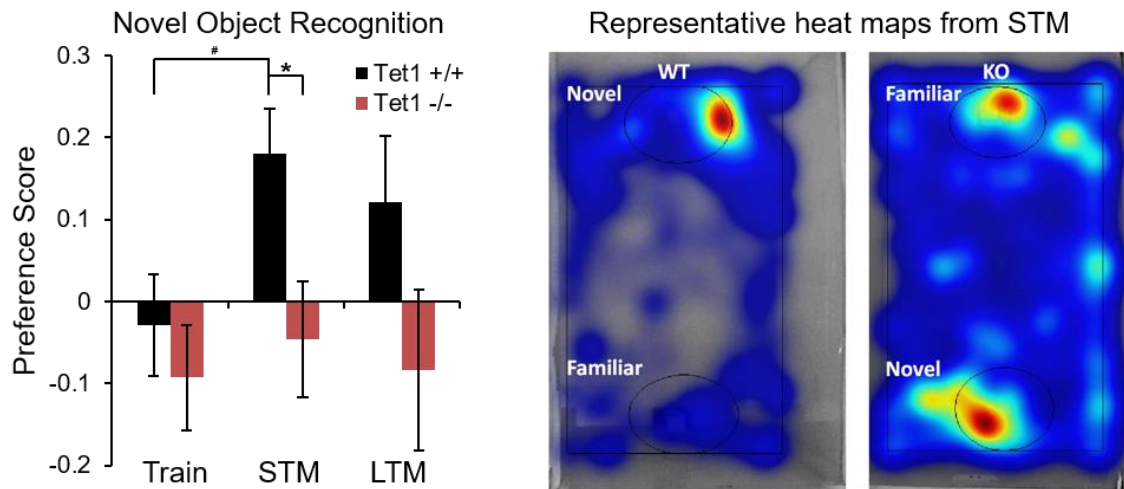
Figure 19: *Tet1^Δe4-/-* mice display impaired episodic memory

(Left) *Tet1^Δe4-/-* mice showed a minor deficit in short-term memory (STM) in the novel object exploration [effect of genotype: F(1,48)=3.877, *p*=0.055]. Train=training phase; LTM=long-term memory. n= 21 (-/-) & 29(+/+). Data are presented as mean ± SEM. (Right) Heat maps made from a pair of mice during the STM phase. Red color indicates more and blue indicates less time spent in a given area.

genotypes. Spatial learning (Morris water maze), social memory (social transmission of food preference), and associative memory (fear-conditioning) did not differ between

Tet1^Δe4-/- mice and their *Tet1^+/+* littermates (Figure 20).
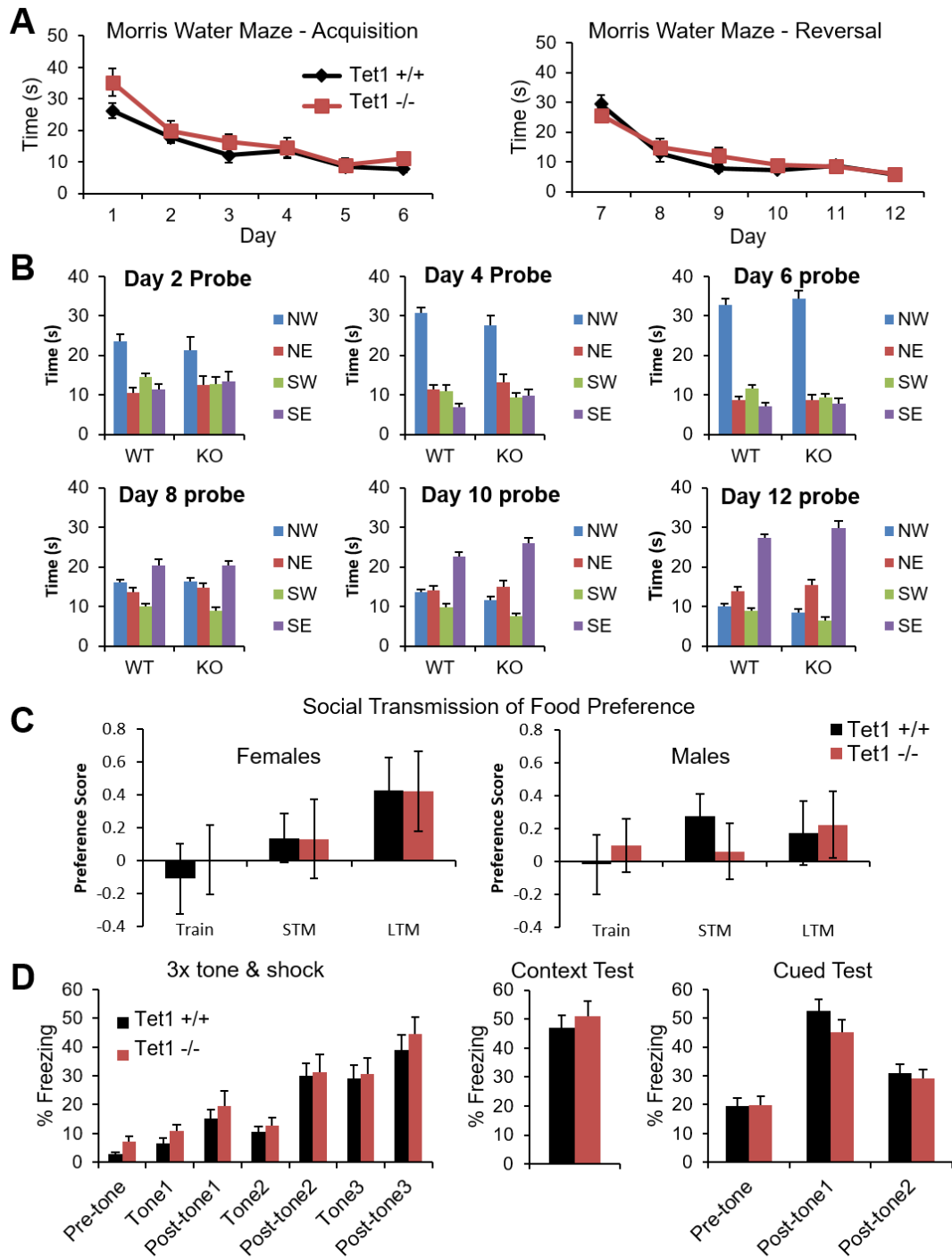
Figure 20: *Tet1*$^{\Delta e4-/-}$ mice display normal spatial learning, social memory, and associative memory

(A) *Tet1^{Δe4-/-}* mice performed similarly to WT in both acquisition and reversal of Morris water maze. n= 11 (-/-) & 16(+/+). **(B)** *Tet1^{Δe4-/-}* (KO) mice performed similarly to WT in the probe tests of Morris water maze. NW=northwest, NE=northeast, SW=southwest, SE=southeast quandrants. n= 11 (-/-) & 16(+/+). **(C)** *Tet1^{Δe4-/-}* mice performed similarly to WT in the social transmission of food preference test. n= 14M&7F(-/-) & 11M&7F(+/+). **(D)** *Tet1^{Δe4-/-}* mice display similar freezing levels as WT in the learning phase, context test, and cued test of fear conditioning. n= 21 (-/-) & 30(+/+). All data are presented as mean ± SEM.

3.3.2 Normal synaptic plasticity and transmission in *Tet1^{Δe4}* Mutant Mice

Based on the long-term potentiation impairment observed in the *Dnmt1/3a* double knockout (Feng et al., 2010) and dysregulation of *Npas4* in *Tet1^{Δe4-/-}* mice, we predicted a deficit in synaptic plasticity. Synaptic transmission and plasticity as measured by hippocampal LTP, however, were not altered in *Tet1^{Δe4-/-}* mice (Figure 21).
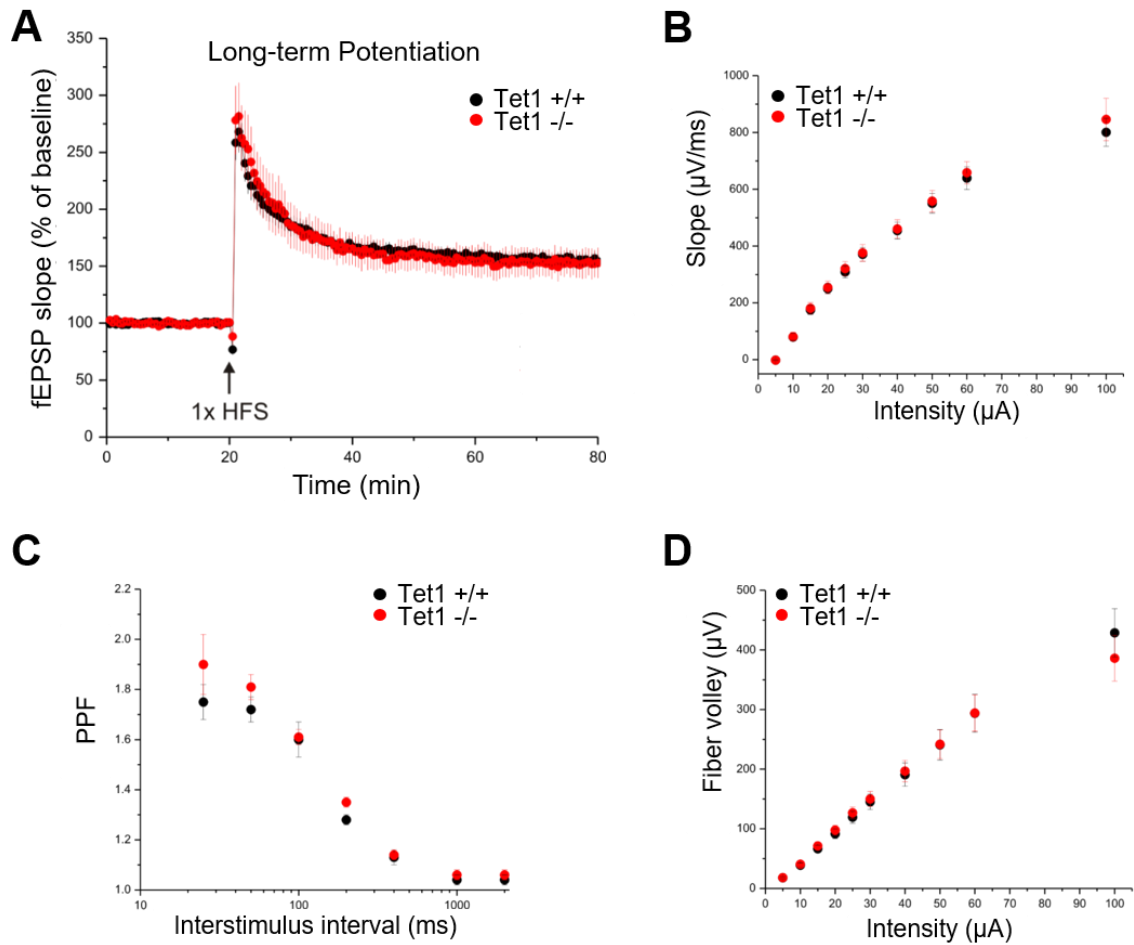
Figure 21: *Tet1^{Δe4-/-}* **mice have normal synaptic transmission and plasticity**

(A) Long-term potentiation (LTP) in CA1 of *Tet1^{Δe4-/-}* (LTP, 153 ± 12 %) was not different from *Tet1^{+/+}* (LTP; 156 ± 6 %). Arrow indicates the time of stimulation (HFS, 100 Hz, 1 second). (B) Baseline synaptic transmission not different in hippocampal CA1 of *Tet1^{Δe4-/-}* mice. (C) Paired pulse facilitation (PPF) not different in hippocampal CA1 of *Tet1^{Δe4-/-}* mice indicating normal pre-synaptic function. (D) Fiber volley not different in hippocampal CA1 of *Tet1^{Δe4-/-}* mice indicating normal pre-synaptic function. (For A-D; -/-:8 slices from 5 mice, +/+: 11 slices from 6 mice; 6 to 8 weeks old).

3.4 Conclusions

We performed the most extensive battery of behavioral tests on *Tet1* knockout

mice to date and identified several new phenotypes. While the observance of

hypoactivity in *Tet1*$^{\Delta e4-/-}$ mice is interesting, the cause is not completely clear.

Hypoactivity and reduced center time in the open field test is often suggested to be

anxiety related but there is controversy in the direct translatability of behavior in the

open field to behavior in the home cage (Careau et al., 2012; Prut and Belzung, 2003).

Possibly supporting an anxiety-like behavior, the number of times mice urinated or

number of boli during the neurophysiological screen was slightly increased in *Tet1*$^{\Delta e4-/-}$

mice (Table 2). Further exploration of anxiety-like behavior could be explored in the

elevated plus-maze and zero-maze.

We have made the first connection between TET1 and its role social behaviors.

The observance of agonistic behaviors and decreased maternal care is particularly

interesting, given the evidence for the role of *Oxtr* in social behaviors. While the three-

chamber test is often used to evaluate sociability and preference for social novelty, our

results were inconclusive. The scoring of the behavior data for the three-chamber test

was automated by software which can sometimes be prone to glitches while tracking the

mice. A blind hand scoring of the videos is necessary to validate the automated scoring.

While we did not observe differences in spatial learning and memory (water-

maze) or associative memory (fear-conditioning) as was previously reported, we did

observe a deficit to short-term episodic memory (Kumar et al., 2015; Rudenko et al., 2013; Zhang et al., 2013).

Our finding of no difference in synaptic transmission or plasticity as measured by hippocampal LTP replicates the same finding in $Tet1^{\Delta e5}$ mice (Kumar et al., 2015; Rudenko et al., 2013). TET1 could affect long-term depression (LTD) or LTP in other brain regions. Indeed, $Tet1^{\Delta e5}$ mice also showed normal hippocampal LTP but increased hippocampal LTD (Rudenko et al., 2013).

4. Generation and Initial Characterization of Tet3 Mutant (Tet3Δe7-9) Mice

4.1 Introduction

We used a similar rationale for generating Tet3 knockout mice as was used in generating and profiling the *Tet1*[Δe4-/-] mice. All three TET proteins have the enzymatic dioxygenase domain that has been demonstrated to catalyze the oxidation of 5mC to 5hmC (Tahiliani et al., 2009). TET3, like TET1 but unlike TET2, have a known CXXC domain is known to bind CpG rich DNA (Tahiliani et al., 2009). The expression profile of of *Tet3* differs the greatest from *Tet1* and *Tet2* which are expressed at higher levels in ESCs than *Tet3* (Szwagierczak et al., 2010; Wossidlo et al., 2011). Our data and others support that *Tet3* is expressed at higher levels than *Tet1* in the adult brain, suggesting a more prominent role for TET3 in the brain (Szwagierczak et al., 2010). Our finding of unchanged 5hmC levels in the brain of *Tet1*[Δe4-/-] mice, suggest TET2 and TET3 may be more responsible for the conversion of 5mC to 5hmC in the adult brain. We used gene targeting approach to create a new line of Tet3 mutant mice to study the role of TET3 in the brain and behavior.

4.2 Methods

4.2.1 Generation of *Tet3*$^{\Delta e7-9}$ mice

We created a floxed construct of *Tet3* exons 7 to 9 using the recombineering

method described by Liu and colleagues (Liu et al., 2003). The 129SvEv BAC clone

(BMQ-341J3) covering the *Tet3* gene was first identified *in silico* using the NCBI Map

Viewer (www.ncbi.nlm.nih.gov/projects/mapview) and obtained from Geneservice

(www.geneservice.co.uk) (Adams et al., 2005). The BAC was electroporated into SW102

E. coli and confirmed by digestion with EcoRI (Figure 22A) (Warming et al., 2005).
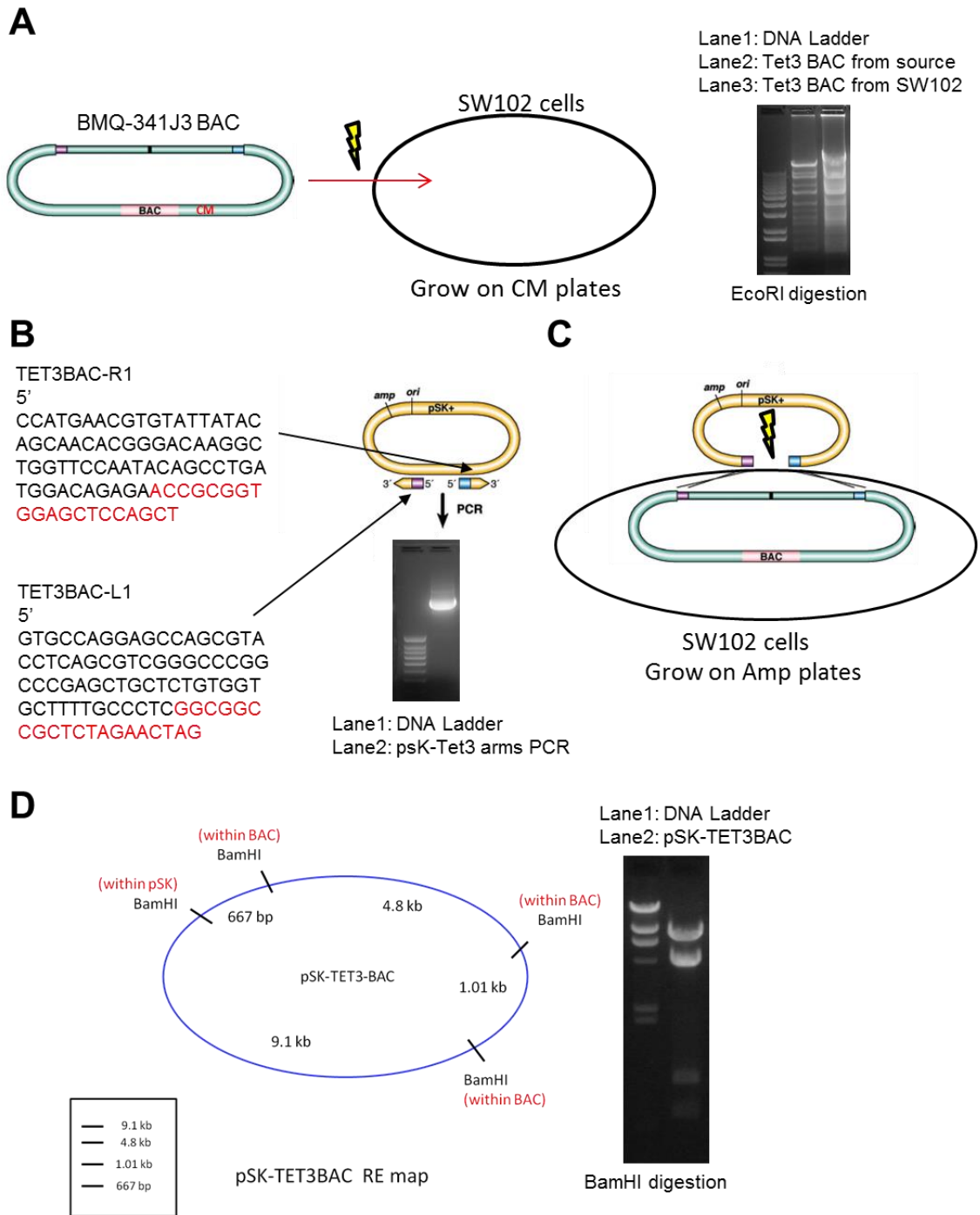
Figure 22: Generation of *Tet3* targeting construct (part 1)

Primers containing *Tet3* "arms" were designed and used to amplify the pBluescript SK+ (psK) plasmid (Figure 22B). The amplified product was electroporated into the SW102 cells containing the BAC (Figure 22C). Correct incorporation of the 12.6 kb genomic fragment of the BAC containing exons 5 to 11 of *Tet3* (pSK-TET3-BAC) was confirmed by BamHI digestion (Figure 22D). Primers containing *Tet3* "arms" designed to target the genomic insertion site of 83,326,157bp (mm9) were used to amplify the PL452 plasmid containing a neo cassette flanked by two loxP sites (Figure 23A). The amplified product was electroporated into the SW102 cells containing the pSK-TET3-BAC plasmid (Figure 23B) and correct recombination was confirmed by BamHI digestion (pSK-TET3BAC-LoxP1) (Figure 23C). Pure pSK-TET3BAC-LoxP1 plasmid was recovered and electroporated into SW106 *E. coli* containing an arabinose-inducible Cre gene (Figure 23D). 10% arabinose was used to induce Cre expression in the SW106 cells containing the pSK-TET3BAC-LoxP1 plasmid. Excision of the neo cassette was confirmed by PCR and digestion by BamHI (pSK-TET3BAC-LoxP1EX) (Figure 23E). Another set of primers containing *Tet3* "arms" designed to target the genomic insertion site of 83,322,660bp (mm9) were used to amplify the PL451 plasmid containing a neo cassette flanked by two
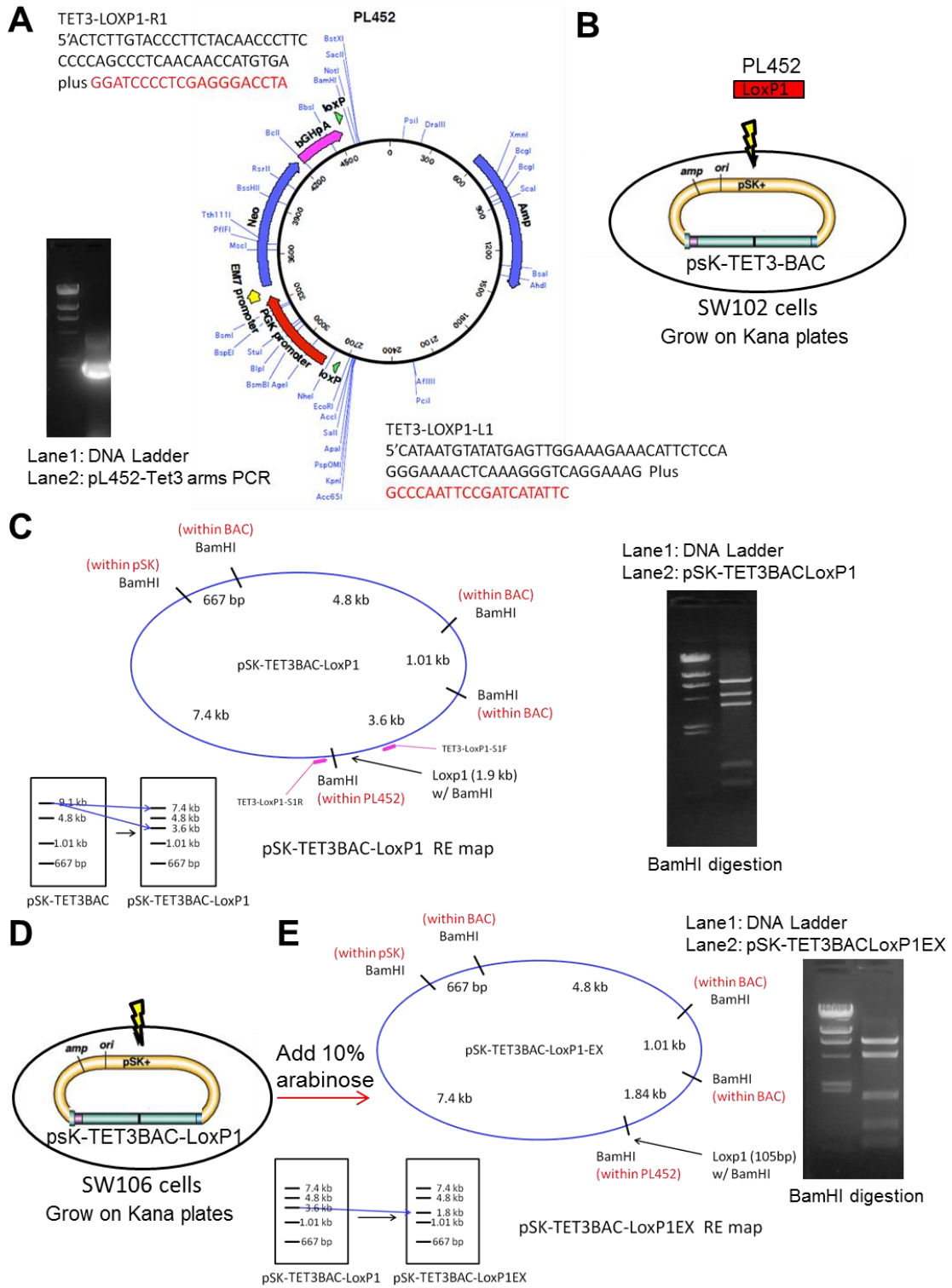
Figure 23: Generation of *Tet3* targeting construct (part 2)

frt sites and one loxP site (Figure 24A). The amplified product was electroporated into

the SW106 cells containing the pSK-TET3BAC-LoxP1EX plasmid (Figure 24B)and

correct recombination was confirmed by BamHI digestion (pSK-TET3BAC-LoxP1EX-P2)

(Figure 24C). The pSK-TET3BAC-LoxP1EX-P2 plasmid was isolated and confirmed by

sequencing. To confirm that excision of *Tet3* exons 7-9 would occur *in vivo*, 10%

arabinose was used to induce Cre expression in an aliquot of SW106 cells containing the

purified pSK-TET3BAC-LoxP1EX-P2 plasmid. Proper excision of *Tet3* exons 7-9 was

confirmed by BamHI digestion (pSK-TET3BAC-PostCre) (Figure 24D). The expected

digestion patterns of the final pSK-TET3BAC-LoxP1EX-P2 plasmid by BamHI and

HindIII were also confirmed (Figure 24E). The finalized plasmid was linearized with

NotI and electroporated into R1 129/Sv mouse embryonic stem cells (ESCs) at the Duke

Neurotransgenic Laboratory. Neo-resistant colonies were picked after 7-8 days of

selection and correctly recombinant clones were identified by Southern blot analysis

using both a 5′ and 3′ probe. *Tet3$^{e7-9\,+/f}$* ESCs were injected into blastocysts resulting in 8

chimeric male mice which were bred to C57BL/6J mice (Jackson Labs, Stock No. 000664)

to obtain germline transmission of the floxed allele.

A

TET3-LOXP2-L1
5'ATCTTTAATAGTAAAGCGTGCAGGAGTGTGGAG
AGCAGGTGGCCTCCCCATGCTCTTGCT Plus
GCTTGATATCGAATTCCGAAG

TET3-LOXP2-R1
5'AAGGGCAAGTCCTCAAGGATAGAGGGGGCAAG
AGGTGGTGACACTGGGGGAGCCGGCAGA Plus
GGCCGCTCTAGAACTAGTGGA

PL451
Constructed by Pentao Liu

Lane1: DNA Ladder
Lane2: pL451-Tet3 arms PCR

B

PL451
LoxP2

SW106 cells
Grow on Kana plates

C

PL451 LoxP2
PCR product
1,905 bp
21 bp
BamHI

(within BAC)
BamHI

(within pSK)
BamHI
667 bp

6.0 kb

752 bp
(within BAC)
BamHI

pSK-TET3BAC-LoxP1-EX
1.01 kb

7.4 kb
1.84 kb
BamHI
(within BAC)

BamHI
(within PL452)

Lane1: DNA Ladder
Lane3: mixed population
Lane2: pSK-TET3BAC
LoxP1EX-P2

pSK-TET3BAC-LoxP1EX-P2 RE map

BamHI digestion

pSK-TET3BAC-LoxP1EX
- 7.4 kb
- 4.8 kb
- 1.8 kb
- 1.01 kb
- 667 bp

pSK-TET3BAC-LoxP1EX-P2
- 7.4 kb
- 6.0 kb
- 1.8 kb
- 1.01 kb
- 752 bp
- 667 bp

D

After 10% arabinose

pSK-TET3BAC-LoxP1EX-P2
- 7.4 kb
- 6.0 kb
- 1.8 kb
- 1.01 kb
- 752 bp
- 667 bp

pSK-TET3BAC-Post Cre
- 7.4 kb
- 6.0 kb
- 667 bp

Lane1: DNA Ladder
Lane3: pSK-TET3BAC
LoxP1EX-P2
Lane2: pSK-TET3BAC
-PostCre

E

Lane1: DNA Ladder
Lanes2-4: NotI digestion
(1 band: 17.6 kb)
Lane5: BamHI digestion
(6 bands: 7.4 kb, 6 kb,
1.8 kb, 1 kb, 752 & 667
bps)
Lane6: HindIII digestion
(2 bands: 10.1 & 7.5 kb)

Figure 24: Generation of *Tet3* targeting construct (part 3)

4.2.2 PCR genotyping

DNA genotyping was routinely done by PCR using the primers listed in Appendix A. A three primer PCR reaction was used to amplify wild-type (218bp), floxed (323bp), and exon7-9 deleted (155bp) alleles.

4.3 Results

We have successfully generated *Tet3* mutant mice. We designed our *Tet3* targeting construct to delete exons seven to nine, which include the dioxygenase catalytic domain (*Tet3*$^{\Delta e7-9}$) (Figure 25A). Deletion of exons seven to nine causes a frameshift leading to a premature stop codon in exon 10 (Figure 25B). We used Southern blot analysis to confirm recombination at both the 3′ and 5′ ends of the construct (Figure 25C & 25D).

Three low percentage chimeric male mice were generated from the first round of blastocyst injections of *Tet3* targeted ESCs but breeding with C57BL/6J females failed to produce germline transmission of the targeted allele. A second round of injections produced an additional five high percentage chimeric male mice. Germline transmission
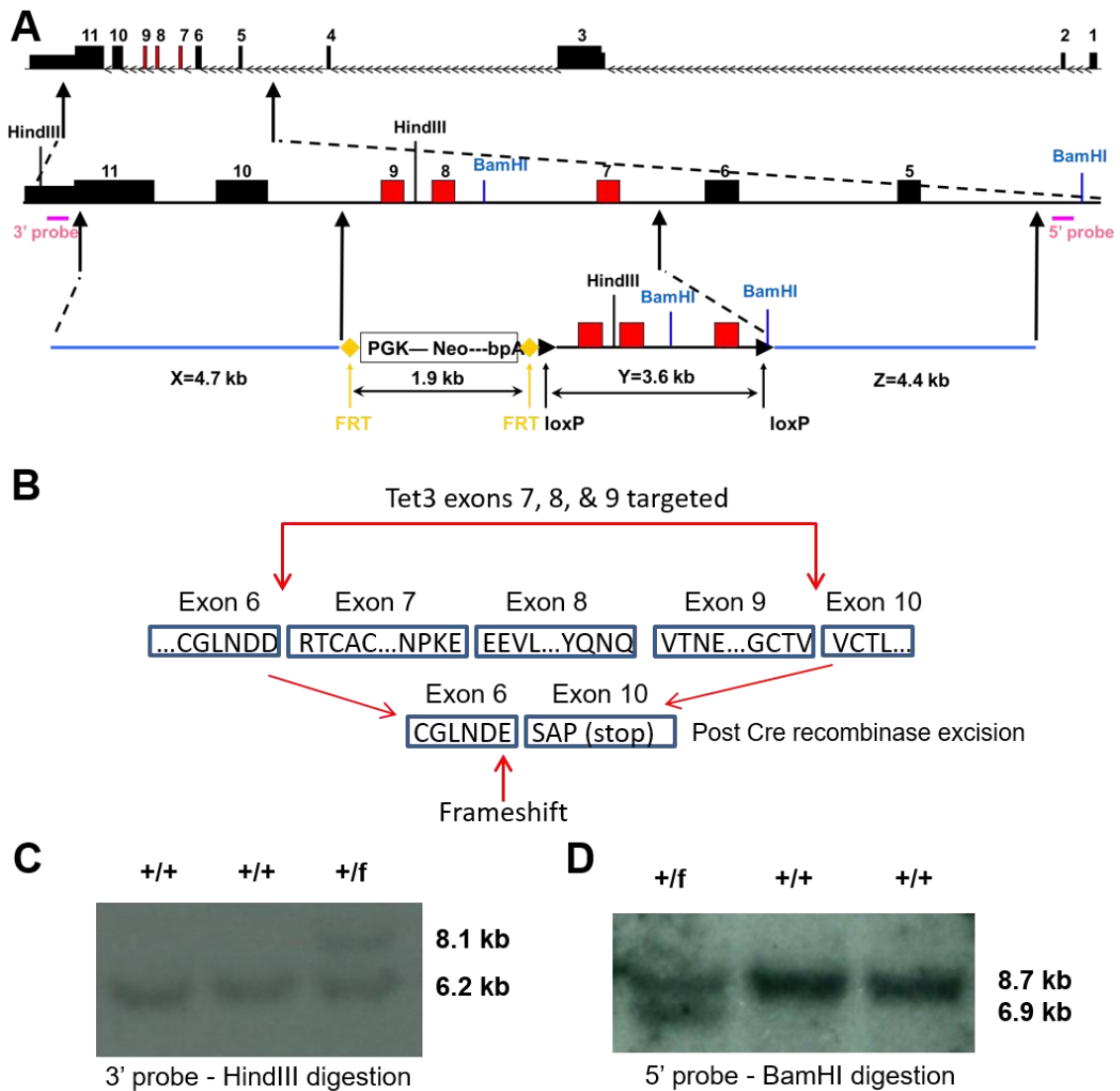
Figure 25: Generation of *Tet3* Mutant (*Tet3*$^{\Delta e7\text{-}9}$) Mice

(A) *Tet3* genomic structure and conditional targeting vector. Full length Tet3 is shown at the top, the targeted region is shown in the middle, and the floxed targeting construct is shown on the bottom. Exons 7-9, containing the catalytic domain, is targeted in this mouse. **(B)** After the Cre-induced excision of exon s 7-9, the catalytic domain is removed resulting in a frameshift and premature stop codon in the remaining sequence. **(C)** Southern analysis of electroporated ESCs after HindIII digestion using a 3′ radiolabeled probe. Wild-type (+/+) and recombinant floxed clones (+/f) are shown. **(D)** Southern analysis of electroporated ESCs after BamHI digestion using a 5′ radiolabeled probe.

81

of the $Tet3$ exon 7-9 targeted allele ($Tet3^{e7-9f}$) was confirmed by genotyping F1 offspring

of chimeric males (Figure 26A). As noted in Figure 25A, the targeted $Tet3$ exon 7-9 is a

floxed allele, thereby allowing us to produce both conventional and conditional $Tet3$

deletion mice. $Tet3^{e7-9f}$ mice were bred to CMV-Cre mice to obtain germline transmission

of the deleted exons 7-9 ($Tet3^{\Delta e7-9}$). After several paired mating attempts of $Tet3^{\Delta e7-9}$

heterozygotes failed to produce homozygous deleted mice, we concluded that complete

loss of TET3 is embryonically lethal. $Tet3^{e7-9f}$ mice were then bred to a conditional

knockout mouse expressing Cre recombinase driven by a Nestin promoter. Nestin-cre is

expressed throughout the central and peripheral nervous system by embryonic day 11

(E11) (Tronche et al., 1999). We noted during the breeding of $Tet3^{e7-9f}$ male mice positive

for Nestin-cre, deletion of $Tet3$ would often occur in the germline (red box, Figure 26B).

Breeding with only Nestin-cre females mostly resolved the issue. We confirmed the

nervous system specificity of Nestin-cre driven deletion of $Tet3$ in a Nestin-cre/$Tet3^{e7-9\ +/f}$

mouse (Figure26C). Homozygous $Tet3^{e7-9\ f/f}$ mice expresssing Nestin-cre are partially

lethal as few mice were produced from breeding pairs. The few that did result from

breeding were considerably smaller in size than their littermates. $Tet3^{e7-9f}$ mice were also

bred with mice expressing a forebrain-specific cre driven by Camk2a and backcrossed to

a C57BL/6J background for future studies. Homozygous $Tet3^{e7-9\ f/f}$ mice expresssing

Camk2a-cre were generated at normal Mendelian ratios with no observable phenotype.
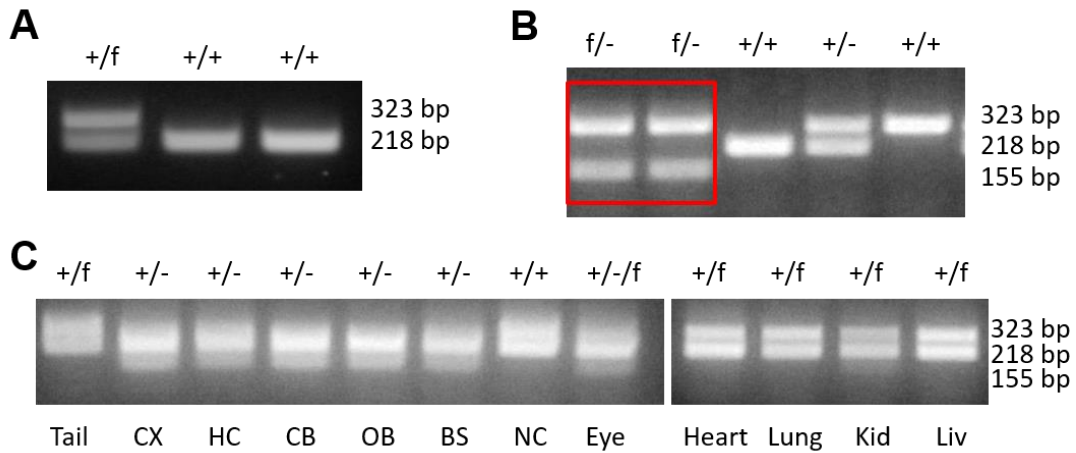
Figure 26: *Tet3* **genotyping results**

(A) *Tet3* **genotyping reveals germline transmission of** *Tet3*^{e7-9f} **(+/f) allele. (B) Genotyping of offspring from nestin-cre males consistently reveals germline deletion of** *Tet3* **(f/- genotype). (C) Nestin-cre/***Tet3***^{+/f} mouse tissue genotyping reveals deletion of** *Tet3* **exons 7-9 in the cortex (CX), hippocampus (HC), cerebellum (CB), olfactory bulb (OB), brain stem (BS); partial deletion in the eye and kidney (Kid); and no deletion in the tail, nasal cavity (NC), heart, lung, and liver (Liv).**

4.4 Conclusions

Conventional *Tet3*^{Δe7-9} mice are embryonic lethal but can survive if TET3-

deficiency in the brain. The initial *Tet3* knockout study also reported that mice are

homozygous lethal (Gu et al., 2011). Female mice that have a germline specific deletion

of *Tet3*, have normal growth and morphology but reduced fecundity (Gu et al., 2011).

5hmC was not detected in male pronuclei in zygotes from germline-deleted *Tet3* female

mice, while 5hmC was present in germline-deleted *Tet3* male mice, indicating that TET3

is expressed from female pronuclei and functions to convert 5mC to 5hmC in the male

pronuclei (Gu et al., 2011).

Our generation of *Tet3* brain-conditional knockout mice allows us to study the function of TET3 both in the developing and adult brain. We previously tested whether hippocampal expression of *Tet* genes was activity-dependent and found *Tet1* downregulated but *Tet3* upregulated in *Tet1*^{+/+} mice after ECS, although neither reached significance (Figure 6B). The trend toward increased *Tet3* expression after ECS is also in agreement with a similar observation reported in cultured neurons (Yu et al., 2015). It would be interesting to repeat our electroconvulsive stimulation experiment in the *Tet3* brain knockout mice to see if TET3 regulates activity-dependent neural gene expression.

5. Discussion and Future Directions

5.1 The role of TET1 in DNA methylation dynamics

This is the first study to clearly identify early prenatal development as a critical period for TET1 function, suggested by previous *in vitro* evidence (Xu et al., 2011). It is known that genome-wide demethylation occurs after fertilization (Mayer et al., 2000; Oswald et al., 2000; Surani et al., 2007). *Tet3*, along with replication-dependent dilution, has been implicated in both the rapid demethylation of the paternal genome and slower demethylation of the maternal genome (Shen et al., 2014). Genome-wide demethylation is complete by the blastocyst stage, which is followed by *de novo* methylation during gastrulation (Bao et al., 2009; Seisenberger et al., 2012). Promoters with low or intermediate but not high CpG content become hypermethylated during this time (Borgel et al., 2010). TET1 may function to protect the high CpG content promoters from hypermethylation. This is supported by our finding that the *Oxtr* CpG island (CGI) is hypermethylated in E14.5 cerebrum as well as mesodermal and endodermal tissues but not ESCs.

The most parsimonious explanation would be that without TET1, the *Oxtr* CGI becomes hypermethylated during this onset of *de novo* methylation between E4.5 to 7.5 and the aberrant methylation is then propagated in every cell from that point (Figure 27). Rather than a role in active demethylation, the *Oxtr* data supports a role for TET1
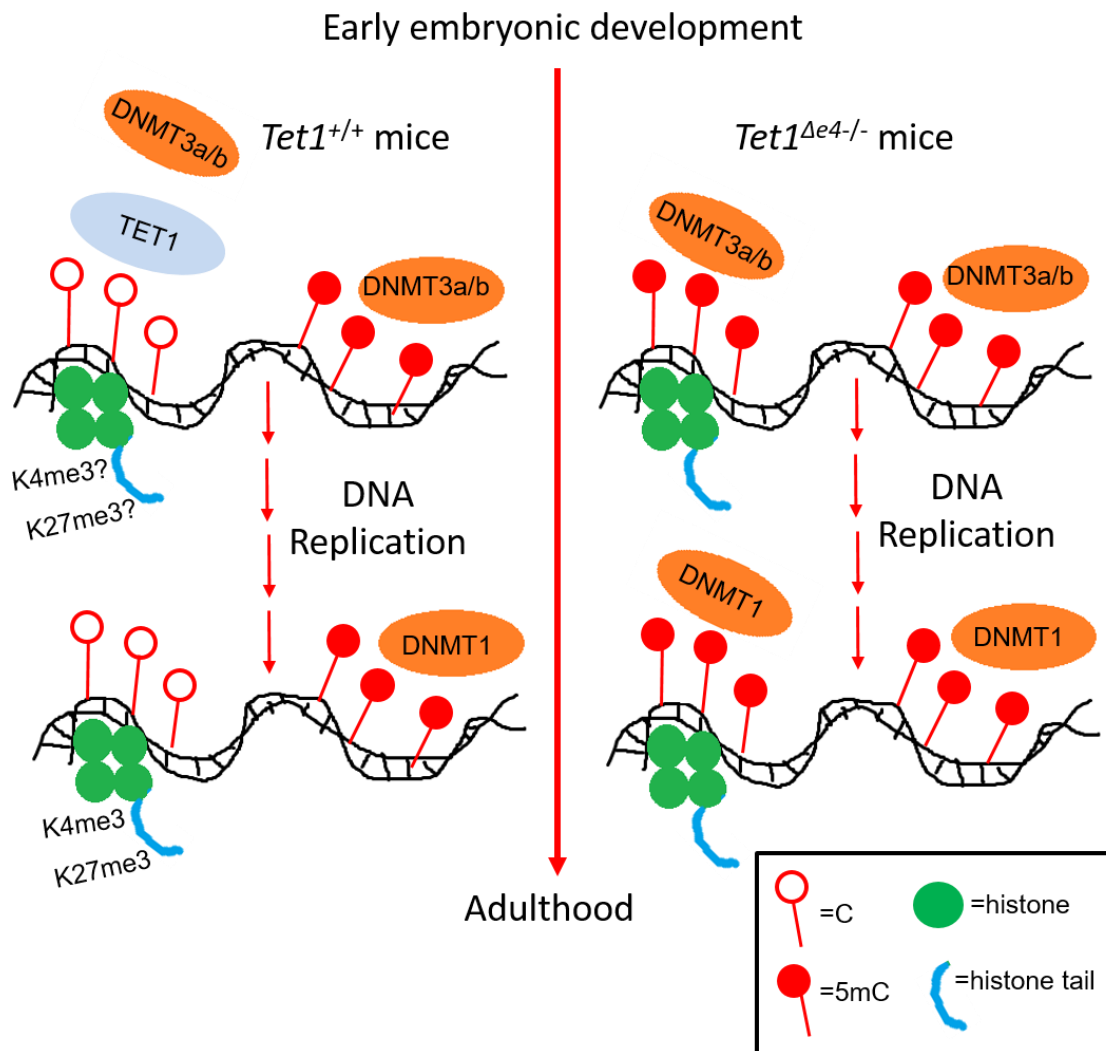
Figure 27: Proposed model for TET1 activity in early development

in preventing *de novo* methylation as has previously been suggested (Jin et al., 2014; Xu

et al., 2011). In addition, the finding of intermediate hypermethylation of *Oxtr* in

heterozygous *Tet1^Δe4+/-* mice suggests that proper establishment of DNA methylation

during development is sensitive to levels of TET1.

Consistent with the finding that TET1 is preferentially bound to CGIs in mouse

ESCs (Xu et al., 2011), we found that depletion of TET1 in the mouse cortex leads to

enrichment of hypermethylated *Tet1*-DMRs in intragenic CGIs. The enrichment suggests

a unique role for TET1 in regulating DNA methylation at intragenic vs promoter CGIs.

Computationally examining the similarities among these hypermethylated CGIs and the

differences between CGIs that are TET1-independent may reveal additional information

about the genomic regions that TET1 regulates. For instance, the hypermethylated CGIs

may share a similar sequence motif, chromatin structure, or chromatin binding partners.

Several *Tet1* knockout, knockdown, and overexpression studies have generated

genome-wide expression, methylation, and TET1 chromatin binding data sets from

different tissues and different stages of development. It would be worthwhile to take a

closer look at these data sets to understand how TET1 functions at particular genomic

loci. For example, it would be interesting to compare the list of CGIs that become *de novo*

methylated during normal embryonic development to TET1 ChIP data. If TET1 is indeed

protecting specific CGIs from hypermethylation, one would predict that TET1 would be

absent from those CGIs that normally become methylated.

Surprisingly, while *Npas4* was hypermethylated in young, naïve mice from either

a mixed or C57Bl/6J background, we did not observe a difference in older mice that had

been through a battery of cognitive tests. It would be interesting to follow this up to see

if *Npas4* methylation in modified by age or experience. Also, future experiments could

examine if there is a correlation between performance in memory-related behaviors and

Npas4 methylation state.

5.2 **The role of TET1 in the regulation of oxytocin receptor**

We assume that less OXTR protein is being produced due to the *Oxtr*

hypermethylation and decreased gene expression, although we did not directly prove it.

We attempted to quantify OXTR protein by Western blot, but our antibody was non-

specific and results were uninterpretable. Another experiment we are currently

performing to test whether oxytocin receptor functionality is impaired is through brain

slice physiology. A recent study demonstrated that oxytocin signaling in the prefrontal

cortex causes interneurons, expressing the oxytocin receptor, to fire (Nakajima et al.,

2014). We are administering oxytocin to slice cultures to see if spike transmission is

decreased in *Tet1*$^{\Delta e4-/-}$ mice.

The exact molecular effect of the hypermethylation in the *Oxtr* BS2 and BS3

remains incomplete. We observed altered histone modifications in the BS2 and BS3

regions suggesting that TET1-mediated establishment of proper *Oxtr* methylation has an

effect on the chromatin structure in the region. While the hypermethylation at *Oxtr* and

Npas4 is likely an accumulation of 5mC and not 5hmC, future studies could distinguish

the content by oxidative bisulfite sequencing.

5.3 The role of TET1 in maternal care, agonistic, and cognitive behaviors

The role of oxytocin and the oxytocin receptor in the neurocircuitry involved in maternal behavior has been well documented (D'Cunha et al., 2011; Olazabal and Young, 2006; Pedersen and Prange, 1979; Pedersen et al., 2006; Shahrokh et al., 2010). Repeated exposure to pups and treatment with sodium butyrate, an HDAC inhibitor, lead to increased oxytocin expression and increased maternal behavior in nulliparous female mice, suggesting an epigenetic effect of pup retrieval (Stolzenberg et al., 2012). In mice, both $Oxtr^{-/-}$ dams and $Oxtr^{-/-}$ virgin females take longer to retrieve pups and spend less time crouching over them in the pup retrieval test (Takayanagi et al., 2005). In addition to aberrant maternal behavior, $Oxtr^{-/-}$ males are more aggressive in the resident intruder test demonstrated by an increase in number and duration of attacks (Takayanagi et al., 2005). Our findings of increased threatening behaviors and decreased maternal care in $Tet1^{\Delta e4-/-}$ mice mimic the findings observed in $Oxtr^{-/-}$ mice and support the dysregulation of $Oxtr$ in causing these behavioral deficits. We acknowledge, however, that in addition to down-regulation of $Oxtr$, there are other dysregulated genes in our $Tet1^{\Delta e4-/-}$ that may confound the interpretation of behavioral phenotypes.

There are few experiments that could be done to more directly link the $Oxtr$ finding with the impaired maternal care and agonistic behaviors in $Tet1^{\Delta e4-/-}$ mice. $Tet1^{\Delta e4-/-}$ mice could be treated with a regimen of oxytocin and tested to see if behaviors are rescued. Behaviors would be rescued assuming that the cause for the behavioral

deficits is due to insufficient response to oxytocin in $Tet1^{\Delta e4-/-}$ mice. Interestingly, intracerebral administration of oxytocin has been shown to rescue the aggression and social and learning deficits in $Oxtr^{-/-}$ mice (Sala et al., 2011). Future experiments could further explore if $Tet1^{\Delta e4-/-}$ mice show the other behavioral deficits observed in $Oxt^{-/-}$ and $Oxtr^{-/-}$ mice such as impairments in sociosexual behavior, sociability and preference for social novelty, and cognitive flexibility (Lee et al., 2008; Nakajima et al., 2014; Takayanagi et al., 2005; Winslow and Insel, 2002).

In any physiological process where DNA methylation has been involved, the *Tet1* and *Tet3* knockout mice present an opportunity for testing their involvement. These would even include studies of behavioral conditions, such as exercise or environmental enrichment, or nutrition. Interestingly, several studies have shown that oxytocin receptor expression is sensitive to neonatal handling and social enrichment (Carter, 2007; Curley et al., 2009). In particular, due to our discovery of the early critical window of establishment of *Oxtr* methylation, future human studies may examine how very early environmental exposures might affect *Tet1* regulation and thus affect *Oxtr* methylation.

5.4 Implications on human studies

Several human studies have found associations between *OXTR* DNA hypermethylation in the human homologous regions of BS2 and BS3 and a wide spectrum of behavioral traits and neuropsychiatric disorders including autism spectrum disorders (ASD) (Bell et al., 2015; Cecil et al., 2014; Dadds et al., 2014; Gregory et al.,

2009; Jack et al., 2012; Puglia et al., 2015; Reiner et al., 2015; Unternaehrer et al., 2012;

Ziegler et al., 2015) (Figure 28). Until now, any mechanism for the cause of
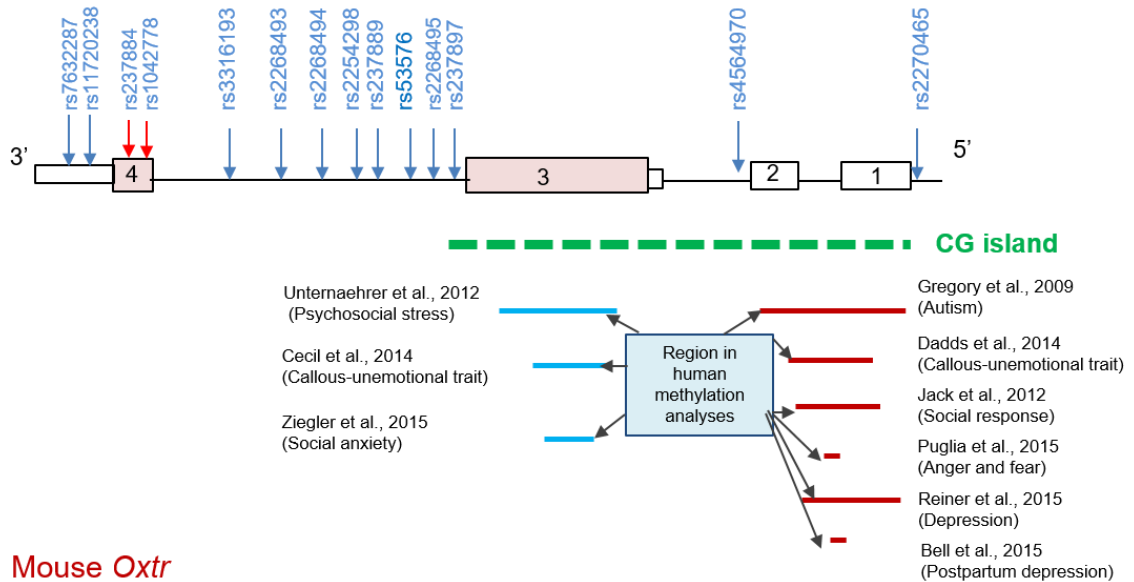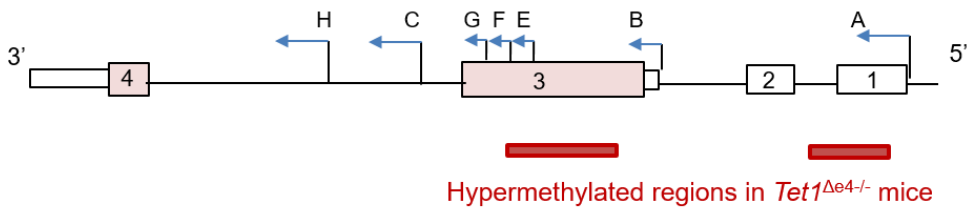
Figure 28: Diagram of human and mouse oxytocin receptors

Human *OXTR* SNPs and methylated regions that have been associated with autism spectrum disorders (ASD) and other neurobehavioral features are indicated. Mouse *Oxtr* mRNA TSSs as well as the BS2 and BS3 regions which are hypermethylated in *Tet1$^{\Delta e4-/-}$* mice are indicated.

hypermethylation was entirely unknown. Our study provides the first evidence of a

mechanism for *OXTR* hypermethylation with accompanying altered histone

modifications. In addition, multiple human studies have found significant association

91

between genomic variants in *OXTR* and autism spectrum disorders (ASD) (Jacob et al., 2007; Lerer et al., 2008; LoParo and Waldman, 2015; Wu et al., 2005).

As we expect the complex transcriptional regulation of *Oxtr* we uncovered in mice to be highly conserved in humans, our findings provide valuable information to re-evaluate whether different OXTR isoforms are likely affected in these studies. Of particular interest, our finding that *Oxtr* is hypermethylated in tissues from all germ layers supports the use of peripheral blood in neurodevelopmental studies. Furthermore, our finding that TET1 has a dosage-sensitive effect on *Oxtr* methylation is particularly interesting considering *TET1* mutations found in ASD are heterozygous. In fact, a TET1 protein-disrupting rare *de novo* variant and *TET1* misexpression have been implicated in ASD (Sanders et al., 2012; Zhubi et al., 2014). Another recent link between TET proteins and *OXTR* regulation was suggested from a study that found *OXTR* among the top 25% of genes enriched with 5hmC in human cerebellum (Wang et al., 2012). Altogether, our discovery of the involvement of TET1 in the epigenetic regulation of *Oxtr* and the complex transcriptional structure of *Oxtr* provide novel insights into understanding the role of OXTR and TET1 in brain function and in neuropsychiatric disorders. These findings will inform future disease related genetic and epigenetic study designs related to *OXTR*.

5.5 Additional future directions

Now that we have generated a list of genes dysregulated in $Tet1^{\Delta e4-/-}$ mice after ECS treatment, there are opportunities for follow-up. In the case of *Npas4* and *Oxtr*, dysregulation was also observed without stimulation. It is unclear whether the dysregulation of the other genes in our study will only be observed after inducing activity. Initially, our gene list could be compared to those reported in the $Tet1^{\Delta e5-/-}$ mouse study of unstimulated hippocampus (Rudenko et al., 2013). Any genes that do not overlap would be candidates for dysregulation specifically after ECS treatment.

Further behavioral studies may also examine *Tet1*-deficiency on a different genetic background. While C57BL/6 mice are widely used in behavior studies, they are also more susceptible to pain, show more dominant behaviors, have increased preference for alcohol and are susceptible to hearing loss (Mogil et al., 1999; Sarna et al., 2000)(Pierce et al., 1998; Willott et al., 2013).

With the increasing identification of abnormal epigenetic marks associated with human disease, there is a growing need to identify epigenetic therapies that can target a specific genetic locus. Would therapies that remove DNA methylation at regulatory regions of neural genes, such as *Oxtr* or *Shank3*, ameliorate the associated behavioral phenotypes? Towards this goal, there have been recent advances in using the CRISPR (clustered, regularly interspaced, short palindromic repeats)-Cas9 system to epigenetically modify single locus (Thakore et al., 2016; Thakore et al., 2015). As targeted

epigenetic modification in the brain becomes a reality, either by CRISPR or some other means, *Oxtr* could be targeted in *Tet1*$^{\Delta e4-/-}$ mice to see if behavioral deficits are rescued.

Denis Noble argued in his book *The Music of Life: Biology beyond the Genome*, "We sometimes seem to have forgotten that the original question in genetics was not what makes a protein but rather 'what makes a dog a dog, a man a man'" (Noble, 2006). One future area of research would be to examine the evolutionary path of TET proteins, both between species and within species. In order to make more informed inferences from research on mouse *Tet1* to human *TET1*, we need to understand the similarities and differences between them. One computational study has already begun such an analysis (Iyer et al., 2009).

Further exploration of the craniofacial abnormalities observed in *Tet1*$^{\Delta e4-/-}$ mice is warranted. Genes involved in epigenetic regulation have been implicated in human facial abnormalities, including *DNMT3B* in Immunodeficiency Centromeric instability Facial anomalies (ICF) syndrome and *HDAC8* in Cornelia de Lange syndrome (Deardorff et al., 2012; Lana et al., 2012). Interestingly, one of the phenotypes of human ICF syndrome is heterogeneous observed facial anomalies including a flattened nasal bridge (Jiang et al., 2005). Future studies could examine methylation anomalies reported in ICF syndrome to see if there is any overlap in *Tet1*$^{\Delta e4-/-}$ mice. It is not surprising that epigenetically modifying genes have been implicated in craniofacial abnormalities. Stem and progenitor cells undergo differentiation during development, which is regulated, at

least in part, by epigenetic modifications (Jaenisch and Bird, 2003). As neural crest cells are predominantly responsible for craniofacial development (Bildsoe et al., 2013; Santagati and Rijli, 2003), it would be interesting to explore if neural crest genes are dysregulated in $Tet1^{\Delta e4-/-}$ mice. Of note, Matrix gla protein (*Mgp*) was the only gene that was dysregulated in $Tet1^{\Delta e5}$ hippocampus, $Tet1^{\Delta e11-13}$ neural progenitor cells, and our ECS-treated $Tet1^{\Delta e4-/-}$ hippocampus (Figure 7F). Mutations in human *MGP*, an extracellular matrix protein implicated in bone and cartilage growth, causes Keutel syndrome which has characteristic midfacial hypoplasia (Munroe et al., 1999). Although similar to the variability observed in human ICF patients, one of the difficulties in pursuing this direction is the incomplete penetrance and variability of the craniofacial phenotype. It is possible that the $Tet1^{\Delta e4-/-}$ mice that do not survive to weaning have a stronger facial phenotype. In order to better understand the penetrance, experiments including craniofacial measurements, bone morphological staining and immunohistochemistry would need to happen at an embryonic stage or at birth.

Appendix A

Primer pairs used in this study

Sequence (5'-3')	Primer Name	Experiment	Annealing Temp. (C°)
TGTTGAGAAAAACGGCACTG	GF1	DNA Genotyping	59
TCGACTAGAGCTTGCGGAAC	GF2	DNA Genotyping	59
GATAGACCACGTGCCTGGAT	GR1	DNA Genotyping	59
GCATCAATCCTCAGGAAAGG	CF1	cDNA Genotyping	59
TGCACCTACTGCAAGAATCG	CF2	cDNA Genotyping	59
TGGGCCTTTTTCTTTTTGTG	CR1	cDNA Genotyping	59
CTCACCCACAACCACAAACAATTTAA ATACGATTAAATAATATTAATATATT ATCGATTAAATAATAATTAATTAATA TTTGATGTGATGGGTGGTATGG	Dot blot control sequence[a]	Dot blot	N/A
CTCACCCACAACCACAAACA	Dot blot control F[a]	Dot blot	58
CCATACCACCCATCACATCA	Dot blot control R[a]	Dot blot	58
TCCTGCTGTGGGAAGGTATC	Tet1_F	qRT-PCR	59
ACAGGTGCAGGTACGCTTTT	Tet1_R	qRT-PCR	59
AAGGTGCCTCTGGAGTGTTG	Tet2_F	qRT-PCR	59
ACCAAGAAAGCAGCTCGAAA	Tet2_R	qRT-PCR	59
ATGGCCCCACTACTGACCTT	Tet3_F	qRT-PCR	59
TACAATGGGTGCACTGTGGT	Tet3_R	qRT-PCR	59
CGCCATGCAATTTCCACTATCAATAA	Bdnf_Exon 4F	qRT-PCR	60
GCCTTCATGCAACCGAAGTA	Bdnf_Exon 1-6R	qRT-PCR	60
AGTTTCAGGAATTTAAGGAAGCTG	Homer1a_F	qRT-PCR	60
CATGATTGCTGAATTGAATGTGTA	Homer1a_R	qRT-PCR	60
CTGCATCTACACTCGCAAGG	Npas4_F	qRT-PCR	59
GCCACAATGTCTTCAAGCTCT	Npas4_R	qRT-PCR	59

CATGGCCTTCCGTGTTCCT	GAPDH_F	qRT-PCR	59
TGATGTCATCATACTTGGCAGGTT	GAPDH_R	qRT-PCR	59
TTCTTCGTGCAGATGTGGAG	Oxtr_ABEFG_F (black arrows)	qRT-PCR	59
TGTAGATCCATGGGTTGCAG	Oxtr_ABEFG_R (black arrows)	qRT-PCR	59
GTAAATTGGTAGAGGATTAAGTTTTT TTTTATTTTTTG	Npas4_ex_F[b]	Bisulfite-sequencing	58
TATCTCACACAAATCCAATACTAAAA CTATC	Npas4_ex_R[b]	Bisulfite-sequencing	58
TTTTGTTAAGGGTTTTAGATTATTTTA ATTTATGTATTG	Npas4_in_F[b]	Bisulfite-sequencing	58
AACCCAAACTACTCACCTCCAAC	Npas4_in_R[b]	Bisulfite-sequencing	58
AGTTGAGTTTTTTTTAAAAAGATGTA AAG	Oxtr_BS1_F	Bisulfite-sequencing	53
AATTAACCCAAAATTACCTTACCAC	Oxtr_BS1_R	Bisulfite-sequencing	53
GGGTATATTTTTTTGGGGTTTTTTTA	Oxtr_BS2_F	Bisulfite-sequencing	53
ACCATCCACTATAATACAACTTCCC	Oxtr_BS2_R	Bisulfite-sequencing	53
TGGAGATAAGTTTGATATTATTGATT	Oxtr_BS3_F	Bisulfite-sequencing	53
CTTTTTCATAAAACACCTAAACATC	Oxtr_BS3_R	Bisulfite-sequencing	53
TGCTAATGCTCGTCTCTCCA	Oxtr_RACE_R1	5'RACE	59
GAGCAGAGCAGCAGAGGAAG	Oxtr_RACE_R2	5'RACE	59
TGTAGATCCATGGGTTGCAG	Oxtr_RACE_R3	5'RACE	59
GGGTGTACCGAGAGAGACTGA	Oxtr_A_F (blue arrows)	qRT-PCR	59
GGTGACTTCTCGGTGGTGA	Oxtr_A_R (blue arrows)	qRT-PCR	59
TTCTCCTGGTTTGTTTCAGG	Oxtr_B_F (purple arrows)	qRT-PCR	59
CCGAGGTCCAACTCGATACT	Oxtr_B_R (purple arrows)	qRT-PCR	59
GCCGCCTGCTATGGTCTC	Oxtr_ABE_F (green arrows)	qRT-PCR	59
CATCTGCACGAAGAAGAAAGG	Oxtr_ABE_R (green arrows)	qRT-PCR	59
TGCATTTGAGTCCAGTCACC	Oxtr_H_F (yellow arrows)	qRT-PCR	59
GGCAATGATGAAGGCAGAAG	Oxtr_H_R (yellow arrows)	qRT-PCR	59
TTCATCATTGCCATGCTCTT	Oxtr_A-H_F (red arrows)	qRT-PCR	59
TGCTAATGCTCGTCTCTCCA	Oxtr_A-H_R (red arrows)	qRT-PCR	59

CCGCAGGCTAGGTAGGAGTT	Oxtr_5'UTR_F	ChIP-qPCR	60
AGTGGATGGCCTCAGAGATG	Oxtr_5'UTR_R	ChIP-qPCR	60
CACTCGCGCCTCTTCTTT	Oxtr_Exon3_F	ChIP-qPCR	60
GCAAGTATTTGACCAGACGACA	Oxtr_Exon3_R	ChIP-qPCR	60
GCATCACCCGGAGGAGAAAATCGG	GAPDH-F	ChIP-qPCR	60
GTCACGTGTCGCAGAGGAGC	GAPDH-R	ChIP-qPCR	60

Appendix B

List of Tet1Δe4-/- downregulated genes from hippocampus 2 hours after ECS.

Ngp	Fgg	Fgfbp1	Ldhd	Igf2	Acer2	Pamr1
S100a8	Slc26a10	Cdh1	Ndn	Fcrls	As3mt	Nxph3
Rdh7	Mup14	Mst1r	Cyp27a1	Aox3	Bmp7	Npas4
S100a9	H2-Q10	Alox12b	Vmn2r29	Col9a2	Dnahc1	Nid1
Has1	Ldoc1	Gpnmb	Col3a1	Slc22a8	Col5a2	AI854703
Gm13152	Cyp2e1	Cyp3a11	Acta2	Lyz2	Tshz2	Sstr1
Wnt6	Akr1c6	Slc38a5	Ly6g6e	Tlr9	Col6a2	Thbd
Adh1	Serpina1c	Creb3l3	Tfr2	Cd74	Fbln1	Cobl
Hp	Fabp1	Asgr1	Alox8	Itih2	Erdr1	Kcnf1
Ambp	Apoc4	Gc	Tpm2	Cd163	Pnma3	Vtn
Arg1	Aldh3a1	Fgb	Dnahc6	Thbs4	Trim66	Slc5a5
Evpl	Pirt	Vill	Nek10	Gjb2	Ctgf	Oxtr
Apoa5	Zfp648	Barx2	Cd59a	Slc13a3	Eln	Abcb1a
D130017N08Rik	Alb	Mpzl2	Tekt5	Slc6a20a	Zfp772	C4b
Kng1	Lect1	Kctd14	Hhatl	Spp1	Islr	Grm2
Mup20	Ahsg	Crabp2	Rbp4	Pcolce	Lamc3	Lama2
Serpina3k	Serpina1d	C3	Col1a1	Gstm6	Btg2	Alad
Dsc3	Apoc3	Slc22a6	Vwf	Mrc2	Rbp1	Cfh
Capn11	Apoc1	Fmod	Pgam2	Card10	Fn1	Foxo1
Apoa2	Bhmt	Aldh1a2	Resp18	Bgn	Ddr2	Kcna6
Apoa1	Slc47a1	Gpr182	Clec3b	Mid1	Gucy1a3	Oxt
Mup7	Foxc2	Clec14a	Gpx3	Myh11	Zic2	Retnlg
Serpina1b	Mrgprf	Col6a6	Mgp	Lama1	Gpr83	
Henmt1	Hmgcs2	Anxa1	Pla2g4e	Nrsn2	Ccnf	
Serpinc1	Hpx	Slc6a13	Col1a2	Ptgds	Ubc	
Mup3	Gnmt	Slc13a4	Gm13157	1700048O20Rik	Ptprb	
Fga	Slc6a12	Tnxb	Spink8	Fam198b	Igfbp2	

List of Tet1Δe4-/- upregulated genes from hippocampus 2 hours after ECS.

Sub1	Spsb1	Gm14420	Atf3	Prph	LOC100861615
Pdia4	Ddo	Gm14295	Gm14322	Gm3002	Gm3893
Rapgef6	B4galt1	Hspa1b	Clcnka	Ptchd1	Gm5506
Commd6	2900052N01Rik	Serpina3n	1500015A07Rik	Gm3558	Tuba1c
Hspa5	Tle1	Gm14403	Wnk4	Gm10406	
Uggt2	Gm14436	Col15a1	C630043F03Rik	Gm5796	

Appendix C

List of neuronal activity-dependent genes from literature search.

Abcd2	Cdk5rap3	Emp1	H2-K1	Lonrf3	P4ha1	Reep1	Spsb1
Acadvl	Cdkn1a	Enah	Habp4	Lrfn1	P4ha2	Rem2	Srf
Acan	Cdkn1b	Epha2	Haghl	Lrrc3	Pak7	Rere	Srsf7
Acp1	Cds1	Eprs	Hcn1	Maff	Pam	Rerg	Sstr2
Acsl4	Chac1	Eps8	Hdac9	Magel2	Pard6a	Rgs10	St3gal1
Acss1	Chaf1a	Erf	Heca	Man1a	Pax1	Rgs2	Stac
Adamts1	Chml	Errfi1	Herpud1	Map3k2	Pcdh17	Rgs4	Stard4
Adcyap1	Chst15	Etv3	Hiat1	Map3k5	Pcdh8	Rgs7bp	Stc2
Adm	Cited1	Etv5	Hif3a	Mapk6	Pcdh9	Rhbdl3	Stk40
Adora2a	Cited2	Fahd1	Hist1h1d	Mbnl2	Pcf11	Rhoq	Stxbp5
Aff1	Cldn1	Fam107b	Hist1h2bc	Mea1	Pcsk1	Ripk2	Sult2b1
Ager	Cldn25	Fam126b	Hist1h3g	Mecom	Pcsk5	Rnd3	Supt4a
AI836003	Clpb	Fam46a	Hivep3	Med14	Pde4dip	Rnf10	Suv420h2
Akr1c13	Clvs1	Fance	Homer1	Meox1	Pdk3	Rnf128	Sv2c
Alcam	Cntnap1	Fastkd5	Hpgd	Mest	Pdlim1	Rnf217	Svil
Ang	Col15a1	Fbln5	Hsd17b12	Mfap3l	Peg10	Rorb	Tac1
Ankzf1	Commd9	Fbxo18	Hsdl1	Mknk2	Peli1	Rpl22	Tacr3
Apba3	Coq10b	Fbxo33	Hspa14	Mkrn1	Per1	Rspo3	Tes
Arc	Cort	Fen1	Hspa1a	Mkrn3	Per2	Samd4	Tfcp2
Areg	Creb1	Fezf2	Hspa4	Mlf1	Pex11a	Sap30	Tgfb2
Arg2	Creld2	Fgf9	Hspa4l	Mllt3	Pex13	Sars2	Tgm3
Arhgap20	Crem	Fgfr1	Hspb3	Morc4	Pfkfb4	Sc4mol	Tgoln1
Arhgap29	Crh	Fgfr2	Hspb8	Mpp3	Phf10	Sc5d	Tiparp
Arih1	Crhbp	Fkbp5	Htr5b	Mpp7	Phka2	Scg2	Tll1
Arl5b	Cryl1	Flnb	Hunk	Mpz	Pim3	Scn3a	Tmed8
Arpp21	Csrnp1	Fmnl1	Ier2	Msh2	Plagl1	Scn8a	Tmem33
Arsa	Ctgf	Fndc3b	Ier3	Msh3	Plat	Sdc2	Tmem47
Asf1a	Cxxc4	Fndc9	Ifrd1	Msi2	Pld2	Serpinb2	Tmem64
Asph	Cyr61	Fos	Igdcc3	Mst1r	Plod2	Sertad1	Tmem74
Asxl1	Cyth1	Fosb	Igf1	Mthfd1l	Pnma2	Sesn2	Tmtc2
Atf3	D16Ertd472e	Fosl2	Igf2bp2	Mthfd2	Pnoc	Sf1	Tmtc4
Atp10d	D3Bwg0562e	Foxk1	Il1a	Mxd4	Pold1	Sf3a2	Tnfrsf12a
Atp1b1	Dab1	Frmd6	Inhba	Mycl1	Polr2e	Sfmbt2	Tnip1
Atp2c1	Dact2	Frmpd3	Ints12	Mylk	Popdc3	Sgk1	Tob2
Atp5s	Dars	Fzd3	Invs	Myo7a	Pou3f1	Sgtb	Tpbg
Azi1	Ddit4	Fzd8	Irf1	Mypop	Ppp1r3c	Sh3rf3	Tpm3
B630005N14Rik	Ddx27	Gabpb1	Irf2bp1	Nab1	Ppp1r3e	Sik1	Traip
Baz1a	Ddx3y	Gadd45b	Itgb8	Nampt	Prkca	Sik2	Trib1
Baz2b	Dio2	Gadd45g	Itpr1	Nat6	Prkg2	Sik3	Trib3
BC022687	Dlc1	Galnt18	Itprip	Ndel1	Prok2	Sirpa	Trim66
Bdnf	Dll1	Galnt9	Jak2	Nedd9	Prox1	Sirt1	Trmt10b
Bhlhe40	Dmtf1	Gas2l3	Jmjd1c	Nek4	Prrt1	Sla	Tyk2

Boc	Dmxl1	Gch1	Jun	Nfil3	Psme4	Slc16a1	Tyro3
Bphl	Dnahc8	Gck	Junb	Nfkbid	Pten	Slc25a3	Ubfd1
Braf	Dnajb1	Gdf10	Kcna1	Nfkbiz	Ptger3	Slc25a36	Ubl3
Btg2	Dnajc1	Gem	Kcna4	Nfya	Ptger4	Slc25a37	Ubn1
Btk	Dnmt1	Gfap	Kcnf1	Nicn1	Ptgs2	Slc27a1	Unc45a
C1ql3	Dok3	Gfod1	Kcnh2	Nme6	Pthlh	Slc2a1	Usp2
C2cd4a	Dusp1	Gkap1	Kcnj3	Nnmt	Ptp4a3	Slc2a3	Usp3
C330006P03Rik	Dusp14	Gla	Kcnj4	Npas4	Ptpn20	Slc35a1	Usp9x
Cacng5	Dusp16	Gm13889	Kcnk1	Nppc	Ptpru	Slc40a1	Vgf
Cad	Dusp4	Gm5124	Kcns2	Nptx2	Purb	Slc4a7	Vkorc1
Calcrl	Dusp5	Gm7120	Keap1	Nr4a1	Pvrl3	Slc5a6	Wdr54
Camk2d	Dusp6	Gmeb2	Kif18a	Nr4a2	Rab11fip2	Slc6a17	Wdr90
Cant1	E2f5	Gmpr	Kif1b	Nr4a3	Rab39	Slc6a6	Wls
Cartpt	E530001K10Rik	Gnai2	Kif22	Nrf1	Rab3c	Slc7a1	Xrcc1
Casp7	Egf	Gnb1	Kitl	Nrip3	Rabgap1l	Slc7a3	Zc3h12c
Cbln1	Egr1	Gpr12	Klf4	Nrn1	Rad51	Slc7a8	Zc3h6
Cc2d1b	Egr2	Gpr19	Klf5	Nrp1	Rai14	Slit2	Zfp105
Cckbr	Egr3	Gpr22	Klf9	Nrsn1	Ralgapa1	Snhg1	Zfp143
Ccnd3	Egr4	Gpr26	Klhl4	Nudt4	Rap1b	Snord22	Zfp688
Ccno	Ehd4	Gpr3	Lamb3	Omg	Rasa4	Sorcs3	Zfyve19
Ccnt1	Eif4ebp1	Gpr50	Leng8	Opn3	Rasgrp1	Sowahb	Zhx2
Cd34	Elac2	Gprin2	Lin7a	Osbpl3	Rbbp6	Sox12	Zkscan14
Cdc14b	Ell2	Gpt2	Lipg	Osgin2	Rbfox2	Spata2l	Zscan2
Cdc26	Elmo1	Grasp	Lmna	Otud1	Rbm11	Spry2	Zwint
Cdh11	Emd	Grk5	Lmo2	Ovca2	Rbm15	Spry4	

Appendix D

List of Tet1-Differentially Methylated Regions in promoter CpG islands in cortex

between Tet1Δe4-/- and Tet1+/+.

Ppp1r2-ps3	Aatk	Il1rl2	Gm5868	Gldn	L3mbtl4	Bhlhb9
E130201H02Rik	Spag16	Gm5878	Npb	Tmem235	Fam120c	Zdhhc15
Trim58	Itpka	Ptchd3	4930524B15Rik	Pnmt	Mmp9	Rab39b
Lect1	Ttc22	Gm5124	Abcb7	Spata22	Klhl40	Nnat
Mycs	Grid2ip	Gm5294	Ddx26b	Amn	Spesp1	Espn
D130017N08Rik	Gpi1	P2rx2	Henmt1	Dnd1	Slc47a1	Nap1l5
Kcne1l	Tnxb	Il12rb2	Slc5a1	Zmat1	Dnmt3a	Gcsh
Abhd16b	Ubqln2	1700020D05Rik	Oxtr	Taf9b	Trpm6	Ngb
Chst5	Zbtb18	Marc1	Foxi2	Bend6	Hmgn5	Cdx1
Nkpd1	Chrne	Spaca1	Shank1	Irs3	Gspt2	Lox
Pfn3	Pcdh19	Krt83	Comp	Acads	Mpp1	Gpm6b
Arxes2	Zar1	Spag6	Cdcp1	Shank2	Col9a2	1700045I19Rik
Ush1g	Scnn1b	Gabre	Gpx1	Ndufc2	Rasip1	Pgr15l
Htr1f	Gfra3	Sycp3	H2-Q5	Otop2	Zfp180	Cdk16
Zfp185	Lbx2	Prps2	Gal	Ccdc177	Cdc42ep5	Lamc3
Alkbh6	Rhcg	Gsn	Zxdb	Hccs	Lyl1	Eva1b
Prtn3	Cspg4	AI854703	Speg	Rab9	Cilp2	Zfp36
Fam26f	Hsd17b1	Ggn	Cpxm2	Adad1	Fbxo39	Il27ra
Krt7	1700106J16Rik	Ccdc151	Insl3	Ndn	Atxn7	Itga11
Abcb1a	Rxfp3	Gpr64	Kremen2	Kcng4	Tdrd6	1700058G18Rik
Zfp872	Esx1	Fsip1	Mfsd7a	Cyb5b	Ammecr1	Jph4

List of Tet1-Differentially Methylated Regions enriched in intragenic CpG islands in cortex between Tet1Δe4-/- and Tet1+/+.

Prdm6	Cacna1a	Tmem150b	Ptprs	Rimbp2	Tfr2	Pglyrp2
Evpl	F12	Kcnip1	Syt7	Muc2	Ncf1	Gucy1b3
Trat1	Sh3pxd2a	Dlgap1	Tmem151a	Arhgap27	Auts2	Zbtb17
Atg7	Rnft2	Ppp1r13l	Slc1a3	Krt42	Plcxd1	Msantd3
Alox5ap	Tcp11	Celf6	Gm4827	4921506M07Rik	Chrna10	Stx1a
Ccdc42b	Stx11	Klc1	Ptchd2	Gpc2	Zfp444	Sirt4
Ppm1h	Obscn	Oprd1	Dos	Map3k10	Evpl	Zfp282
Cacna1b	Trim7	Tcte1	Gpr179	Begain	Wnk4	Irgc1
Actn1	Dlgap3	Aff3	Dmrt3	Zbed3	Cnp	Rsph6a
Cbfa2t3	Zfhx3	Crb2	Jph2	Shank3	Flt4	Marveld3
Tnfrsf1a	Zc3h12d	Proser2	Nr2f6	Neurl1b	Zbtb7c	Kcnn1
1700019B03Rik	Dupd1	Rspo1	Robo3	2900008C10Rik	Pik3ap1	Dock3
Srcin1	Cd80	Nod1	Tbxa2r	Paqr7	Ppfia4	Dscaml1
Cdh20	Araf	Plekhf1	Myl4	Podn	Slc29a4	Tmprss9
Mmp28	C77080	Hapln4	Abr	Fryl	Atp2b2	Ngfr
3632454L22Rik	Slc6a9	Wnt3	Arhgap39	BC018242	Pml	Myo10
Rbpjl	Slc8a2	Esr2	Ccdc88b	Grm1	Epb4.1l2	Mdga1
Sod3	Bai1	Cyp4f39	Tbc1d25	Tmem132e	Exoc3l4	Tmem151a
Dusp8	Tbx5	Srrm2	Rd3	Coro6	Kifc2	Tas1r1
6330408A02Rik	Kcnh2	Wnk4	Cflar	Myh3	Lca5l	Wdfy3
Fam110a	Vgll4	Pdgfb	Gpr162	Ror2	Ptprs	Grm5
Fam189b	Art1	Abcg5	Tshz1	Zbtb20	Neurl1b	Zfp30
Ano1	Cdh23	Ltbp3	Tmem2	Espnl	Rapgef2	Kcnn4
Abca16	Gfod1	Ano7	Caly	Rtkn	Plch2	Mark4
Nedd4l	Wscd2	Atg16l2	Trim72	Ptov1	Gpr153	Vipr1
Runx1	Jakmip3	Kcnj14	Grm2	Clec3b	Dysf	Grm2

Drd4	Lingo1	Rinl	Mgat5b	Smarca4	Trpm1	Nhsl1
Mamld1	Hs3st3b1	Nfix	Wnt3	C2cd4c	Ercc2	Arhgap22
Zfp648	Btnl9	Comp	Ppap2a	Fgf18	Exoc8	Panx2
Jph2	Osbp2	Sowahc	Elfn2	Map3k13	Smad6	
Arhgap23	Gfod1	Tbkbp1	Nhlh1	Lims2	Scara5	
Socs5	Grid1	Tnfrsf13b	Neurl3	Pcdh19	Slc4a8	
Lgr6	Gjb1	Sema5b	Pglyrp3	Bcl2	Tonsl	
Art3	Ankrd35	Pdxdc1	Elfn1	Spen	Scarf2	

References

(1997). Mutant mice and neuroscience: recommendations concerning genetic background. Banbury Conference on genetic background in mice. Neuron 19, 755-759.

Adams, D.J., Quail, M.A., Cox, T., van der Weyden, L., Gorick, B.D., Su, Q., Chan, W.I., Davies, R., Bonfield, J.K., Law, F., *et al.* (2005). A genome-wide, end-sequenced 129Sv BAC library resource for targeting vector construction. Genomics 86, 753-758.

Agranoff, B.W., Davis, R.E., Casola, L., and Lim, R. (1967). Actinomycin D blocks formation of memory of shock-avoidance in goldfish. Science 158, 1600-1601.

Alsina-Llanes, M., De Brun, V., and Olazabal, D.E. (2015). Development and expression of maternal behavior in naive female C57BL/6 mice. Dev Psychobiol 57, 189-200.

Amir, R.E., Van den Veyver, I.B., Wan, M., Tran, C.Q., Francke, U., and Zoghbi, H.Y. (1999). Rett syndrome is caused by mutations in X-linked MECP2, encoding methyl-CpG-binding protein 2. Nat Genet 23, 185-188.

Bachman, M., Uribe-Lewis, S., Yang, X., Williams, M., Murrell, A., and Balasubramanian, S. (2014). 5-Hydroxymethylcytosine is a predominantly stable DNA modification. Nat Chem 6, 1049-1055.

Bao, S., Tang, F., Li, X., Hayashi, K., Gillich, A., Lao, K., and Surani, M.A. (2009). Epigenetic reversion of post-implantation epiblast to pluripotent embryonic stem cells. Nature 461, 1292-1295.

Bell, A.F., Carter, C.S., Steer, C.D., Golding, J., Davis, J.M., Steffen, A.D., Rubin, L.H., Lillard, T.S., Gregory, S.P., Harris, J.C., and Connelly, J.J. (2015). Interaction between oxytocin receptor DNA methylation and genotype is associated with risk of postpartum depression in women without depression in pregnancy. Front Genet 6, 243.

Bergman, Y., and Cedar, H. (2013). DNA methylation dynamics in health and disease. Nat Struct Mol Biol 20, 274-281.

Bernstein, B.E., Mikkelsen, T.S., Xie, X., Kamal, M., Huebert, D.J., Cuff, J., Fry, B., Meissner, A., Wernig, M., Plath, K., *et al.* (2006). A bivalent chromatin structure marks key developmental genes in embryonic stem cells. Cell 125, 315-326.

Bildsoe, H., Loebel, D.A., Jones, V.J., Hor, A.C., Braithwaite, A.W., Chen, Y.T., Behringer, R.R., and Tam, P.P. (2013). The mesenchymal architecture of the cranial mesoderm of mouse embryos is disrupted by the loss of Twist1 function. Dev Biol 374, 295-307.

Booth, M.J., Branco, M.R., Ficz, G., Oxley, D., Krueger, F., Reik, W., and Balasubramanian, S. (2012). Quantitative sequencing of 5-methylcytosine and 5-hydroxymethylcytosine at single-base resolution. Science 336, 934-937.

Borgel, J., Guibert, S., Li, Y., Chiba, H., Schubeler, D., Sasaki, H., Forne, T., and Weber, M. (2010). Targets and dynamics of promoter DNA methylation during early mouse development. Nat Genet 42, 1093-1100.

Brakeman, P.R., Lanahan, A.A., O'Brien, R., Roche, K., Barnes, C.A., Huganir, R.L., and Worley, P.F. (1997). Homer: a protein that selectively binds metabotropic glutamate receptors. Nature 386, 284-288.

Brenet, F., Moh, M., Funk, P., Feierstein, E., Viale, A.J., Socci, N.D., and Scandura, J.M. (2011). DNA methylation of the first exon is tightly linked to transcriptional silencing. PLoS One 6, e14524.

Brown, J.R., Ye, H., Bronson, R.T., Dikkes, P., and Greenberg, M.E. (1996). A defect in nurturing in mice lacking the immediate early gene fosB. Cell 86, 297-309.

Brummelte, S., Mc Glanaghy, E., Bonnin, A., and Oberlander, T.F. (2016). Developmental changes in serotonin signaling: Implications for early brain function, behavior and adaptation. Neuroscience.

Careau, V., Bininda-Emonds, O.R., Ordonez, G., and Garland, T., Jr. (2012). Are voluntary wheel running and open-field behavior correlated in mice? Different answers from comparative and artificial selection approaches. Behav Genet 42, 830-844.

Carter, C.S. (2007). Sex differences in oxytocin and vasopressin: implications for autism spectrum disorders? Behav Brain Res 176, 170-186.

Cecil, C.A., Lysenko, L.J., Jaffee, S.R., Pingault, J.B., Smith, R.G., Relton, C.L., Woodward, G., McArdle, W., Mill, J., and Barker, E.D. (2014). Environmental risk, Oxytocin Receptor Gene (OXTR) methylation and youth callous-unemotional traits: a 13-year longitudinal study. Mol Psychiatry 19, 1071-1077.

Cedar, H., and Bergman, Y. (2009). Linking DNA methylation and histone modification: patterns and paradigms. Nat Rev Genet 10, 295-304.

Colak, D., Zaninovic, N., Cohen, M.S., Rosenwaks, Z., Yang, W.Y., Gerhardt, J., Disney, M.D., and Jaffrey, S.R. (2014). Promoter-bound trinucleotide repeat mRNA drives epigenetic silencing in fragile X syndrome. Science 343, 1002-1005.

Cole, A.J., Abu-Shakra, S., Saffen, D.W., Baraban, J.M., and Worley, P.F. (1990). Rapid rise in transcription factor mRNAs in rat brain after electroshock-induced seizures. J Neurochem 55, 1920-1927.

Consortium, E.P. (2012). An integrated encyclopedia of DNA elements in the human genome. Nature 489, 57-74.

Crawley, J., and Goodwin, F.K. (1980). Preliminary report of a simple animal behavior model for the anxiolytic effects of benzodiazepines. Pharmacol Biochem Behav 13, 167-170.

Crepaldi, L., Policarpi, C., Coatti, A., Sherlock, W.T., Jongbloets, B.C., Down, T.A., and Riccio, A. (2013). Binding of TFIIIC to sine elements controls the relocation of activity-dependent neuronal genes to transcription factories. PLoS Genet 9, e1003699.

Curley, J.P., Davidson, S., Bateson, P., and Champagne, F.A. (2009). Social enrichment during postnatal development induces transgenerational effects on emotional and reproductive behavior in mice. Front Behav Neurosci 3, 25.

D'Cunha, T.M., King, S.J., Fleming, A.S., and Levy, F. (2011). Oxytocin receptors in the nucleus accumbens shell are involved in the consolidation of maternal memory in postpartum rats. Horm Behav 59, 14-21.

Dadds, M.R., Moul, C., Cauchi, A., Dobson-Stone, C., Hawes, D.J., Brennan, J., and Ebstein, R.E. (2014). Methylation of the oxytocin receptor gene and oxytocin blood levels in the development of psychopathy. Dev Psychopathol 26, 33-40.

Dawlaty, M.M., Ganz, K., Powell, B.E., Hu, Y.C., Markoulaki, S., Cheng, A.W., Gao, Q., Kim, J., Choi, S.W., Page, D.C., and Jaenisch, R. (2011). Tet1 is dispensable for maintaining pluripotency and its loss is compatible with embryonic and postnatal development. Cell Stem Cell 9, 166-175.

Deardorff, M.A., Bando, M., Nakato, R., Watrin, E., Itoh, T., Minamino, M., Saitoh, K., Komata, M., Katou, Y., Clark, D., *et al.* (2012). HDAC8 mutations in Cornelia de Lange syndrome affect the cohesin acetylation cycle. Nature 489, 313-317.

Dityatev, A., Schachner, M., and Sonderegger, P. (2010). The dual role of the extracellular matrix in synaptic plasticity and homeostasis. Nat Rev Neurosci 11, 735-746.

Esteller, M., Garcia-Foncillas, J., Andion, E., Goodman, S.N., Hidalgo, O.F., Vanaclocha, V., Baylin, S.B., and Herman, J.G. (2000). Inactivation of the DNA-repair gene MGMT and the clinical response of gliomas to alkylating agents. N Engl J Med 343, 1350-1354.

Feng, J., Zhou, Y., Campbell, S.L., Le, T., Li, E., Sweatt, J.D., Silva, A.J., and Fan, G. (2010). Dnmt1 and Dnmt3a maintain DNA methylation and regulate synaptic function in adult forebrain neurons. Nat Neurosci 13, 423-430.

Ficz, G., Branco, M.R., Seisenberger, S., Santos, F., Krueger, F., Hore, T.A., Marques, C.J., Andrews, S., and Reik, W. (2011). Dynamic regulation of 5-hydroxymethylcytosine in mouse ES cells and during differentiation. Nature 473, 398-402.

French, P.J., O'Connor, V., Voss, K., Stean, T., Hunt, S.P., and Bliss, T.V. (2001). Seizure-induced gene expression in area CA1 of the mouse hippocampus. Eur J Neurosci 14, 2037-2041.

Frommer, M., McDonald, L.E., Millar, D.S., Collis, C.M., Watt, F., Grigg, G.W., Molloy, P.L., and Paul, C.L. (1992). A genomic sequencing protocol that yields a positive display of 5-methylcytosine residues in individual DNA strands. Proceedings of the National Academy of Sciences of the United States of America 89, 1827-1831.

Globisch, D., Munzel, M., Muller, M., Michalakis, S., Wagner, M., Koch, S., Bruckl, T., Biel, M., and Carell, T. (2010). Tissue distribution of 5-hydroxymethylcytosine and search for active demethylation intermediates. PLoS One 5, e15367.

Goldsmith, J.F., Brain, P.F., and Benton, D. (1978). Effects of the duration of individual or group housing on behavioural and adrenocortical reactivity in male mice. Physiol Behav 21, 757-760.

Gregory, S.G., Connelly, J.J., Towers, A.J., Johnson, J., Biscocho, D., Markunas, C.A., Lintas, C., Abramson, R.K., Wright, H.H., Ellis, P., *et al.* (2009). Genomic and epigenetic evidence for oxytocin receptor deficiency in autism. BMC Med 7, 62.

Grove, M., Demyanenko, G., Echarri, A., Zipfel, P.A., Quiroz, M.E., Rodriguiz, R.M., Playford, M., Martensen, S.A., Robinson, M.R., Wetsel, W.C., *et al*. (2004). ABI2-deficient mice exhibit defective cell migration, aberrant dendritic spine morphogenesis, and deficits in learning and memory. Mol Cell Biol 24, 10905-10922.

Gu, T.P., Guo, F., Yang, H., Wu, H.P., Xu, G.F., Liu, W., Xie, Z.G., Shi, L., He, X., Jin, S.G., *et al*. (2011). The role of Tet3 DNA dioxygenase in epigenetic reprogramming by oocytes. Nature 477, 606-610.

Guan, J.S., Haggarty, S.J., Giacometti, E., Dannenberg, J.H., Joseph, N., Gao, J., Nieland, T.J., Zhou, Y., Wang, X., Mazitschek, R., *et al*. (2009). HDAC2 negatively regulates memory formation and synaptic plasticity. Nature 459, 55-60.

Guan, Z., Giustetto, M., Lomvardas, S., Kim, J.H., Miniaci, M.C., Schwartz, J.H., Thanos, D., and Kandel, E.R. (2002). Integration of long-term-memory-related synaptic plasticity involves bidirectional regulation of gene expression and chromatin structure. Cell 111, 483-493.

Guo, J.U., Ma, D.K., Mo, H., Ball, M.P., Jang, M.H., Bonaguidi, M.A., Balazer, J.A., Eaves, H.L., Xie, B., Ford, E., *et al*. (2011a). Neuronal activity modifies the DNA methylation landscape in the adult brain. Nat Neurosci 14, 1345-1351.

Guo, J.U., Su, Y., Zhong, C., Ming, G.L., and Song, H. (2011b). Hydroxylation of 5-methylcytosine by TET1 promotes active DNA demethylation in the adult brain. Cell 145, 423-434.

Gupta, S., Kim, S.Y., Artis, S., Molfese, D.L., Schumacher, A., Sweatt, J.D., Paylor, R.E., and Lubin, F.D. (2010). Histone methylation regulates memory formation. J Neurosci 30, 3589-3599.

Hajkova, P., Ancelin, K., Waldmann, T., Lacoste, N., Lange, U.C., Cesari, F., Lee, C., Almouzni, G., Schneider, R., and Surani, M.A. (2008). Chromatin dynamics during epigenetic reprogramming in the mouse germ line. Nature 452, 877-881.

Hansen, R.S., Wijmenga, C., Luo, P., Stanek, A.M., Canfield, T.K., Weemaes, C.M., and Gartler, S.M. (1999). The DNMT3B DNA methyltransferase gene is mutated in the ICF immunodeficiency syndrome. Proceedings of the National Academy of Sciences of the United States of America 96, 14412-14417.

He, Y.F., Li, B.Z., Li, Z., Liu, P., Wang, Y., Tang, Q., Ding, J., Jia, Y., Chen, Z., Li, L., *et al.* (2011). Tet-mediated formation of 5-carboxylcytosine and its excision by TDG in mammalian DNA. Science 333, 1303-1307.

Hitti, F.L., and Siegelbaum, S.A. (2014). The hippocampal CA2 region is essential for social memory. Nature 508, 88-92.

Huang, Y., Pastor, W.A., Shen, Y., Tahiliani, M., Liu, D.R., and Rao, A. (2010). The behaviour of 5-hydroxymethylcytosine in bisulfite sequencing. PLoS One 5, e8888.

Ito, S., D'Alessio, A.C., Taranova, O.V., Hong, K., Sowers, L.C., and Zhang, Y. (2010). Role of Tet proteins in 5mC to 5hmC conversion, ES-cell self-renewal and inner cell mass specification. Nature 466, 1129-1133.

Ito, S., Shen, L., Dai, Q., Wu, S.C., Collins, L.B., Swenberg, J.A., He, C., and Zhang, Y. (2011). Tet proteins can convert 5-methylcytosine to 5-formylcytosine and 5-carboxylcytosine. Science 333, 1300-1303.

Iyer, L.M., Tahiliani, M., Rao, A., and Aravind, L. (2009). Prediction of novel families of enzymes involved in oxidative and other complex modifications of bases in nucleic acids. Cell Cycle 8, 1698-1710.

Jabbari, K., and Bernardi, G. (2004). Cytosine methylation and CpG, TpG (CpA) and TpA frequencies. Gene 333, 143-149.

Jack, A., Connelly, J.J., and Morris, J.P. (2012). DNA methylation of the oxytocin receptor gene predicts neural response to ambiguous social stimuli. Front Hum Neurosci 6, 280.

Jacob, S., Brune, C.W., Carter, C.S., Leventhal, B.L., Lord, C., and Cook, E.H., Jr. (2007). Association of the oxytocin receptor gene (OXTR) in Caucasian children and adolescents with autism. Neurosci Lett 417, 6-9.

Jaenisch, R., and Bird, A. (2003). Epigenetic regulation of gene expression: how the genome integrates intrinsic and environmental signals. Nat Genet 33 Suppl, 245-254.

Jiang, Y.H., Sahoo, T., Michaelis, R.C., Bercovich, D., Bressler, J., Kashork, C.D., Liu, Q., Shaffer, L.G., Schroer, R.J., Stockton, D.W., *et al.* (2004). A mixed epigenetic/genetic model for oligogenic inheritance of autism with a limited role for UBE3A. Am J Med Genet A 131, 1-10.

Jiang, Y.L., Rigolet, M., Bourc'his, D., Nigon, F., Bokesoy, I., Fryns, J.P., Hulten, M., Jonveaux, P., Maraschio, P., Megarbane, A., *et al.* (2005). DNMT3B mutations and DNA methylation defect define two types of ICF syndrome. Hum Mutat 25, 56-63.

Jin, C., Lu, Y., Jelinek, J., Liang, S., Estecio, M.R., Barton, M.C., and Issa, J.P. (2014). TET1 is a maintenance DNA demethylase that prevents methylation spreading in differentiated cells. Nucleic Acids Res 42, 6956-6971.

Jones, B.J., and Roberts, D.J. (1968). A rotarod suitable for quantitative measurements of motor incoordination in naive mice. Naunyn Schmiedebergs Arch Exp Pathol Pharmakol 259, 211.

Jones, P.A. (2012). Functions of DNA methylation: islands, start sites, gene bodies and beyond. Nat Rev Genet 13, 484-492.

Kaas, G.A., Zhong, C., Eason, D.E., Ross, D.L., Vachhani, R.V., Ming, G.L., King, J.R., Song, H., and Sweatt, J.D. (2013). TET1 controls CNS 5-methylcytosine hydroxylation, active DNA demethylation, gene transcription, and memory formation. Neuron 79, 1086-1093.

Kafri, T., Ariel, M., Brandeis, M., Shemer, R., Urven, L., McCarrey, J., Cedar, H., and Razin, A. (1992). Developmental pattern of gene-specific DNA methylation in the mouse embryo and germ line. Genes Dev 6, 705-714.

Kim, T.K., Hemberg, M., Gray, J.M., Costa, A.M., Bear, D.M., Wu, J., Harmin, D.A., Laptewicz, M., Barbara-Haley, K., Kuersten, S., *et al.* (2010). Widespread transcription at neuronal activity-regulated enhancers. Nature 465, 182-187.

Koh, K.P., Yabuuchi, A., Rao, S., Huang, Y., Cunniff, K., Nardone, J., Laiho, A., Tahiliani, M., Sommer, C.A., Mostoslavsky, G., *et al.* (2011). Tet1 and Tet2 regulate 5-hydroxymethylcytosine production and cell lineage specification in mouse embryonic stem cells. Cell Stem Cell 8, 200-213.

Kriaucionis, S., and Heintz, N. (2009). The nuclear DNA base 5-hydroxymethylcytosine is present in Purkinje neurons and the brain. Science 324, 929-930.

Kubota, Y., Kimura, T., Hashimoto, K., Tokugawa, Y., Nobunaga, K., Azuma, C., Saji, F., and Murata, Y. (1996). Structure and expression of the mouse oxytocin receptor gene. Mol Cell Endocrinol 124, 25-32.

Kumar, D., Aggarwal, M., Kaas, G.A., Lewis, J., Wang, J., Ross, D.L., Zhong, C., Kennedy, A., Song, H., and Sweatt, J.D. (2015). Tet1 Oxidase Regulates Neuronal Gene Transcription, Active DNA Hydroxy-methylation, Object Location Memory, and Threat Recognition Memory. Neuroepigenetics 4, 12-27.

Kusui, C., Kimura, T., Ogita, K., Nakamura, H., Matsumura, Y., Koyama, M., Azuma, C., and Murata, Y. (2001). DNA methylation of the human oxytocin receptor gene promoter regulates tissue-specific gene suppression. Biochem Biophys Res Commun 289, 681-686.

Lalonde, R., and Strazielle, C. (2008). Relations between open-field, elevated plus-maze, and emergence tests as displayed by C57/BL6J and BALB/c mice. J Neurosci Methods 171, 48-52.

Lam, A.L., Pazin, D.E., and Sullivan, B.A. (2005). Control of gene expression and assembly of chromosomal subdomains by chromatin regulators with antagonistic functions. Chromosoma 114, 242-251.

Lana, E., Megarbane, A., Tourriere, H., Sarda, P., Lefranc, G., Claustres, M., and De Sario, A. (2012). DNA replication is altered in Immunodeficiency Centromeric instability Facial anomalies (ICF) cells carrying DNMT3B mutations. Eur J Hum Genet 20, 1044-1050.

Lee, H.J., Caldwell, H.K., Macbeth, A.H., Tolu, S.G., and Young, W.S., 3rd (2008). A conditional knockout mouse line of the oxytocin receptor. Endocrinology 149, 3256-3263.

Lee, W.H., Morton, R.A., Epstein, J.I., Brooks, J.D., Campbell, P.A., Bova, G.S., Hsieh, W.S., Isaacs, W.B., and Nelson, W.G. (1994). Cytidine methylation of regulatory sequences near the pi-class glutathione S-transferase gene accompanies human prostatic carcinogenesis. Proceedings of the National Academy of Sciences of the United States of America 91, 11733-11737.

Lerer, E., Levi, S., Salomon, S., Darvasi, A., Yirmiya, N., and Ebstein, R.P. (2008). Association between the oxytocin receptor (OXTR) gene and autism: relationship to Vineland Adaptive Behavior Scales and cognition. Mol Psychiatry 13, 980-988.

Lin, Y., Bloodgood, B.L., Hauser, J.L., Lapan, A.D., Koon, A.C., Kim, T.K., Hu, L.S., Malik, A.N., and Greenberg, M.E. (2008). Activity-dependent regulation of inhibitory synapse development by Npas4. Nature 455, 1198-1204.

Liu, P., Jenkins, N.A., and Copeland, N.G. (2003). A highly efficient recombineering-based method for generating conditional knockout mutations. Genome Res 13, 476-484.

Lonstein, J.S., and De Vries, G.J. (2000). Sex differences in the parental behavior of rodents. Neurosci Biobehav Rev 24, 669-686.

LoParo, D., and Waldman, I.D. (2015). The oxytocin receptor gene (OXTR) is associated with autism spectrum disorder: a meta-analysis. Mol Psychiatry 20, 640-646.

Lorsbach, R.B., Moore, J., Mathew, S., Raimondi, S.C., Mukatira, S.T., and Downing, J.R. (2003). TET1, a member of a novel protein family, is fused to MLL in acute myeloid leukemia containing the t(10;11)(q22;q23). Leukemia 17, 637-641.

Lubin, F.D., Roth, T.L., and Sweatt, J.D. (2008). Epigenetic regulation of BDNF gene transcription in the consolidation of fear memory. J Neurosci 28, 10576-10586.

Ma, D.K., Jang, M.H., Guo, J.U., Kitabatake, Y., Chang, M.L., Pow-Anpongkul, N., Flavell, R.A., Lu, B., Ming, G.L., and Song, H. (2009). Neuronal activity-induced Gadd45b promotes epigenetic DNA demethylation and adult neurogenesis. Science 323, 1074-1077.

Malik, A.N., Vierbuchen, T., Hemberg, M., Rubin, A.A., Ling, E., Couch, C.H., Stroud, H., Spiegel, I., Farh, K.K., Harmin, D.A., and Greenberg, M.E. (2014). Genome-wide identification and characterization of functional neuronal activity-dependent enhancers. Nat Neurosci 17, 1330-1339.

Mamrut, S., Harony, H., Sood, R., Shahar-Gold, H., Gainer, H., Shi, Y.J., Barki-Harrington, L., and Wagner, S. (2013). DNA methylation of specific CpG sites in the promoter region regulates the transcription of the mouse oxytocin receptor. PLoS One 8, e56869.

Mayer, W., Niveleau, A., Walter, J., Fundele, R., and Haaf, T. (2000). Demethylation of the zygotic paternal genome. Nature 403, 501-502.

Millan, M.J. (2013). An epigenetic framework for neurodevelopmental disorders: from pathogenesis to potential therapy. Neuropharmacology 68, 2-82.

Mogil, J.S., Wilson, S.G., Bon, K., Lee, S.E., Chung, K., Raber, P., Pieper, J.O., Hain, H.S., Belknap, J.K., Hubert, L., *et al.* (1999). Heritability of nociception I: responses of 11 inbred mouse strains on 12 measures of nociception. Pain 80, 67-82.

More, L. (2008). Intra-female aggression in the mouse (Mus musculus domesticus) is linked to the estrous cycle regularity but not to ovulation. Aggress Behav 34, 46-50.

Morgan, H.D., Dean, W., Coker, H.A., Reik, W., and Petersen-Mahrt, S.K. (2004). Activation-induced cytidine deaminase deaminates 5-methylcytosine in DNA and is expressed in pluripotent tissues: implications for epigenetic reprogramming. J Biol Chem 279, 52353-52360.

Moy, S.S., Nadler, J.J., Perez, A., Barbaro, R.P., Johns, J.M., Magnuson, T.R., Piven, J., and Crawley, J.N. (2004). Sociability and preference for social novelty in five inbred strains: an approach to assess autistic-like behavior in mice. Genes Brain Behav 3, 287-302.

Munroe, P.B., Olgunturk, R.O., Fryns, J.P., Van Maldergem, L., Ziereisen, F., Yuksel, B., Gardiner, R.M., and Chung, E. (1999). Mutations in the gene encoding the human matrix Gla protein cause Keutel syndrome. Nat Genet 21, 142-144.

Munzel, M., Globisch, D., Bruckl, T., Wagner, M., Welzmiller, V., Michalakis, S., Muller, M., Biel, M., and Carell, T. (2010). Quantification of the sixth DNA base hydroxymethylcytosine in the brain. Angew Chem Int Ed Engl 49, 5375-5377.

Nakajima, M., Gorlich, A., and Heintz, N. (2014). Oxytocin modulates female sociosexual behavior through a specific class of prefrontal cortical interneurons. Cell 159, 295-305.

Nardone, S., Sams, D.S., Reuveni, E., Getselter, D., Oron, O., Karpuj, M., and Elliott, E. (2014). DNA methylation analysis of the autistic brain reveals multiple dysregulated biological pathways. Transl Psychiatry 4, e433.

Nibuya, M., Morinobu, S., and Duman, R.S. (1995). Regulation of BDNF and trkB mRNA in rat brain by chronic electroconvulsive seizure and antidepressant drug treatments. J Neurosci 15, 7539-7547.

Noirot, E. (1969). Changes in responsiveness to young in the adult mouse. V. Priming. Anim Behav 17, 542-546.

Olazabal, D.E., and Young, L.J. (2006). Oxytocin receptors in the nucleus accumbens facilitate "spontaneous" maternal behavior in adult female prairie voles. Neuroscience 141, 559-568.

Ono, R., Taki, T., Taketani, T., Taniwaki, M., Kobayashi, H., and Hayashi, Y. (2002). LCX, leukemia-associated protein with a CXXC domain, is fused to MLL in acute myeloid leukemia with trilineage dysplasia having t(10;11)(q22;q23). Cancer Res 62, 4075-4080.

Oswald, J., Engemann, S., Lane, N., Mayer, W., Olek, A., Fundele, R., Dean, W., Reik, W., and Walter, J. (2000). Active demethylation of the paternal genome in the mouse zygote. Curr Biol 10, 475-478.

Park, C.S., Gong, R., Stuart, J., and Tang, S.J. (2006). Molecular network and chromosomal clustering of genes involved in synaptic plasticity in the hippocampus. J Biol Chem 281, 30195-30211.

Pedersen, C.A., and Prange, A.J., Jr. (1979). Induction of maternal behavior in virgin rats after intracerebroventricular administration of oxytocin. Proceedings of the National Academy of Sciences of the United States of America 76, 6661-6665.

Pedersen, C.A., Vadlamudi, S.V., Boccia, M.L., and Amico, J.A. (2006). Maternal behavior deficits in nulliparous oxytocin knockout mice. Genes Brain Behav 5, 274-281.

Piekarz, R.L., and Bates, S.E. (2009). Epigenetic modifiers: basic understanding and clinical development. Clin Cancer Res 15, 3918-3926.

Porton, B., Rodriguiz, R.M., Phillips, L.E., Gilbert, J.W.t., Feng, J., Greengard, P., Kao, H.T., and Wetsel, W.C. (2010). Mice lacking synapsin III show abnormalities in explicit memory and conditioned fear. Genes Brain Behav 9, 257-268.

Prut, L., and Belzung, C. (2003). The open field as a paradigm to measure the effects of drugs on anxiety-like behaviors: a review. Eur J Pharmacol 463, 3-33.

Puglia, M.H., Lillard, T.S., Morris, J.P., and Connelly, J.J. (2015). Epigenetic modification of the oxytocin receptor gene influences the perception of anger and fear in the human brain. Proceedings of the National Academy of Sciences of the United States of America 112, 3308-3313.

Ramamoorthi, K., Fropf, R., Belfort, G.M., Fitzmaurice, H.L., McKinney, R.M., Neve, R.L., Otto, T., and Lin, Y. (2011). Npas4 regulates a transcriptional program in CA3 required for contextual memory formation. Science 334, 1669-1675.

Reiner, I., Van, I.M.H., Bakermans-Kranenburg, M.J., Bleich, S., Beutel, M., and Frieling, H. (2015). Methylation of the oxytocin receptor gene in clinically depressed patients compared to controls: The role of OXTR rs53576 genotype. J Psychiatr Res 65, 9-15.

Ribar, T.J., Rodriguiz, R.M., Khiroug, L., Wetsel, W.C., Augustine, G.J., and Means, A.R. (2000). Cerebellar defects in Ca2+/calmodulin kinase IV-deficient mice. J Neurosci 20, RC107.

Roberts, A.C., Diez-Garcia, J., Rodriguiz, R.M., Lopez, I.P., Lujan, R., Martinez-Turrillas, R., Pico, E., Henson, M.A., Bernardo, D.R., Jarrett, T.M., *et al.* (2009). Downregulation of NR3A-containing NMDARs is required for synapse maturation and memory consolidation. Neuron 63, 342-356.

Rodriguiz, R.M., Colvin, J.S., and Wetsel, W.C. (2011). Neurophenotyping genetically modified mice for social behavior. Methods Mol Biol 768, 343-363.

Rohde, C., Zhang, Y., Reinhardt, R., and Jeltsch, A. (2010). BISMA--fast and accurate bisulfite sequencing data analysis of individual clones from unique and repetitive sequences. BMC Bioinformatics 11, 230.

Rudenko, A., Dawlaty, M.M., Seo, J., Cheng, A.W., Meng, J., Le, T., Faull, K.F., Jaenisch, R., and Tsai, L.H. (2013). Tet1 is critical for neuronal activity-regulated gene expression and memory extinction. Neuron 79, 1109-1122.

Russell, J.A., Leng, G., and Douglas, A.J. (2003). The magnocellular oxytocin system, the fount of maternity: adaptations in pregnancy. Front Neuroendocrinol 24, 27-61.

Sala, M., Braida, D., Lentini, D., Busnelli, M., Bulgheroni, E., Capurro, V., Finardi, A., Donzelli, A., Pattini, L., Rubino, T., *et al.* (2011). Pharmacologic rescue of impaired cognitive flexibility, social deficits, increased aggression, and seizure susceptibility in oxytocin receptor null mice: a neurobehavioral model of autism. Biol Psychiatry 69, 875-882.

Sanders, S.J., Murtha, M.T., Gupta, A.R., Murdoch, J.D., Raubeson, M.J., Willsey, A.J., Ercan-Sencicek, A.G., DiLullo, N.M., Parikshak, N.N., Stein, J.L., *et al.* (2012). De novo mutations revealed by whole-exome sequencing are strongly associated with autism. Nature 485, 237-241.

Santagati, F., and Rijli, F.M. (2003). Cranial neural crest and the building of the vertebrate head. Nat Rev Neurosci 4, 806-818.

Sarna, J.R., Dyck, R.H., and Whishaw, I.Q. (2000). The Dalila effect: C57BL6 mice barber whiskers by plucking. Behav Brain Res 108, 39-45.

Scoville, W.B., and Milner, B. (1957). Loss of recent memory after bilateral hippocampal lesions. J Neurol Neurosurg Psychiatry 20, 11-21.

Seisenberger, S., Andrews, S., Krueger, F., Arand, J., Walter, J., Santos, F., Popp, C., Thienpont, B., Dean, W., and Reik, W. (2012). The dynamics of genome-wide DNA methylation reprogramming in mouse primordial germ cells. Mol Cell 48, 849-862.

Serandour, A.A., Avner, S., Oger, F., Bizot, M., Percevault, F., Lucchetti-Miganeh, C., Palierne, G., Gheeraert, C., Barloy-Hubler, F., Peron, C.L., *et al.* (2012). Dynamic hydroxymethylation of deoxyribonucleic acid marks differentiation-associated enhancers. Nucleic Acids Res 40, 8255-8265.

Shahrokh, D.K., Zhang, T.Y., Diorio, J., Gratton, A., and Meaney, M.J. (2010). Oxytocin-dopamine interactions mediate variations in maternal behavior in the rat. Endocrinology 151, 2276-2286.

Shen, L., Inoue, A., He, J., Liu, Y., Lu, F., and Zhang, Y. (2014). Tet3 and DNA replication mediate demethylation of both the maternal and paternal genomes in mouse zygotes. Cell Stem Cell 15, 459-470.

Smith, Z.D., and Meissner, A. (2013). DNA methylation: roles in mammalian development. Nat Rev Genet 14, 204-220.

Song, C.X., Szulwach, K.E., Fu, Y., Dai, Q., Yi, C., Li, X., Li, Y., Chen, C.H., Zhang, W., Jian, X., *et al.* (2011). Selective chemical labeling reveals the genome-wide distribution of 5-hydroxymethylcytosine. Nat Biotechnol 29, 68-72.

Spiegel, I., Mardinly, A.R., Gabel, H.W., Bazinet, J.E., Couch, C.H., Tzeng, C.P., Harmin, D.A., and Greenberg, M.E. (2014). Npas4 regulates excitatory-inhibitory balance within neural circuits through cell-type-specific gene programs. Cell 157, 1216-1229.

Stolzenberg, D.S., and Rissman, E.F. (2011). Oestrogen-independent, experience-induced maternal behaviour in female mice. J Neuroendocrinol 23, 345-354.

Stolzenberg, D.S., Stevens, J.S., and Rissman, E.F. (2012). Experience-facilitated improvements in pup retrieval; evidence for an epigenetic effect. Horm Behav 62, 128-135.

Surani, M.A., Hayashi, K., and Hajkova, P. (2007). Genetic and epigenetic regulators of pluripotency. Cell 128, 747-762.

Szwagierczak, A., Bultmann, S., Schmidt, C.S., Spada, F., and Leonhardt, H. (2010). Sensitive enzymatic quantification of 5-hydroxymethylcytosine in genomic DNA. Nucleic Acids Res 38, e181.

Tahiliani, M., Koh, K.P., Shen, Y., Pastor, W.A., Bandukwala, H., Brudno, Y., Agarwal, S., Iyer, L.M., Liu, D.R., Aravind, L., and Rao, A. (2009). Conversion of 5-methylcytosine to 5-hydroxymethylcytosine in mammalian DNA by MLL partner TET1. Science 324, 930-935.

Takayanagi, Y., Yoshida, M., Bielsky, I.F., Ross, H.E., Kawamata, M., Onaka, T., Yanagisawa, T., Kimura, T., Matzuk, M.M., Young, L.J., and Nishimori, K. (2005). Pervasive social deficits, but normal parturition, in oxytocin receptor-deficient mice. Proceedings of the National Academy of Sciences of the United States of America 102, 16096-16101.

Taylor, G.A., Rodriguiz, R.M., Greene, R.I., Daniell, X., Henry, S.C., Crooks, K.R., Kotloski, R., Tessarollo, L., Phillips, L.E., and Wetsel, W.C. (2008). Behavioral characterization of P311 knockout mice. Genes Brain Behav 7, 786-795.

Thakore, P.I., Black, J.B., Hilton, I.B., and Gersbach, C.A. (2016). Editing the epigenome: technologies for programmable transcription and epigenetic modulation. Nat Methods 13, 127-137.

Thakore, P.I., D'Ippolito, A.M., Song, L., Safi, A., Shivakumar, N.K., Kabadi, A.M., Reddy, T.E., Crawford, G.E., and Gersbach, C.A. (2015). Highly specific epigenome editing by CRISPR-Cas9 repressors for silencing of distal regulatory elements. Nat Methods 12, 1143-1149.

Tronche, F., Kellendonk, C., Kretz, O., Gass, P., Anlag, K., Orban, P.C., Bock, R., Klein, R., and Schutz, G. (1999). Disruption of the glucocorticoid receptor gene in the nervous system results in reduced anxiety. Nat Genet 23, 99-103.

Unternaehrer, E., Luers, P., Mill, J., Dempster, E., Meyer, A.H., Staehli, S., Lieb, R., Hellhammer, D.H., and Meinlschmidt, G. (2012). Dynamic changes in DNA methylation of stress-associated genes (OXTR, BDNF) after acute psychosocial stress. Transl Psychiatry 2, e150.

van Bokhoven, H. (2011). Genetic and epigenetic networks in intellectual disabilities. Annu Rev Genet 45, 81-104.

Voikar, V., Koks, S., Vasar, E., and Rauvala, H. (2001). Strain and gender differences in the behavior of mouse lines commonly used in transgenic studies. Physiol Behav 72, 271-281.

Wang, T., Pan, Q., Lin, L., Szulwach, K.E., Song, C.X., He, C., Wu, H., Warren, S.T., Jin, P., Duan, R., and Li, X. (2012). Genome-wide DNA hydroxymethylation changes are associated with neurodevelopmental genes in the developing human cerebellum. Human molecular genetics 21, 5500-5510.

Wang, X., McCoy, P.A., Rodriguiz, R.M., Pan, Y., Je, H.S., Roberts, A.C., Kim, C.J., Berrios, J., Colvin, J.S., Bousquet-Moore, D., *et al.* (2011). Synaptic dysfunction and abnormal behaviors in mice lacking major isoforms of Shank3. Human molecular genetics 20, 3093-3108.

Warming, S., Costantino, N., Court, D.L., Jenkins, N.A., and Copeland, N.G. (2005). Simple and highly efficient BAC recombineering using galK selection. Nucleic Acids Res 33, e36.

Waterland, R.A. (2006). Assessing the effects of high methionine intake on DNA methylation. J Nutr 136, 1706S-1710S.

Waterland, R.A., and Jirtle, R.L. (2004). Early nutrition, epigenetic changes at transposons and imprinted genes, and enhanced susceptibility to adult chronic diseases. Nutrition 20, 63-68.

West, A.E., Chen, W.G., Dalva, M.B., Dolmetsch, R.E., Kornhauser, J.M., Shaywitz, A.J., Takasu, M.A., Tao, X., and Greenberg, M.E. (2001). Calcium regulation of neuronal gene expression. Proceedings of the National Academy of Sciences of the United States of America 98, 11024-11031.

Wetsel, W.C., Rodriguiz, R.M., Guillemot, J., Rousselet, E., Essalmani, R., Kim, I.H., Bryant, J.C., Marcinkiewicz, J., Desjardins, R., Day, R., *et al.* (2013). Disruption of the expression of the proprotein convertase PC7 reduces BDNF production and affects learning and memory in mice. Proceedings of the National Academy of Sciences of the United States of America 110, 17362-17367.

Winslow, J.T., and Insel, T.R. (2002). The social deficits of the oxytocin knockout mouse. Neuropeptides 36, 221-229.

Wossidlo, M., Nakamura, T., Lepikhov, K., Marques, C.J., Zakhartchenko, V., Boiani, M., Arand, J., Nakano, T., Reik, W., and Walter, J. (2011). 5-Hydroxymethylcytosine in the mammalian zygote is linked with epigenetic reprogramming. Nat Commun 2, 241.

Wu, H., Coskun, V., Tao, J., Xie, W., Ge, W., Yoshikawa, K., Li, E., Zhang, Y., and Sun, Y.E. (2010). Dnmt3a-dependent nonpromoter DNA methylation facilitates transcription of neurogenic genes. Science 329, 444-448.

Wu, H., D'Alessio, A.C., Ito, S., Xia, K., Wang, Z., Cui, K., Zhao, K., Sun, Y.E., and Zhang, Y. (2011). Dual functions of Tet1 in transcriptional regulation in mouse embryonic stem cells. Nature 473, 389-393.

Wu, S., Jia, M., Ruan, Y., Liu, J., Guo, Y., Shuang, M., Gong, X., Zhang, Y., Yang, X., and Zhang, D. (2005). Positive association of the oxytocin receptor gene (OXTR) with autism in the Chinese Han population. Biol Psychiatry 58, 74-77.

Xi, Y., and Li, W. (2009). BSMAP: whole genome bisulfite sequence MAPping program. BMC Bioinformatics 10, 232.

Xu, Y., Wu, F., Tan, L., Kong, L., Xiong, L., Deng, J., Barbera, A.J., Zheng, L., Zhang, H., Huang, S., *et al.* (2011). Genome-wide regulation of 5hmC, 5mC, and gene expression by Tet1 hydroxylase in mouse embryonic stem cells. Mol Cell 42, 451-464.

Yamaguchi, S., Hong, K., Liu, R., Shen, L., Inoue, A., Diep, D., Zhang, K., and Zhang, Y. (2012). Tet1 controls meiosis by regulating meiotic gene expression. Nature 492, 443-447.

Yildirim, O., Li, R., Hung, J.H., Chen, P.B., Dong, X., Ee, L.S., Weng, Z., Rando, O.J., and Fazzio, T.G. (2011). Mbd3/NURD complex regulates expression of 5-hydroxymethylcytosine marked genes in embryonic stem cells. Cell 147, 1498-1510.

Yu, H., Su, Y., Shin, J., Zhong, C., Guo, J.U., Weng, Y.L., Gao, F., Geschwind, D.H., Coppola, G., Ming, G.L., and Song, H. (2015). Tet3 regulates synaptic transmission and homeostatic plasticity via DNA oxidation and repair. Nat Neurosci 18, 836-843.

Zhang, H., Zhang, X., Clark, E., Mulcahey, M., Huang, S., and Shi, Y.G. (2010). TET1 is a DNA-binding protein that modulates DNA methylation and gene transcription via hydroxylation of 5-methylcytosine. Cell Res 20, 1390-1393.

Zhang, R.R., Cui, Q.Y., Murai, K., Lim, Y.C., Smith, Z.D., Jin, S., Ye, P., Rosa, L., Lee, Y.K., Wu, H.P., *et al.* (2013). Tet1 regulates adult hippocampal neurogenesis and cognition. Cell Stem Cell 13, 237-245.

Zhu, B., Benjamin, D., Zheng, Y., Angliker, H., Thiry, S., Siegmann, M., and Jost, J.P. (2001). Overexpression of 5-methylcytosine DNA glycosylase in human embryonic kidney cells EcR293 demethylates the promoter of a hormone-regulated reporter gene. Proceedings of the National Academy of Sciences of the United States of America 98, 5031-5036.

Zhu, J., and Yao, X. (2009). Use of DNA methylation for cancer detection: promises and challenges. Int J Biochem Cell Biol 41, 147-154.

Zhu, L., Wang, X., Li, X.L., Towers, A., Cao, X., Wang, P., Bowman, R., Yang, H., Goldstein, J., Li, Y.J., and Jiang, Y.H. (2014). Epigenetic dysregulation of SHANK3 in brain tissues from individuals with autism spectrum disorders. Human molecular genetics 23, 1563-1578.

Zhubi, A., Chen, Y., Dong, E., Cook, E.H., Guidotti, A., and Grayson, D.R. (2014). Increased binding of MeCP2 to the GAD1 and RELN promoters may be mediated by an enrichment of 5-hmC in autism spectrum disorder (ASD) cerebellum. Transl Psychiatry 4, e349.

Ziegler, C., Dannlowski, U., Brauer, D., Stevens, S., Laeger, I., Wittmann, H., Kugel, H., Dobel, C., Hurlemann, R., Reif, A., *et al.* (2015). Oxytocin receptor gene methylation: converging multilevel evidence for a role in social anxiety. Neuropsychopharmacology 40, 1528-1538.

Biography

On December 24th of 1980 in Carmichael, California, Aaron Joseph Towers became the 3rd of eventually four children of loving parents, Stephen and Sheryl Towers. After watching a film about genetically modified plants in high school, Aaron fell in love with genetics. He attended Brigham Young University where he majored in Plant Genetics and Biotechnology and graduated with a Bachelor of Science Degree in April, 2006. While there, Aaron had the opportunity to work as a Research Assistant in Dr. Jeff Maughan's plant genetics lab studying, the now trendy, staple food quinoa. Aaron worked two jobs and obtained several scholarships to pay for his education.

Upon graduation, he accepted a one year Oak Ridge Institute for Science and Education (ORISE) fellowship at the FBI Academy to work with Dr. James Robertson. While there, he not only developed genomic real-time PCR assays to detect *Ricinus communis* DNA but fell in love with another fellow, Angela Palermo. After the ORISE fellowship he worked for two years in Dr. Simon Gregory's lab at the Duke Center for Human Genetics where he used microarray technology and bisulfite sequencing to identify genomic and epigenetic factors that may play a role in autism. After gaining these valuable research experiences, he was accepted into Duke University's Program in Genetics and Genomics in order to pursue a PhD in the fall of 2009. By the spring of 2010, he joined Dr. Yong-hui Jiang's lab to begin his research into the field of neuroepigenetics. Aaron and Angela have two boys and are expecting a third child.

Scientific publications

Towers AJ, Li XL, Bey AL, Tremblay MW, Zhang W, Cao X, Wang X, Wang P, Chung L, Duffney LJ, Siecinski SK, Xu S, Kim Y, Kong X, Xie W, Jiang YH. Tet1-deficiency in mice causes transcriptional and epigenetic dysregulation of Oxtr and abnormal social and cognitive behaviors. (Under review at Cell Reports 2/29/2016)

Chung L, Wang X, Zhu L, **Towers AJ**, Kim IH, Jiang YH. Brain Research. Parental origin impairment of synaptic functions and behaviors in cytoplasmic FMRP interacting protein 1 (Cyfip1) deficient mice. 2015 Oct 17; PMID: 26474913

Zhu L, Wang X, Li XL, **Towers A**, Cao X, Wang P, Bowman R, Yang H, Goldstein J, Li YJ, Jiang YH. Hum Mol Genet. Epigenetic dysregulation of SHANK3 in brain tissues from individuals with autism spectrum disorders. 2014 Mar 15;23(6):1563-78. PMID: 24186872

Hara MR, Kovacs JJ, Whalen EJ, Rajagopal S, Strachan RT, Grant W, **Towers AJ**, Williams B, Lam CM, Xiao K, Shenoy SK, Gregory SG, Ahn S, Duckett DR, Lefkowitz RJ. Nature. A stress response pathway regulates DNA damage through β2-adrenoreceptors and β-arrestin-1. 2011 Aug 21;477(7364):349-53. PMID: 21857681

Duncan CG, Killela PJ, Payne CA, Lampson B, Chen WC, Liu J, Solomon D, Waldman T, **Towers AJ**, Gregory SG, McDonald KL, McLendon RE, Bigner DD, Yan H. Integrated genomic analyses identify ERRFI1 and TACC3 as glioblastoma-targeted genes. Oncotarget. 2010 Aug;1(4):265-77. PMID: 21113414

Gregory SG, Connelly JJ, **Towers AJ**, Johnson J, Biscocho D, Markunas CA, Lintas C, Abramson RK, Wright HH, Ellis P, Langford CF, Worley G, Delong GR, Murphy SK, Cuccaro ML, Persico A, Pericak-Vance MA. Genomic and epigenetic evidence for oxytocin receptor deficiency in autism. BMC Med. 2009 Oct 22;7:62. PMID: 19845972

Hari KL, Goates AT, Jain R, **Towers A**, Harpin VS, Robertson JM, Wilson MR, Samant VS, Ecker DJ, McNeil JA, Budowle B. The Microbial Rosetta Stone: a database system for tracking infectious microorganisms. Int J Legal Med. 2009 Jan;123(1):65-9. Epub 2008 Jul 8. PMID: 18607616

Fellowships and academic honors

Top Basic Science Research Abstract – Department of Pediatrics research retreat, 4/2016

2015 ASHG/Charles J. Epstein Trainee Award for Excellence in Human Genetics Research – Semifinalist, American Society of Human Genetics, 7/2015

Oak Ridge Institute for Science and Education Fellowship at the FBI Academy, 6/2006